

# The Galactic Center GeV Excess

**Tim Linden**

CCAPP Postdoctoral Fellow  
Center for Cosmology and Astro-Particle Physics  
The Ohio State University



# The Result

- Observations by the *Fermi Large Area Telescope* have identified an excess in gamma-ray emission in the Galactic center, *compared to the predicted emission from known astrophysical gamma-ray sources.*
- This excess is defined by:
  - 1.) A spectrum which peaks sharply at an energy of  $\sim 2$  GeV, falling off rapidly at lower and higher energies.
  - 2.) A morphology that is spherically symmetric around the dynamical center of our galaxy, and which extends from  $0.1^\circ - 10^\circ$  from the Galactic center.

# The Fermi Large Area Telescope

- Space-based, pair-conversion telescope characterized by:

1.) Energy Range: 30 MeV – 1 TeV

2.) Effective Area:  $\sim 1 \text{ m}^2$

3.) Field of View: 2 sr

4.) Energy Resolution: 10%

5.) Angular Resolution:

a.) 100 MeV:  $10^\circ$

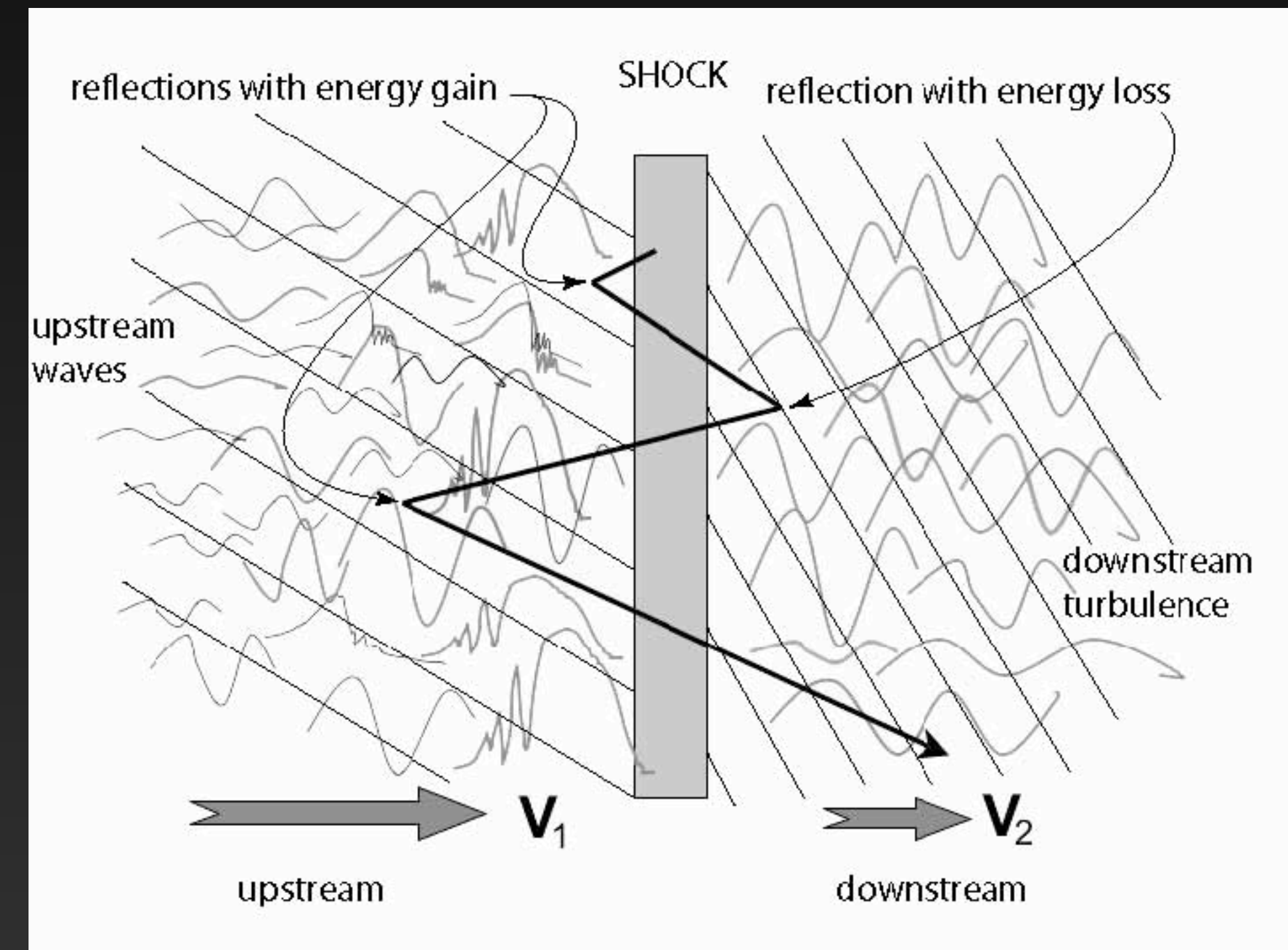
b.) 1 GeV:  $0.8^\circ$

c.) 10 GeV:  $0.1^\circ$



# Gamma-Ray Emission Mechanisms

- Gamma-Ray Emission is non-thermal and requires a source of relativistic cosmic-ray particles.
- Requires a mechanism like 1st order Fermi acceleration
- Most reasonable source of cosmic-rays in the Milky Way are supernova shocks
- Shocks from pulsars, black holes, and magnetohydrodynamic turbulence are also possible contributors.



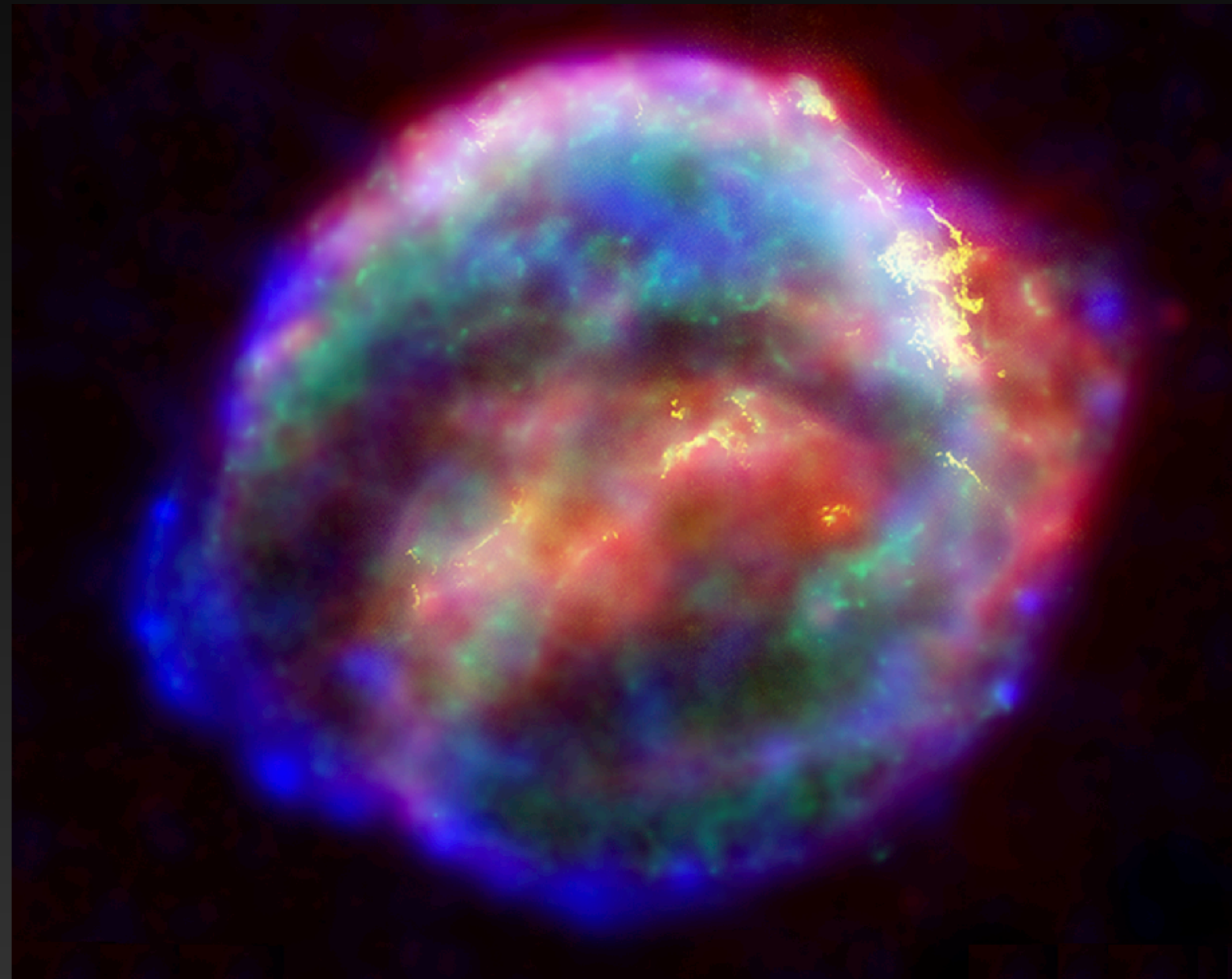
# The Central Molecular Zone

- 400 pc x 80 pc
- $10^7 M_{\odot}$  of gas in Molecular Clouds
- Molecular clouds heated to 50-100K by a significant cosmic-ray component.

# What Generates these Cosmic-Rays?

The Galactic center region is known to contain nearly every known cosmic-ray acceleration mechanism.

- 1.) Supernovae
- 2.) Pulsars
- 3.) Sgr A\*
- 4.) Reacceleration
- 5.) Dark Matter Annihilation?



# The Galactic Center Supernovae

Multiwavelength observations indicate that the Galactic Center is a dense star-forming environment.

2-20% of the total Galactic Star Formation Rate is contained within the Central Molecular Zone.

Each SN injects  $10^{51}$  erg into ISM, 10% in cosmic-rays

2-4% - ISOGAL Survey Immer et al. (2012)

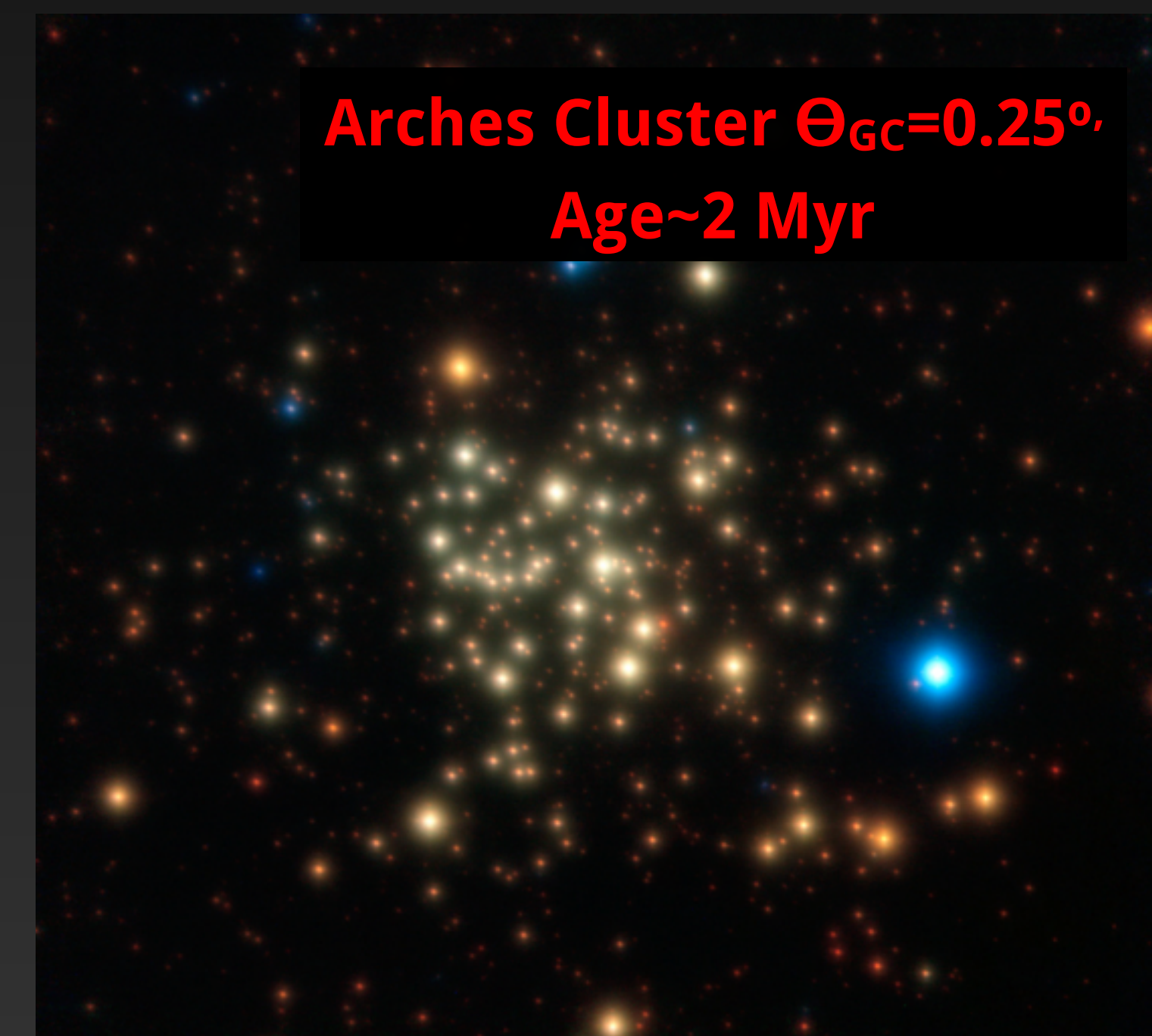
2.5-5% - Young Stellar Objects Yusef-Zadeh et al. (2009)

5-10% - Infrared Flux Longmore et al. (2013)

10-20% - Wolf-Rayet Stars Rosslowe & Crowther (2014)

2% - Far-IR Flux Thompson et al. (2007)

2.5-6% - SN1a Schanne et al. (2007)



# Galactic Center Pulsars



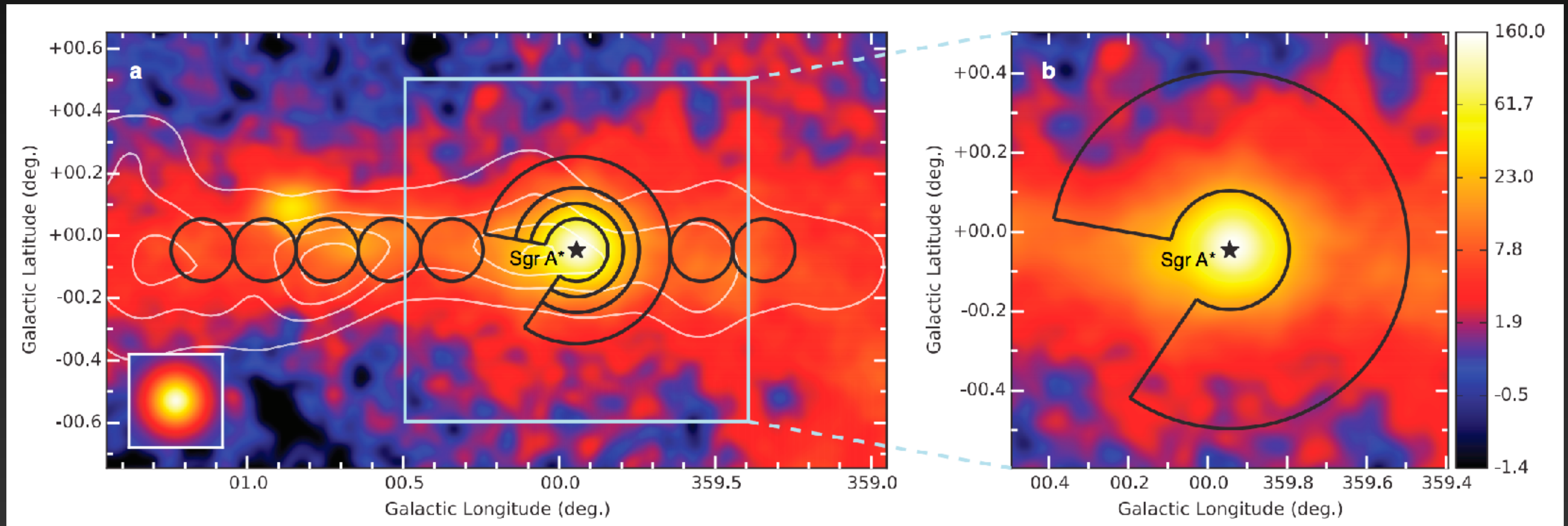
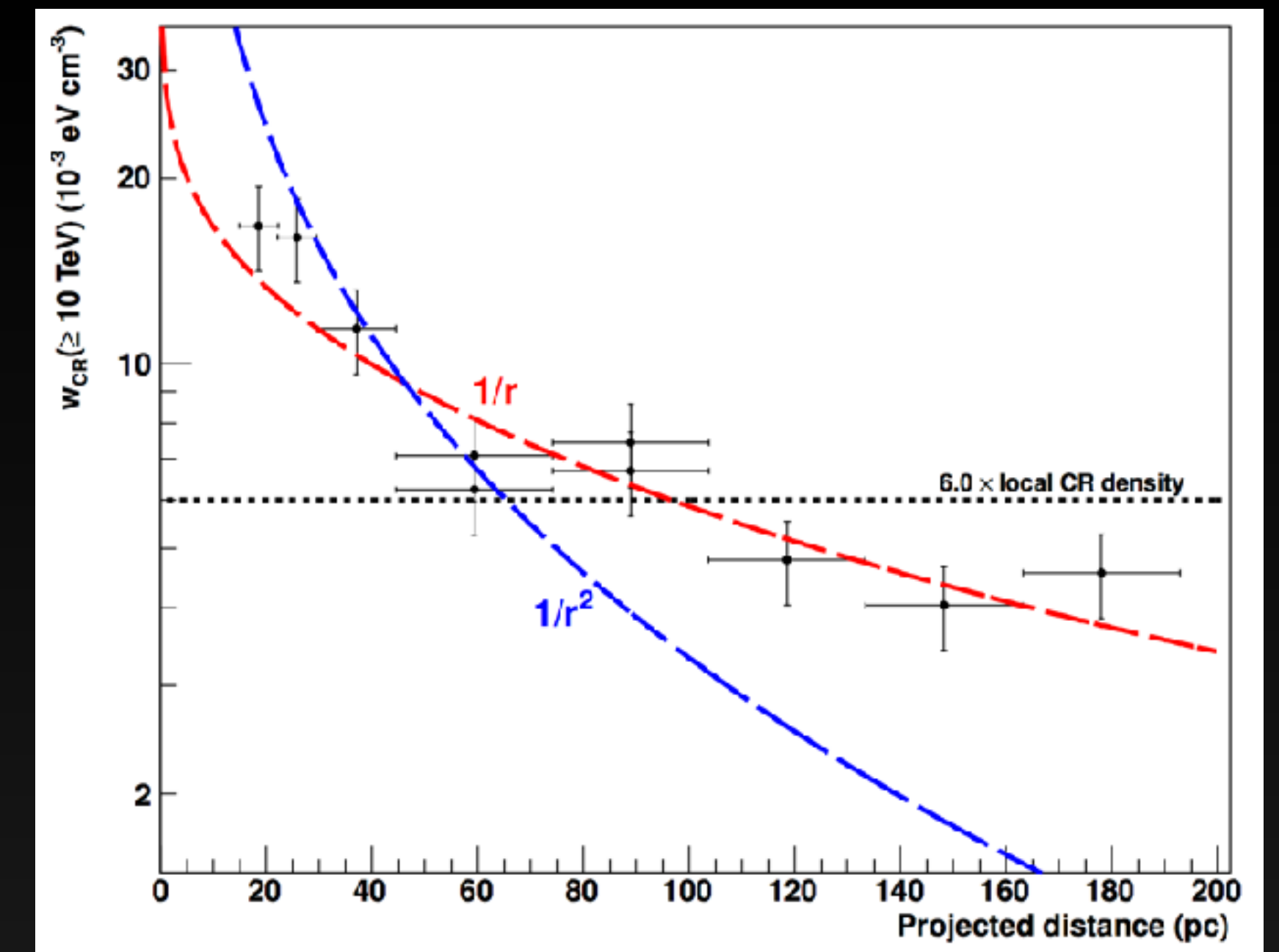
The Galactic Center is expected to host a significant population of both young pulsars (due to its high SFR), and millisecond pulsars (in part from the disruption of Globular Clusters).

Over the lifetime of a young (recycled) pulsar,  $\sim 10^{50}$  erg of energy are released, primarily in the form of relativistic  $e^+e^-$  pairs.

# The Sgr A\* Source

HESS has detected diffuse gamma-ray emission at energies  $\sim 100$  TeV.

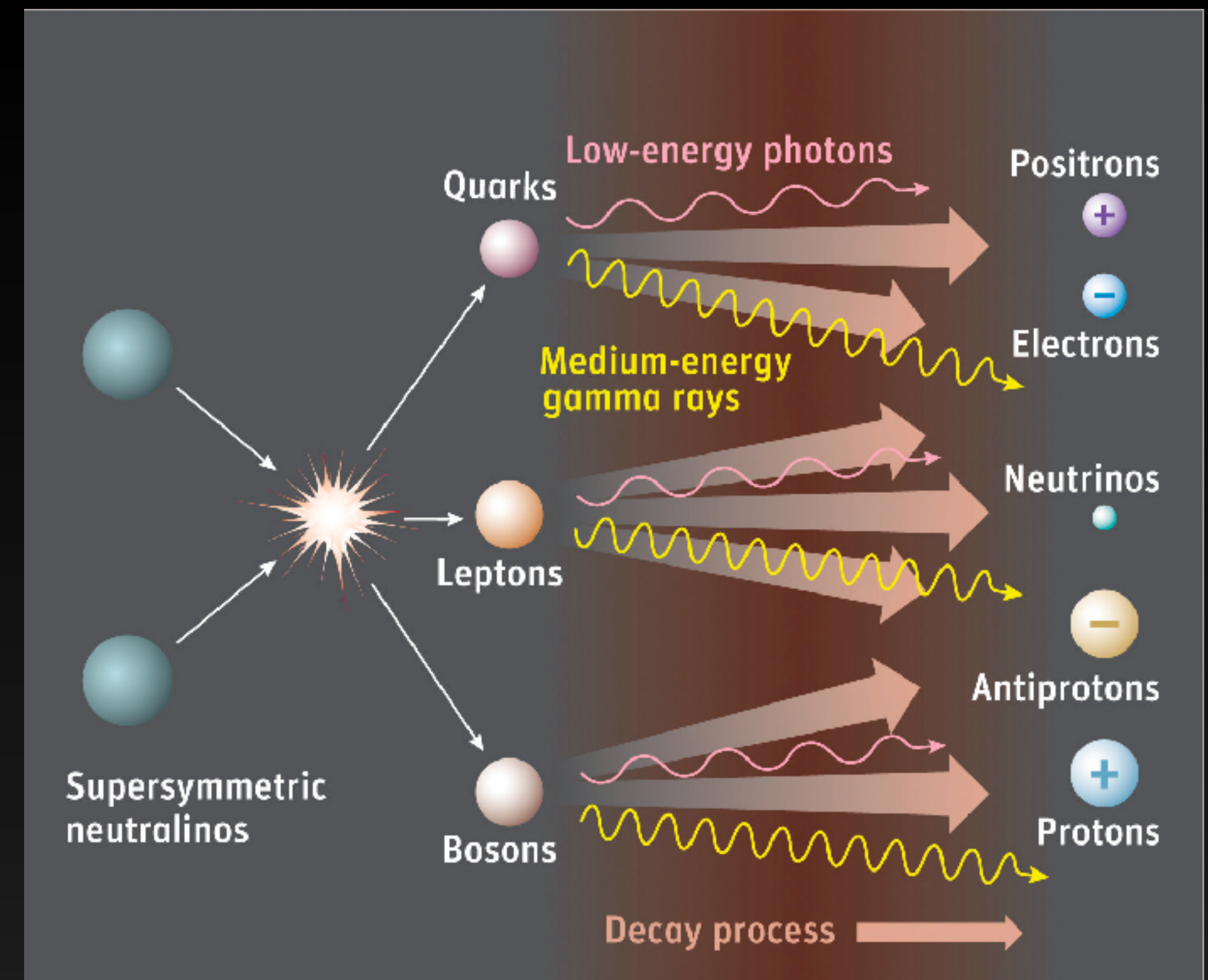
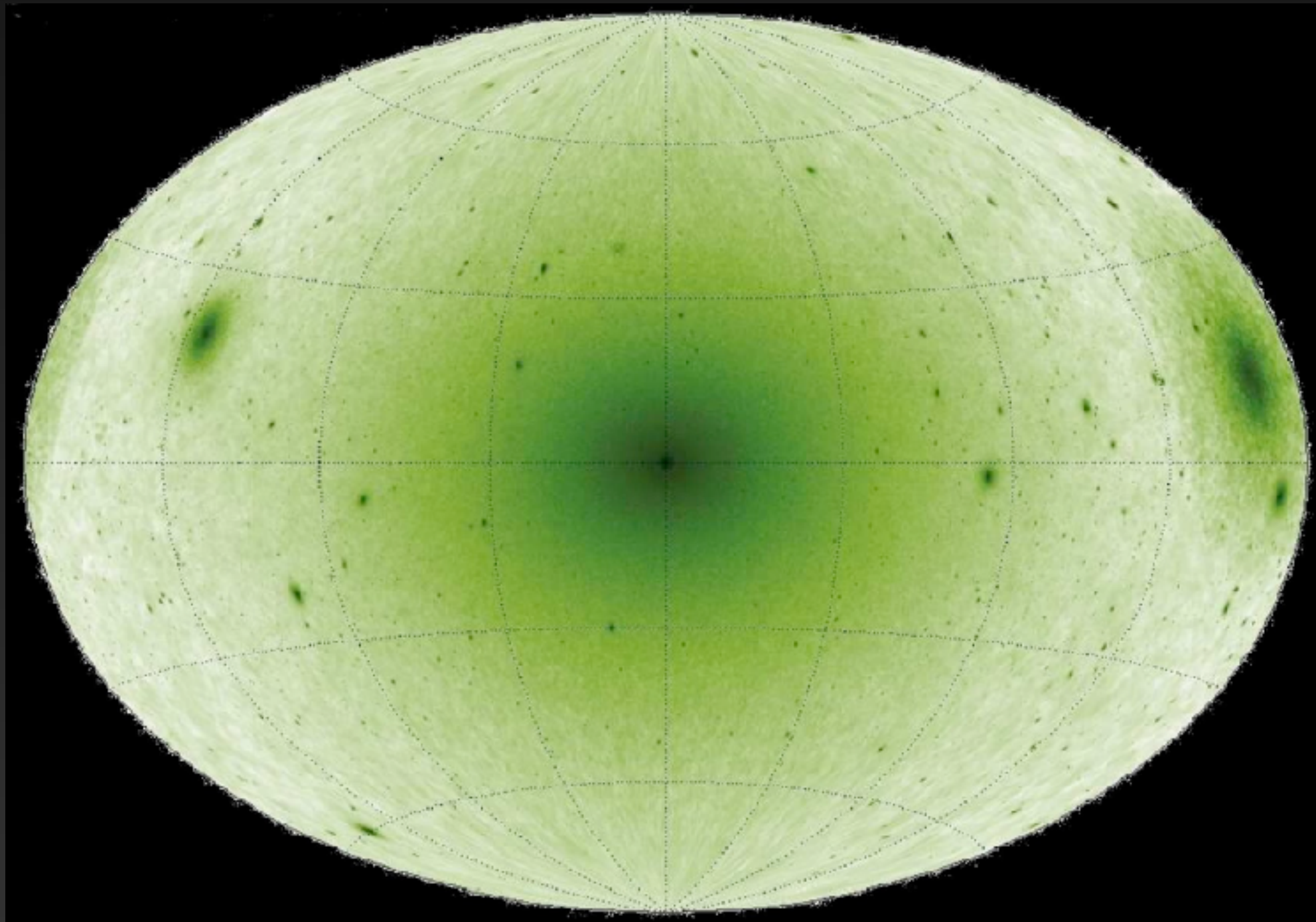
The emission profile is indicative of diffusion from the central BH.



# Dark Matter Annihilation?

WIMPs are currently among the most well-motivated dark matter models.

WIMP annihilation naturally produces a significant cosmic-ray (and gamma-ray) flux.



Dark Matter structure simulations uniformly predict that the GC is the brightest source of WIMP annihilations.

Standard scenarios predict the flux from the GC exceeds dSphs by a factor of  $\sim 100 - 1000$ .

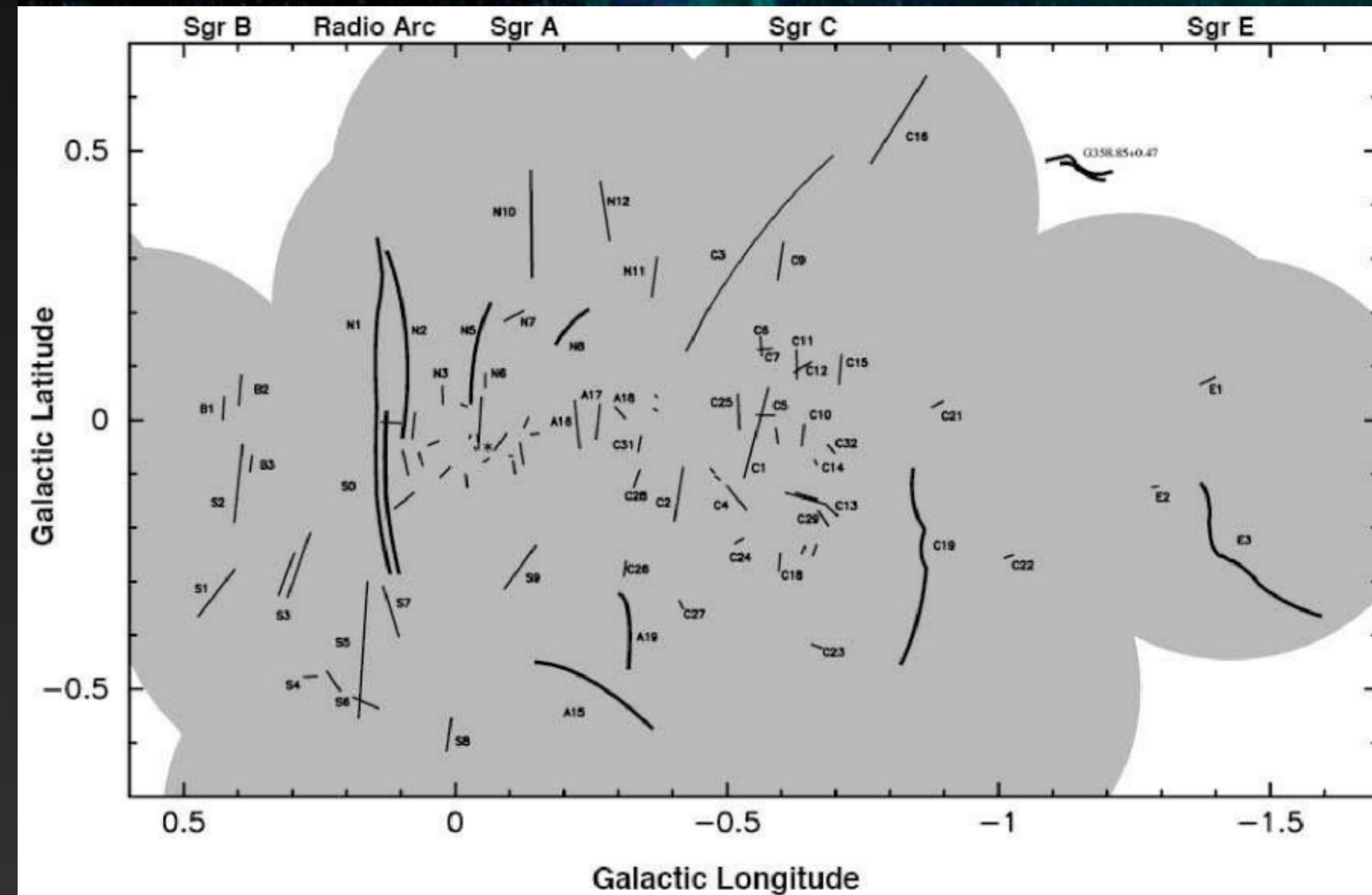
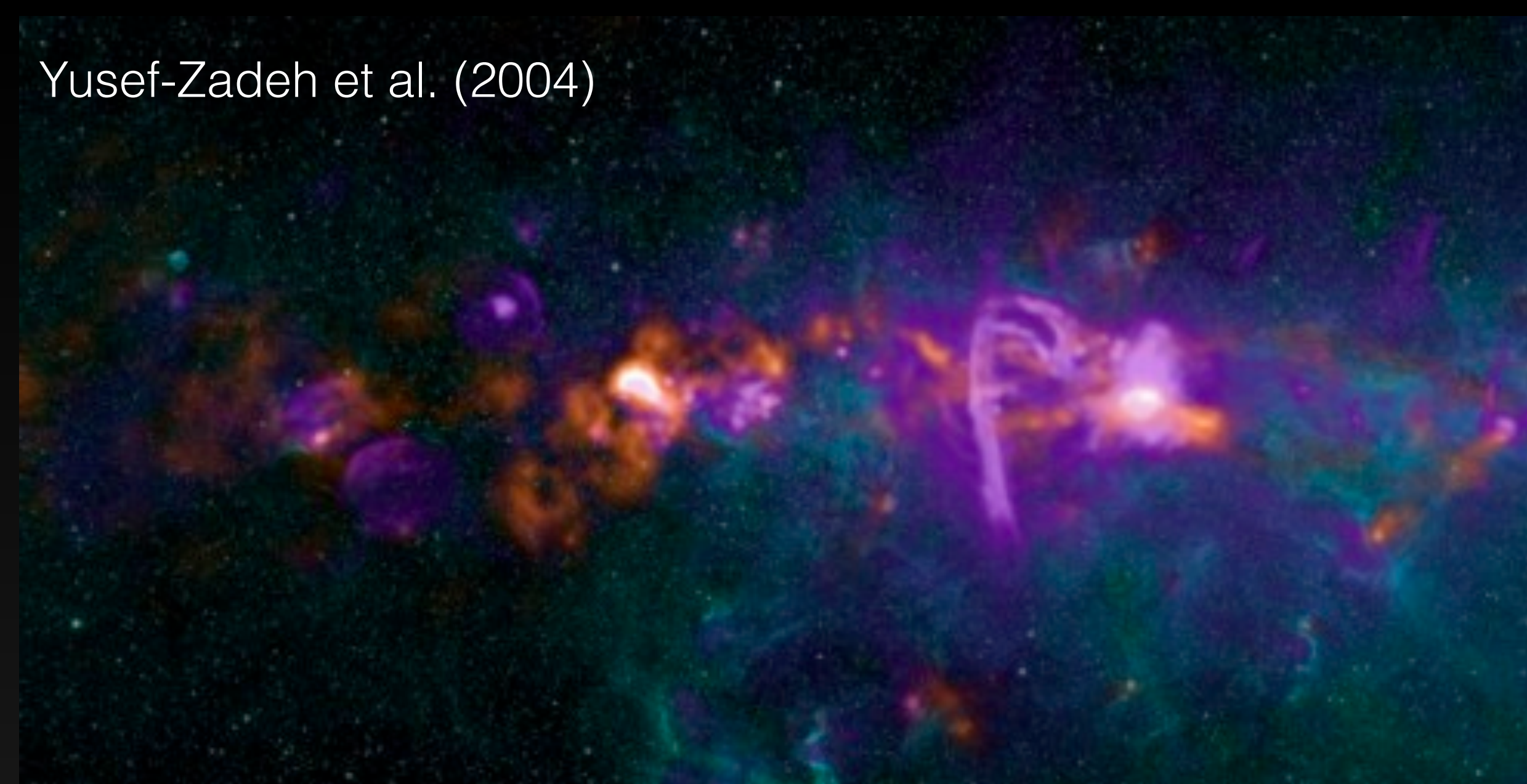
# Reacceleration

More than 80 filamentary structures identified in the central  $2^\circ \times 1^\circ$ .

The best astrophysical explanation involves significant re-acceleration via magnetic reconnection (Lesch & Riech 1992, Lieb et al. (2004).

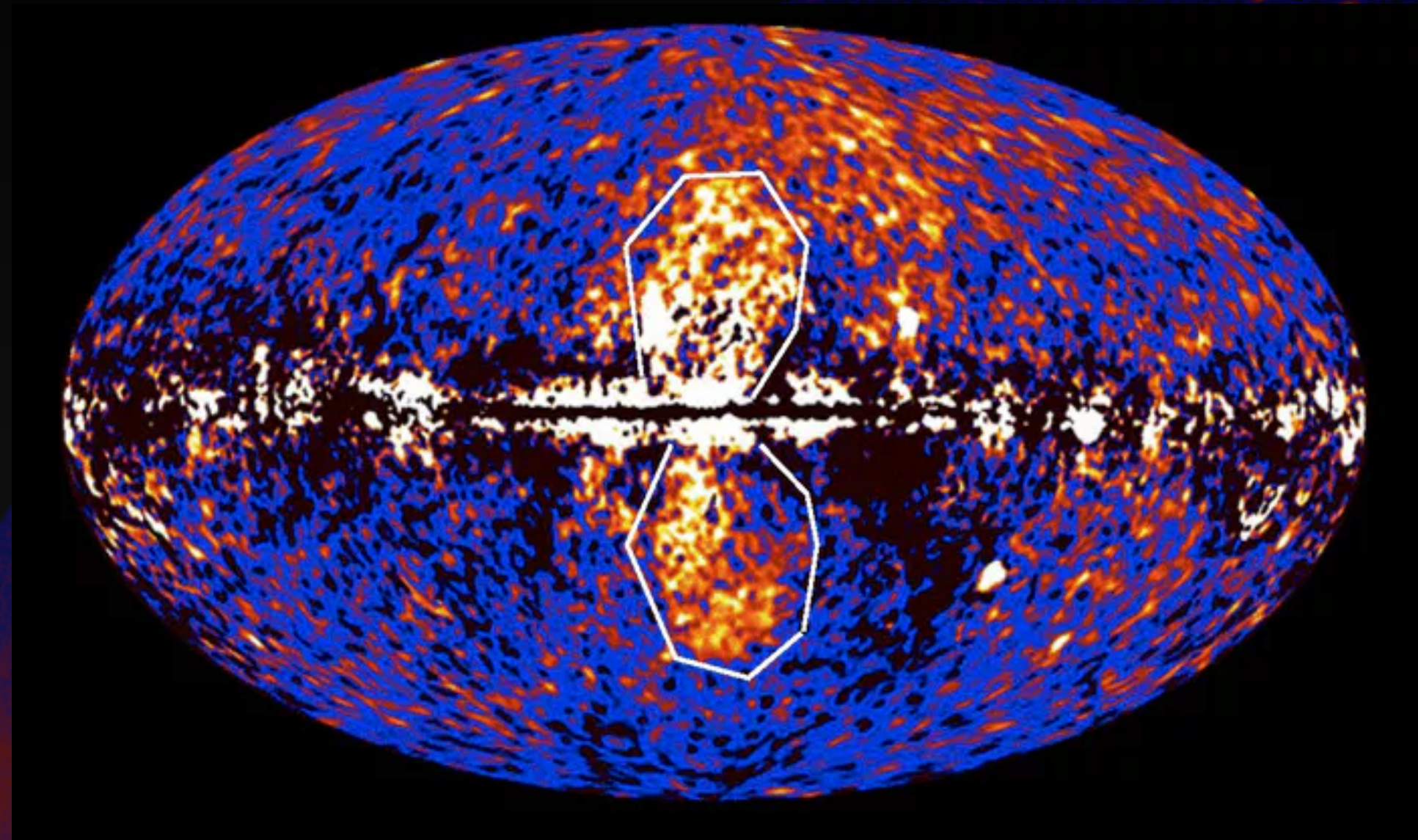
Strong magnetic fields may propagate through the Galactic center, significantly re-accelerating the cosmic-ray population.

Yusef-Zadeh et al. (2004)

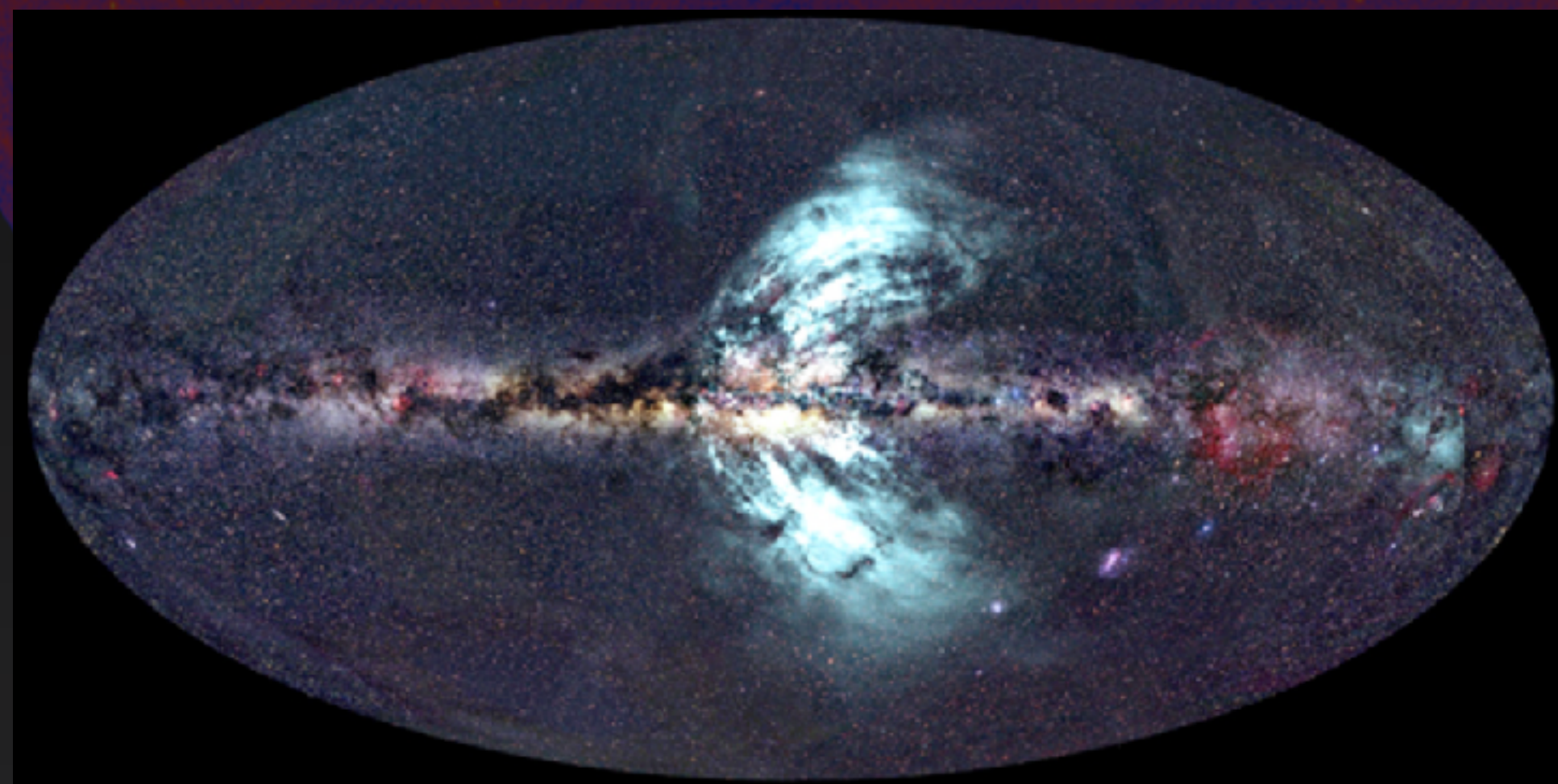


# Non-Thermal Emission (Observables)

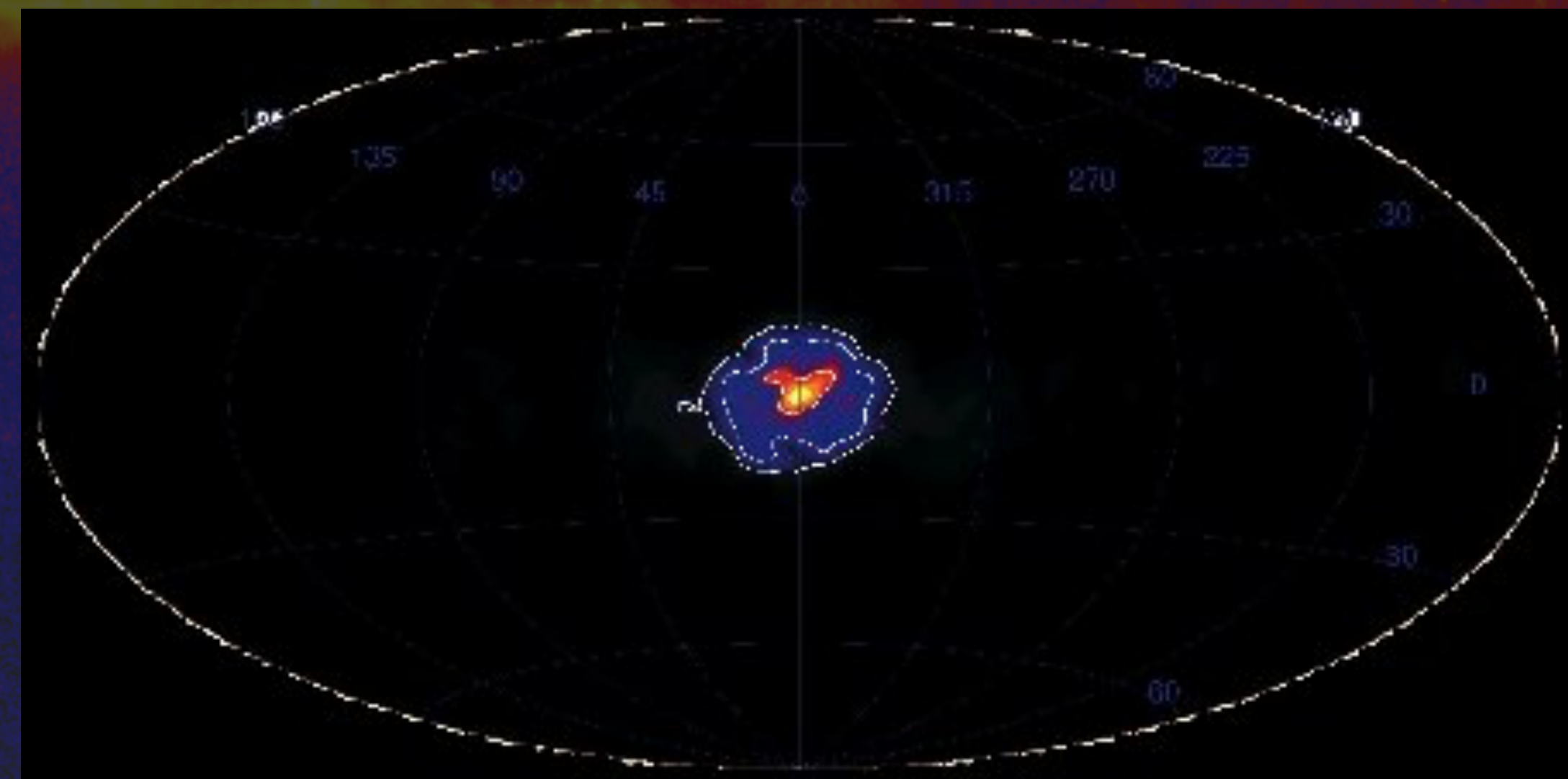
Fermi Bubbles



GeV Excess



WMAP/PLANCK Haze

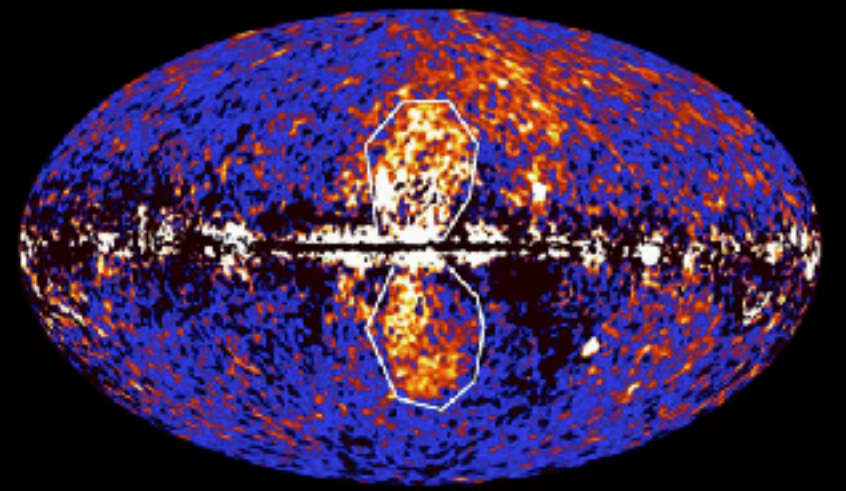


Integral 511 keV Excess

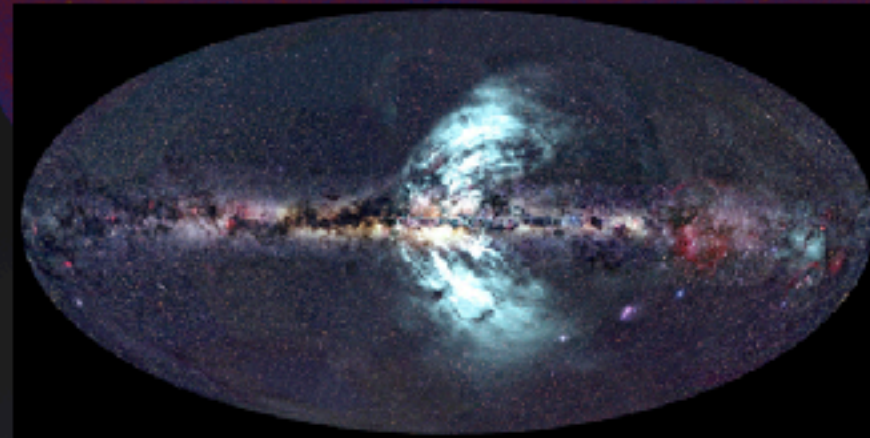
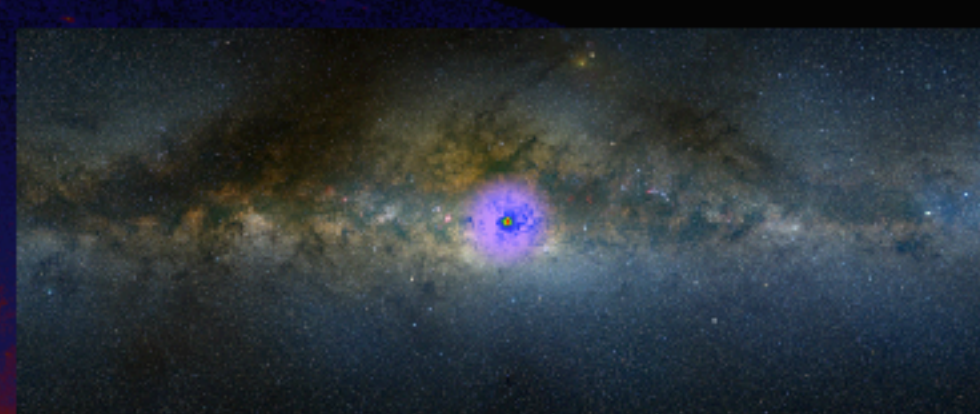
# Non-Thermal Emission (Observables)

## Non-Thermal Emission (Observables)

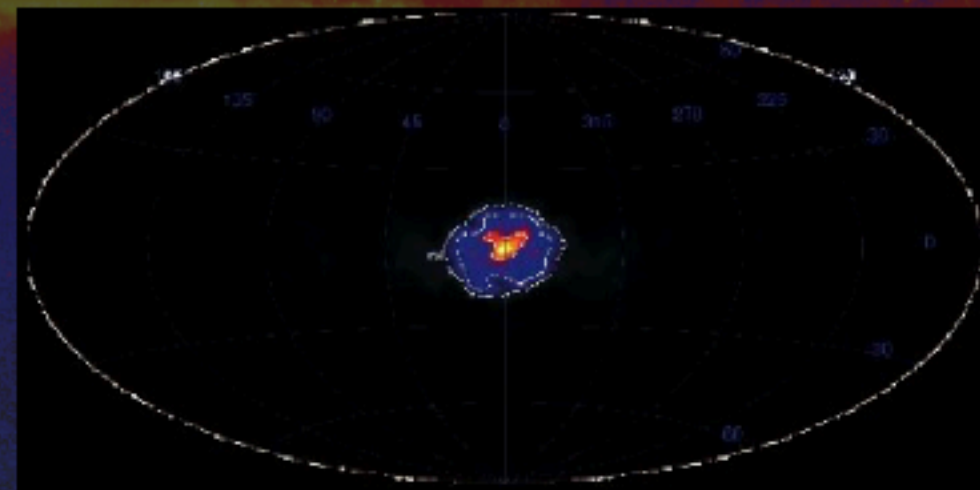
Fermi Bubbles



GeV Excess



WMAP/PLANCK Haze



Integral 511 keV Excess

The photon excesses extend very far from the central molecular region!

**This:**

- (a) Indicates the relative power of Galactic center accelerators, compared to the Galactic plane.
- (b) Provides a large field of view for studies of GC emission.
- (c) Implies that propagation is important!

# Cosmic-Ray Propagation



**Start with a source of  
relativistic cosmic-rays**

# Cosmic-Ray Propagation

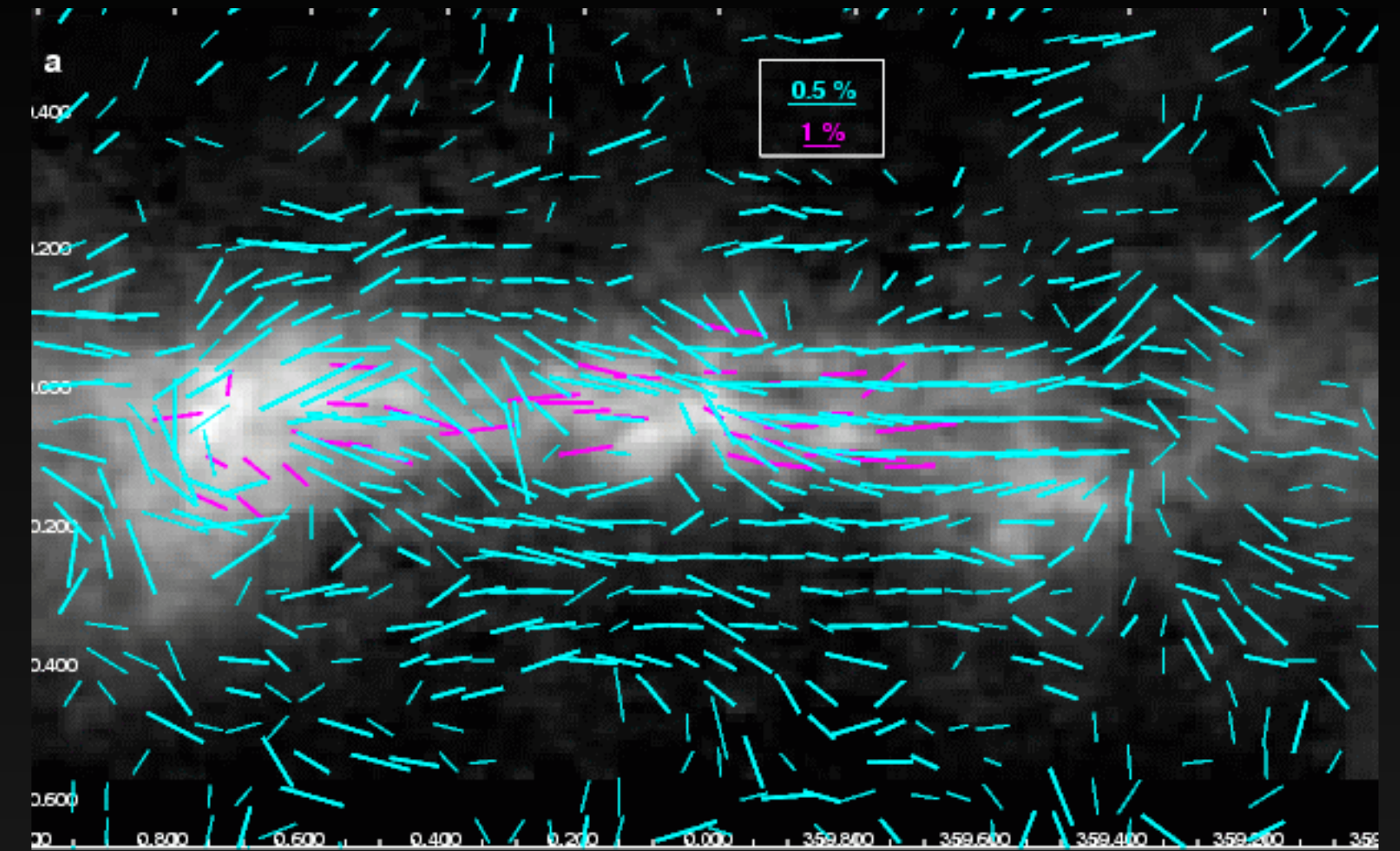


Start with a source of relativistic cosmic-rays

cosmic rays propagate

$$\frac{\partial \psi}{\partial t} = q(\vec{r}, p) + \vec{\nabla} \cdot (D_{xx} \vec{\nabla} \psi - \vec{V} \psi) + \frac{\partial}{\partial p} p^2 D_{pp} \frac{\partial}{\partial p} \frac{1}{p^2} \psi - \frac{\partial}{\partial p} \left[ p \dot{\psi} - \frac{p}{3} (\vec{\nabla} \cdot \vec{V}) \psi \right] - \frac{1}{\tau_f} \psi - \frac{1}{\tau_r} \psi$$

Solved Numerically:  
e.g. Galprop

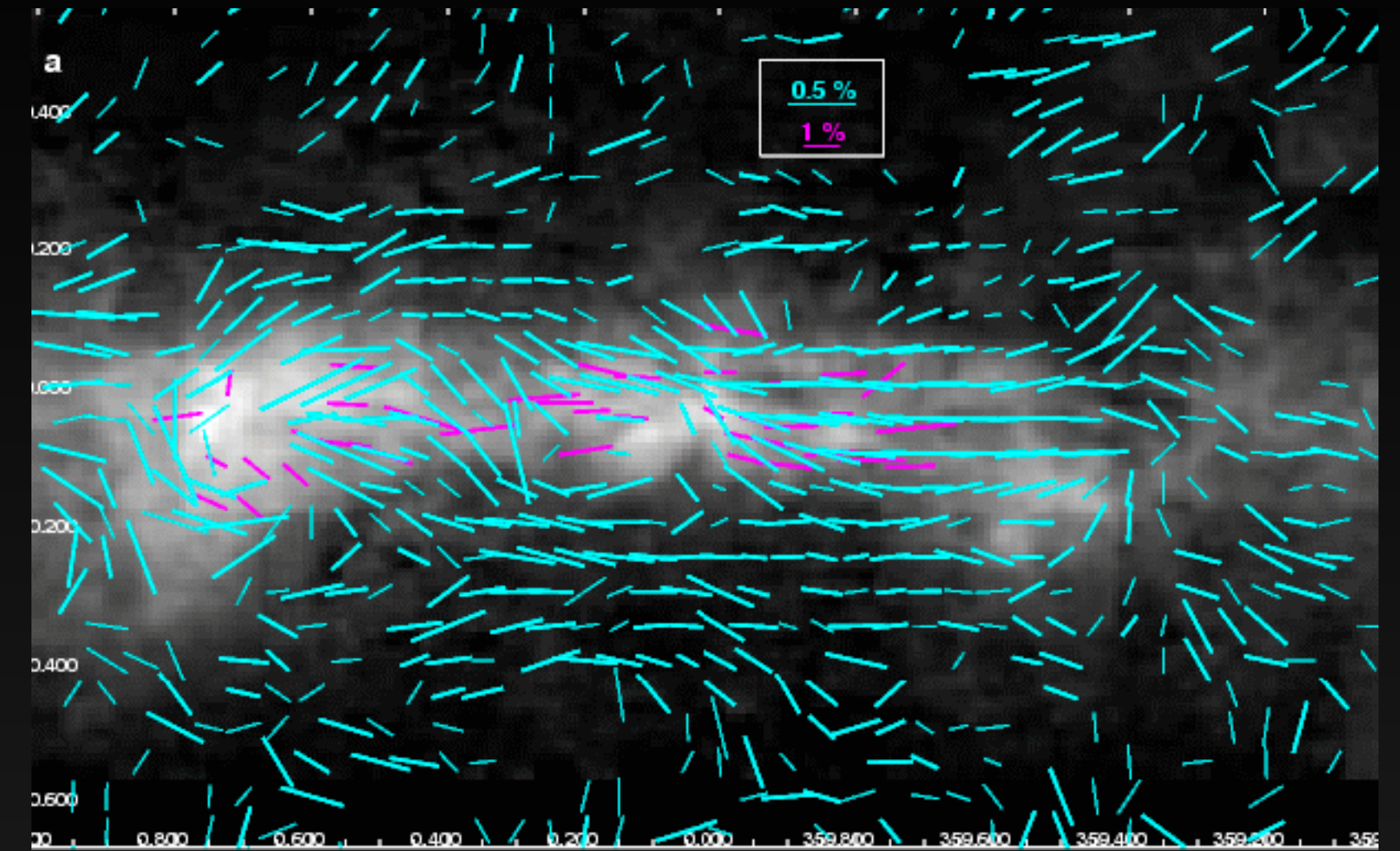


# Cosmic-Ray Propagation



Start with a source of relativistic cosmic-rays

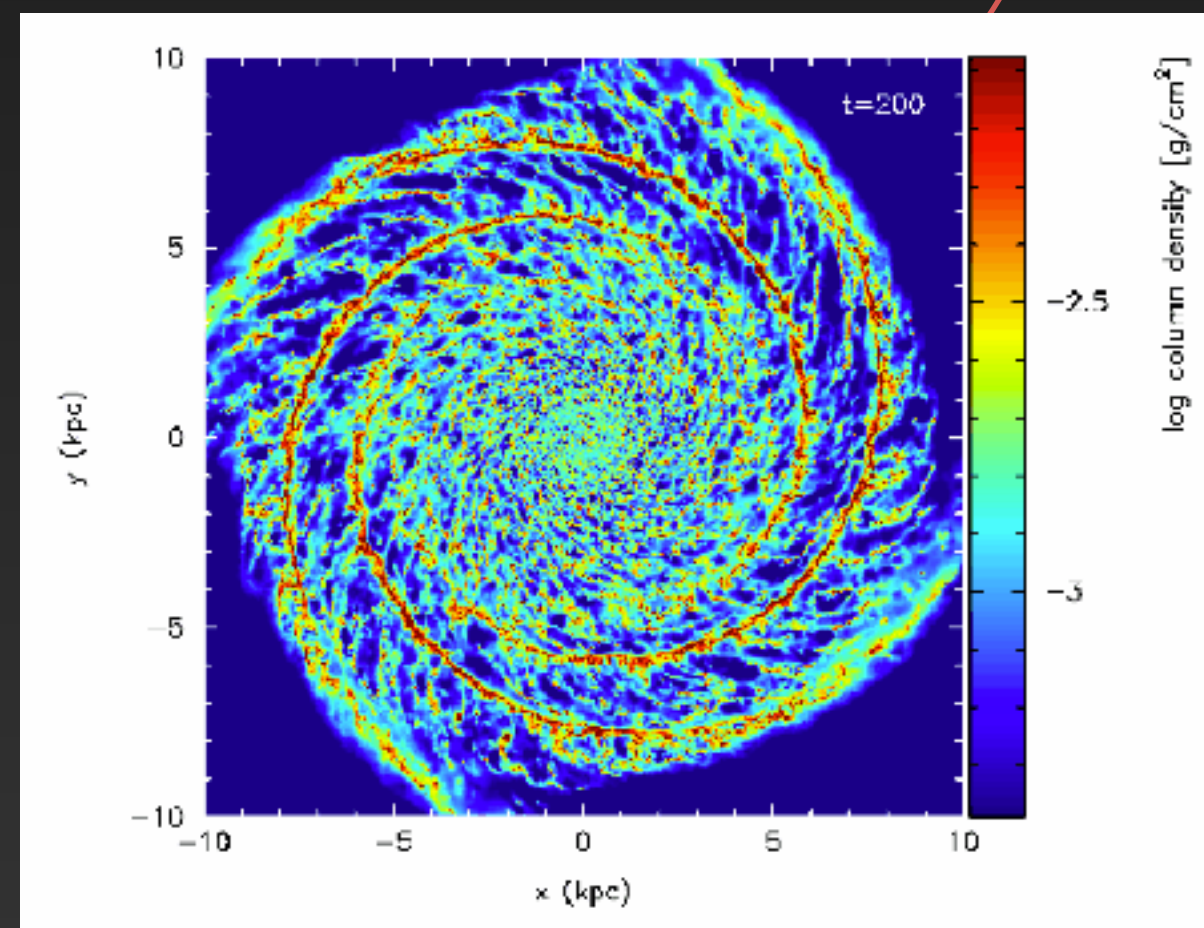
cosmic rays propagate



$$\frac{\partial \psi}{\partial t} = q(\vec{r}, p) + \vec{\nabla} \cdot (D_{xx} \vec{\nabla} \psi - \vec{V} \psi) + \frac{\partial}{\partial p} p^2 D_{pp} \frac{\partial}{\partial p} \frac{1}{p^2} \psi - \frac{\partial}{\partial p} \left[ p \dot{\psi} - \frac{p}{3} (\vec{\nabla} \cdot \vec{V}) \psi \right] - \frac{1}{\tau_f} \psi - \frac{1}{\tau_r} \psi$$

Solved Numerically:  
e.g. Galprop

Gas/ISRF

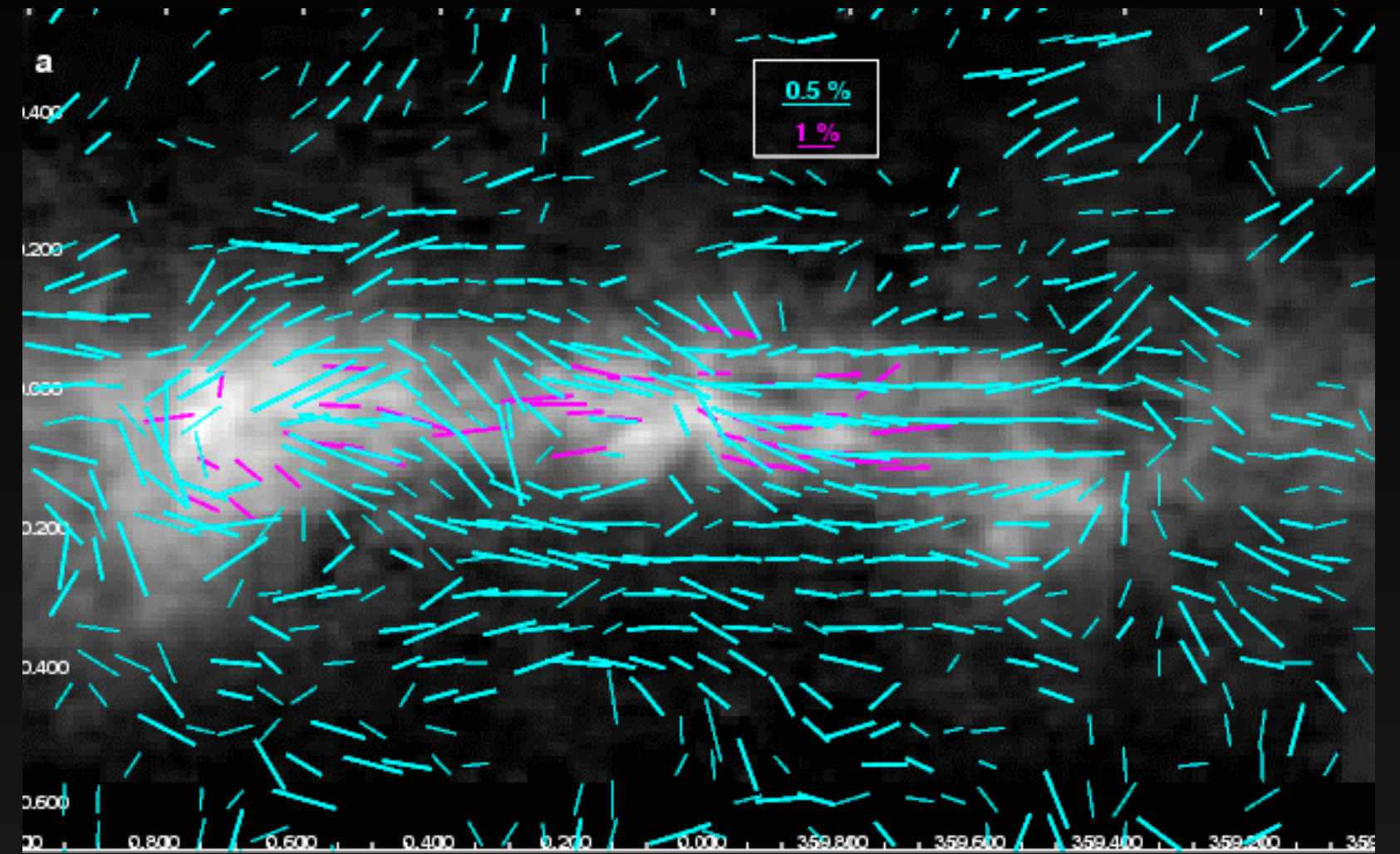


# Cosmic-Ray Propagation



Start with a source of relativistic cosmic-rays

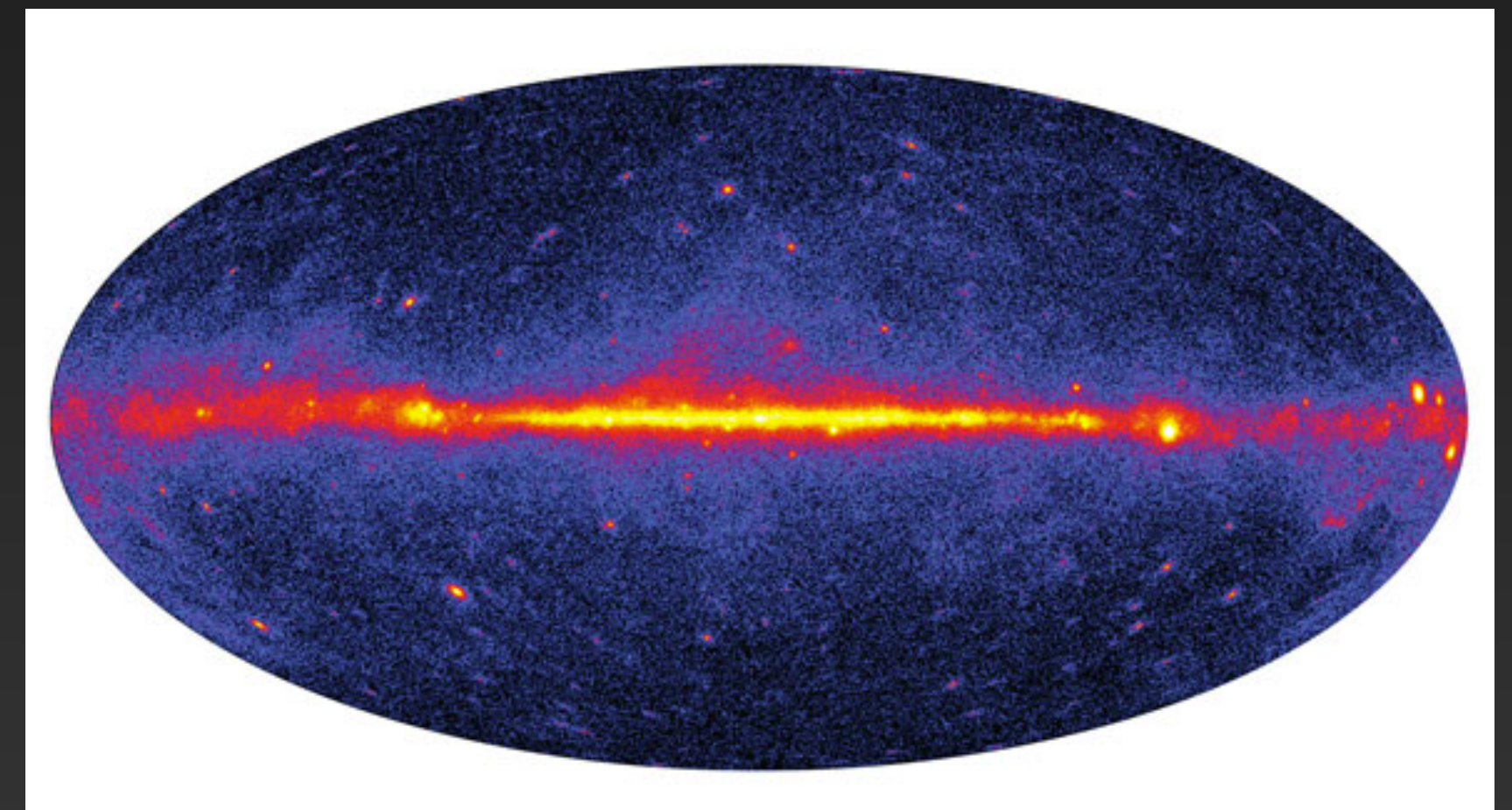
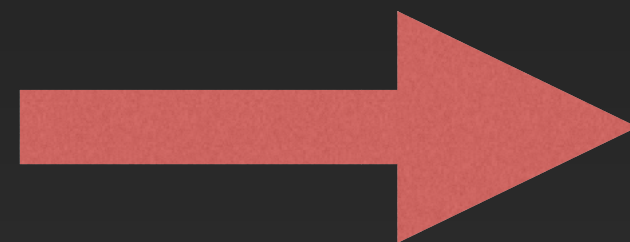
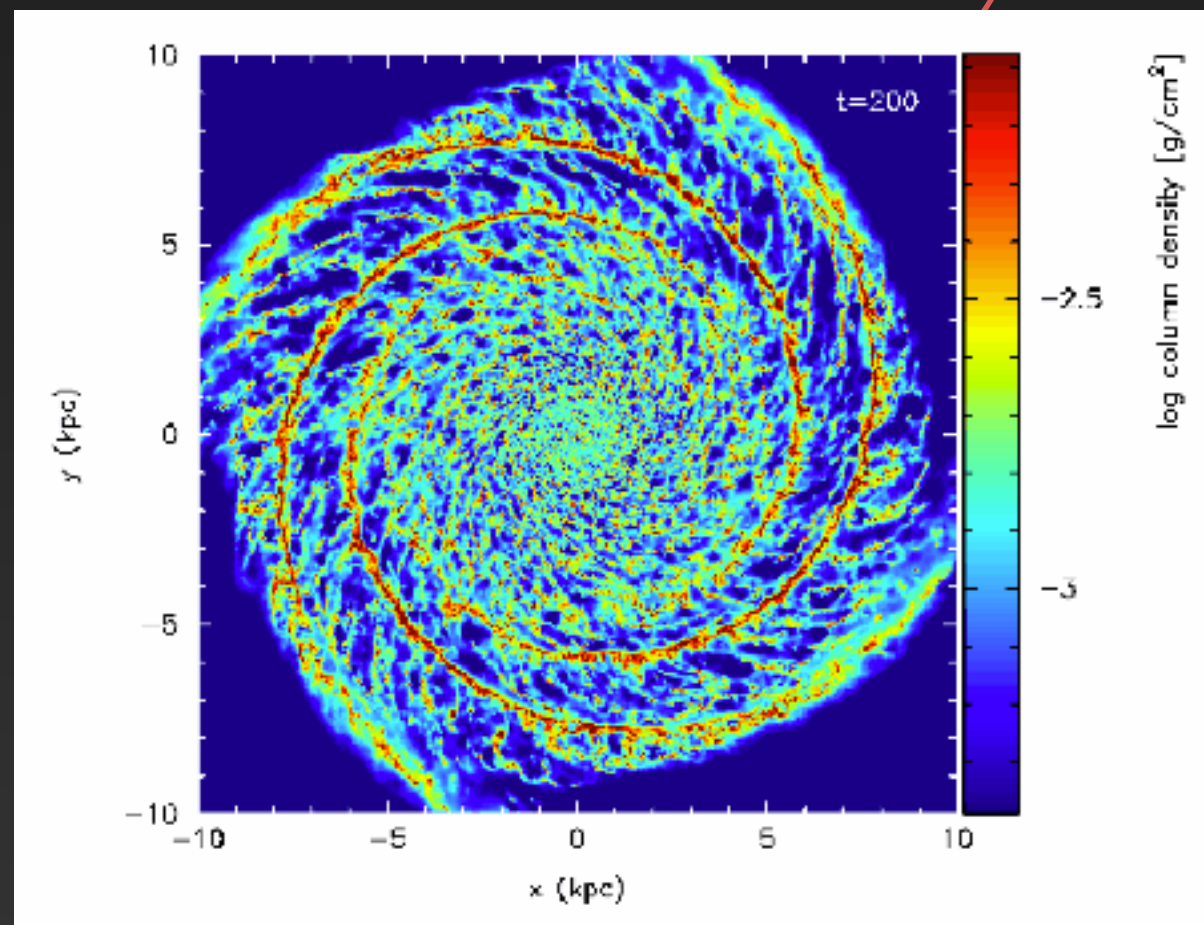
cosmic rays propagate



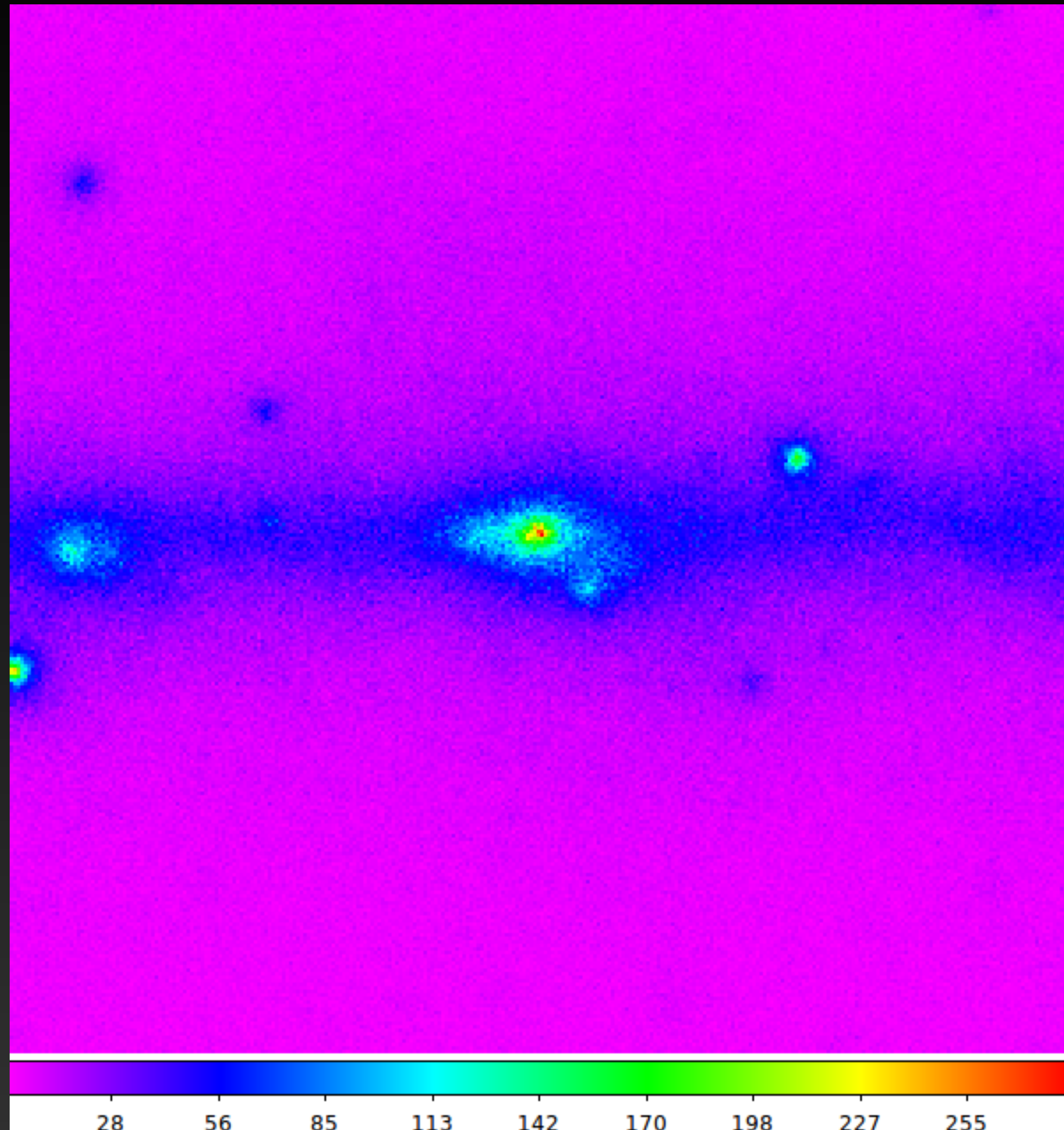
$$\frac{\partial \psi}{\partial t} = q(\vec{r}, p) + \vec{\nabla} \cdot (D_{xx} \vec{\nabla} \psi - \vec{V} \psi) + \frac{\partial}{\partial p} p^2 D_{pp} \frac{\partial}{\partial p} \frac{1}{p^2} \psi - \frac{\partial}{\partial p} \left[ p \dot{\psi} - \frac{p}{3} (\vec{\nabla} \cdot \vec{V}) \psi \right] - \frac{1}{\tau_f} \psi - \frac{1}{\tau_r} \psi$$

Solved Numerically:  
e.g. Galprop

Gas/ISRF

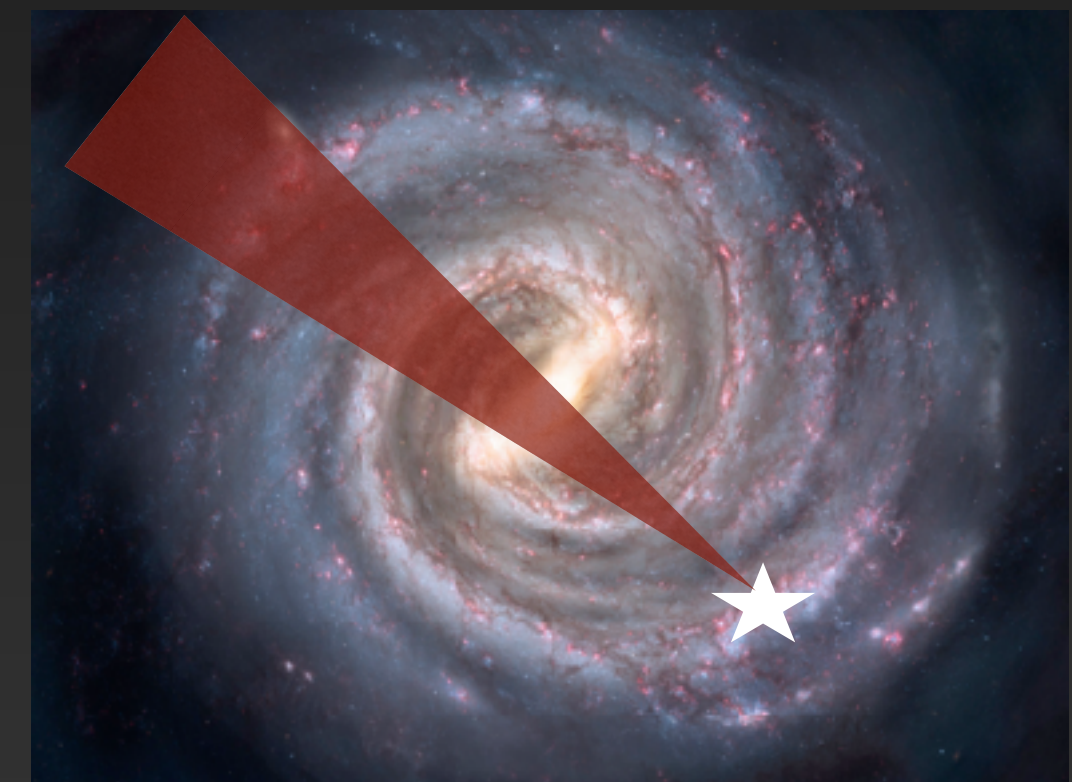


# The Energetics of the Galactic Center

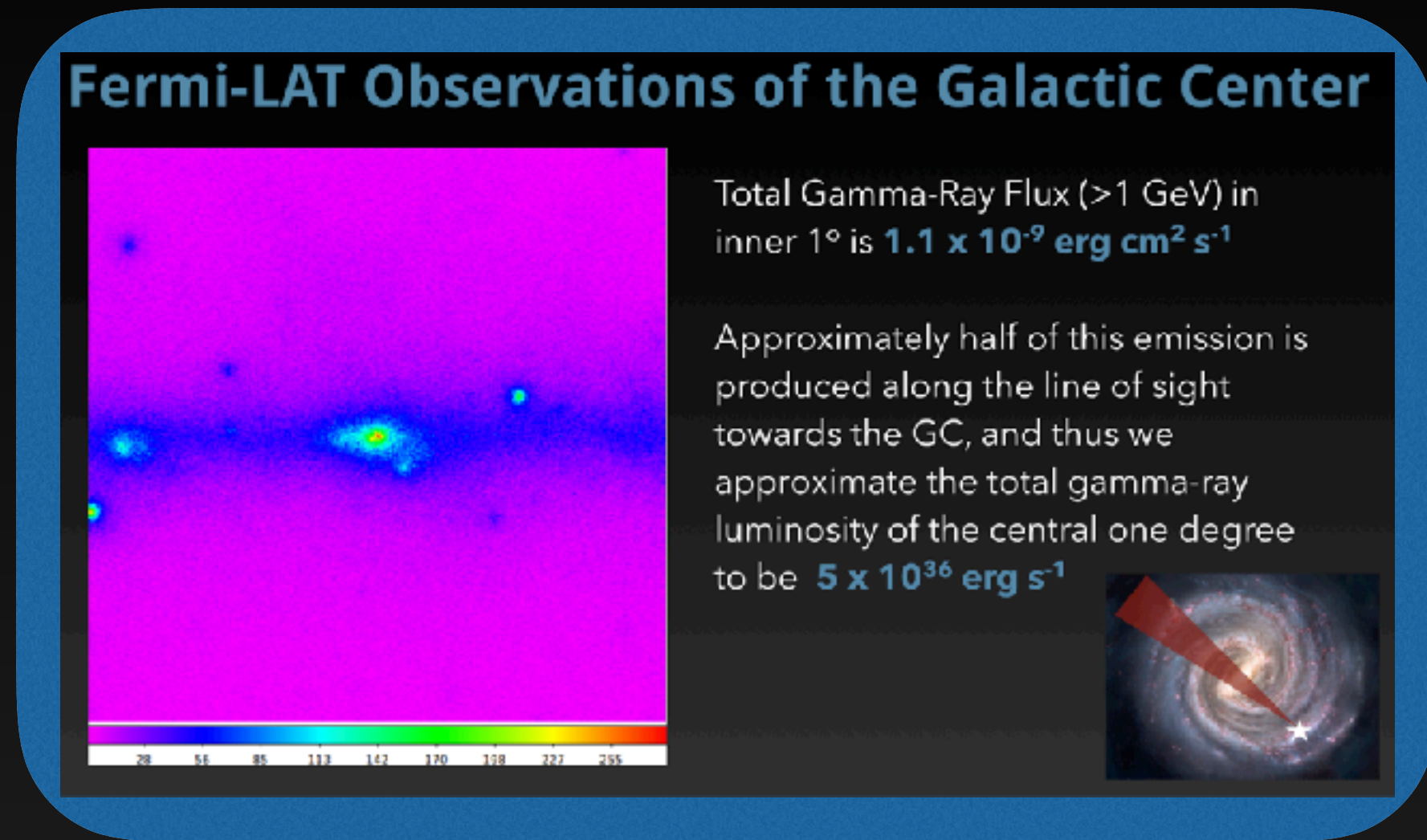


Total Gamma-Ray Flux ( $>1$  GeV) in inner  $1^\circ$  is  **$1.1 \times 10^{-9}$  erg  $\text{cm}^2 \text{s}^{-1}$**

Approximately half of this emission is produced along the line of sight towards the GC, and thus we approximate the total gamma-ray luminosity of the central one degree to be  **$5 \times 10^{36}$  erg  $\text{s}^{-1}$**



# Understanding the Gamma-Ray Source with Energetics



## Supernovae:

A Supernovae produces  $\sim 10^{51}$  erg of energy.

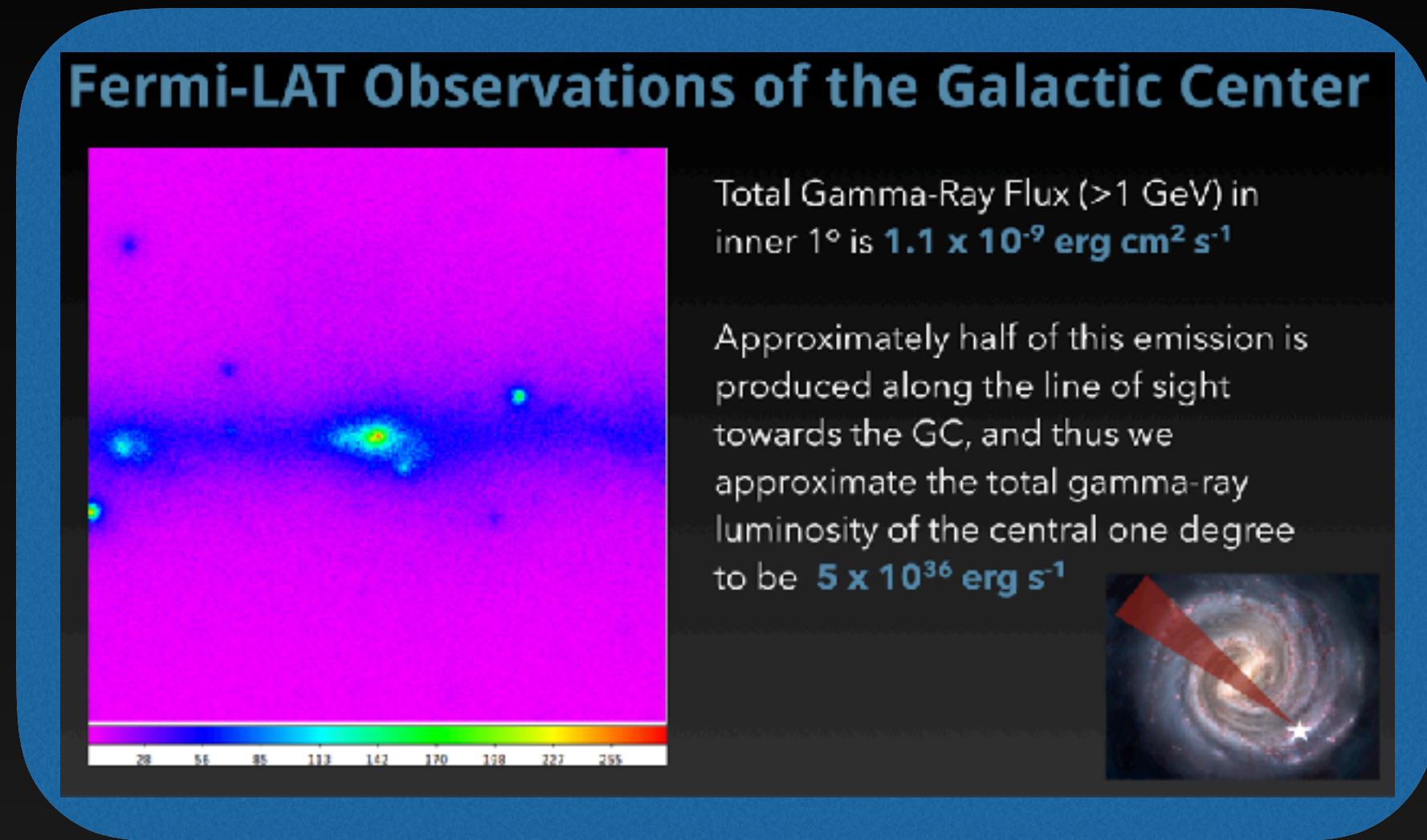
$\sim 10\%$  to CR protons.

Assuming 1 Galactic center SN every 250 years (10% the Galactic Rate), this provides an energy flux of  $1.3 \times 10^{40}$  erg  $\text{s}^{-1}$ .

If these cosmic-rays are trapped for 10 kyr in a 100 pc box ( $D_0 = 5 \times 10^{28}$  cm $^2$  s $^{-1}$ ), filled with Hydrogen gas at density 100 cm $^{-2}$ , this will produce a total gamma-ray emission:

$$6.7 \times 10^{37} \text{ erg s}^{-1} \quad \checkmark$$

# Understanding the Gamma-Ray Source with Energetics



## Pulsars:

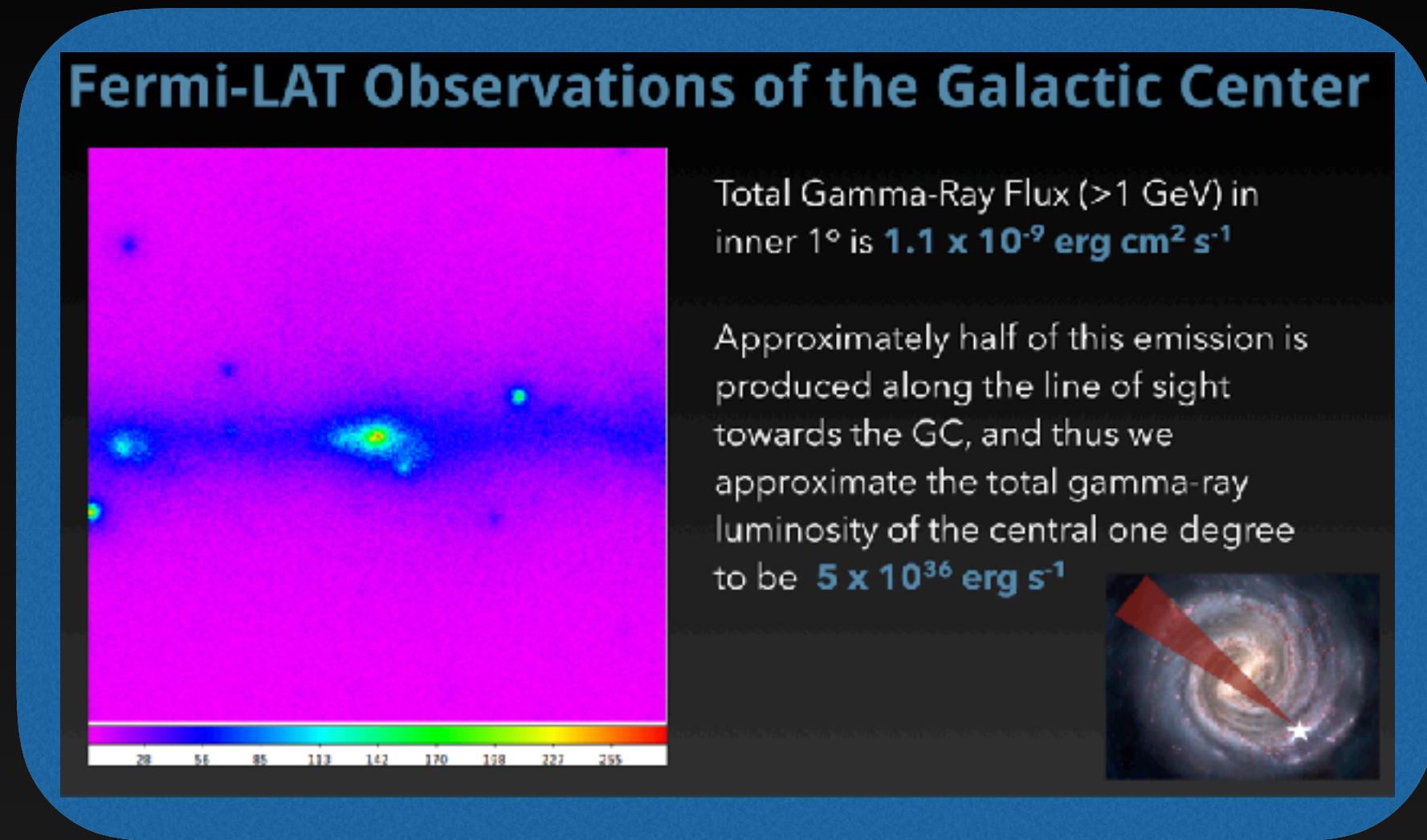
MSPs observed in the galactic field are fit by a population with a mean gamma-ray flux of  $3 \times 10^{34} \text{ erg s}^{-1}$ . (Hooper & Mohlabeng 2015)

Given the population of 129 MSPs among 124 globular clusters (with a total stellar mass  $\sim 5 \times 10^7 M_\odot$ ).

For the  $1 \times 10^9 M_\odot$  of stars formed in the inner degree of the Milky Way, we get:

$$7.7 \times 10^{37} \text{ erg s}^{-1} \quad \checkmark$$

# Understanding the Gamma-Ray Source with Energetics



## Sgr A\*

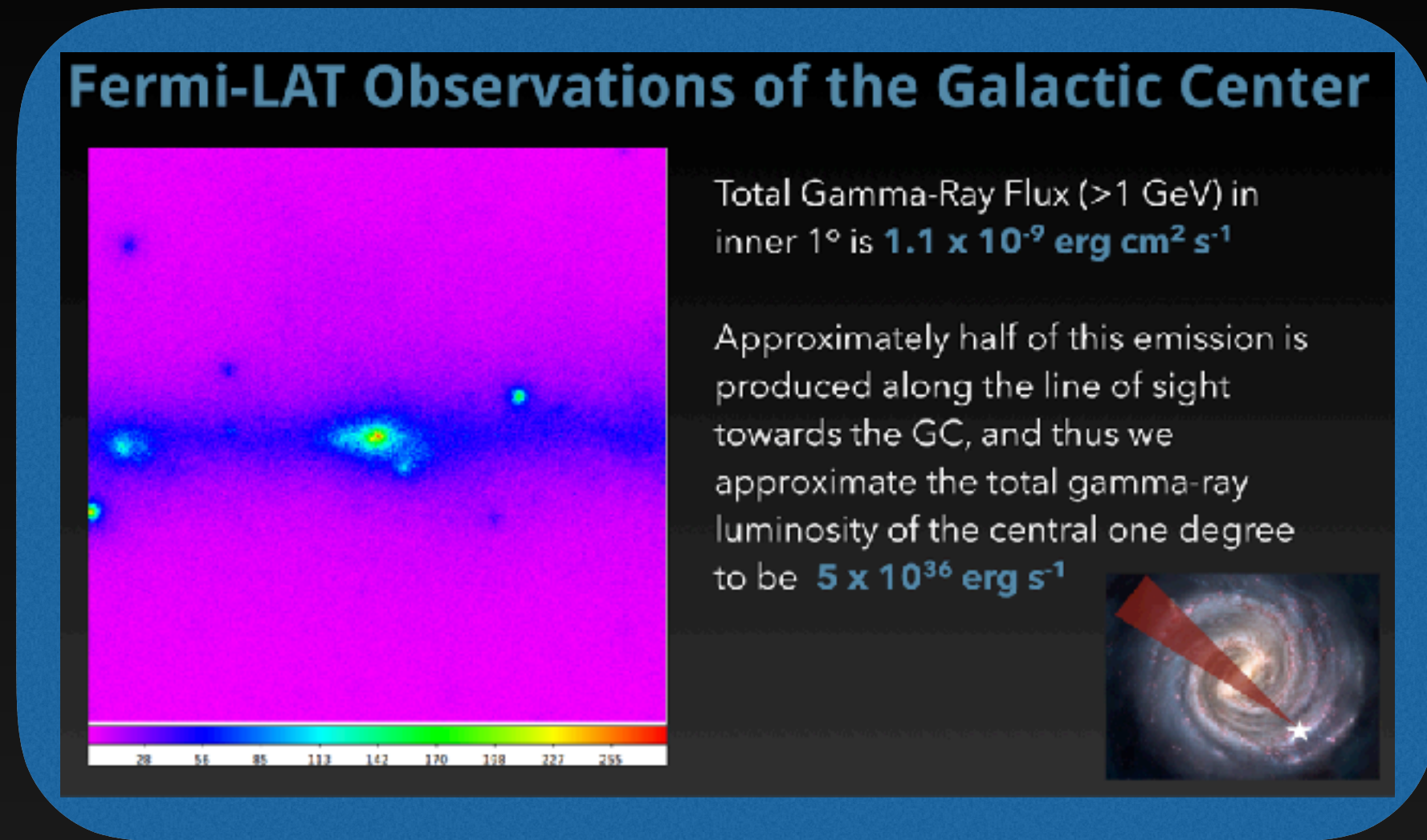
A tidal disruption event releases  $\sim 10^{45} \text{ erg s}^{-1}$  for a period of  $\sim 0.2 \text{ yr}$ .

Sgr A\* is expected to produce a tidal disruption event every  $\sim 10^5 \text{ yr}$ , producing a time-averaged energy output of  $2 \times 10^{39} \text{ erg s}^{-1}$ .

If these CRs are leptonic, and the electrons are trapped in a region with a  $40 \text{ eV cm}^{-3}$  ISRF and a  $200 \mu\text{G}$  B-field the gamma-ray flux from inverse Compton scattering is:

$$7.0 \times 10^{37} \text{ erg s}^{-1} \quad \checkmark$$

# Understanding the Gamma-Ray Source with Energetics



## Dark Matter

For a 35 GeV dark matter particle annihilating at the thermal cross-section to  $bb$ , and a slightly adiabatically contracted  $r^{-1.35}$  density profile.

The dark matter annihilation rate is  $8.6 \times 10^{38} \text{ ann s}^{-1}$ , which produces a gamma-ray flux of:

$$6.9 \times 10^{36} \text{ erg s}^{-1} \quad \checkmark$$

Theorist Conclusion #1:  
Every Model is Correct

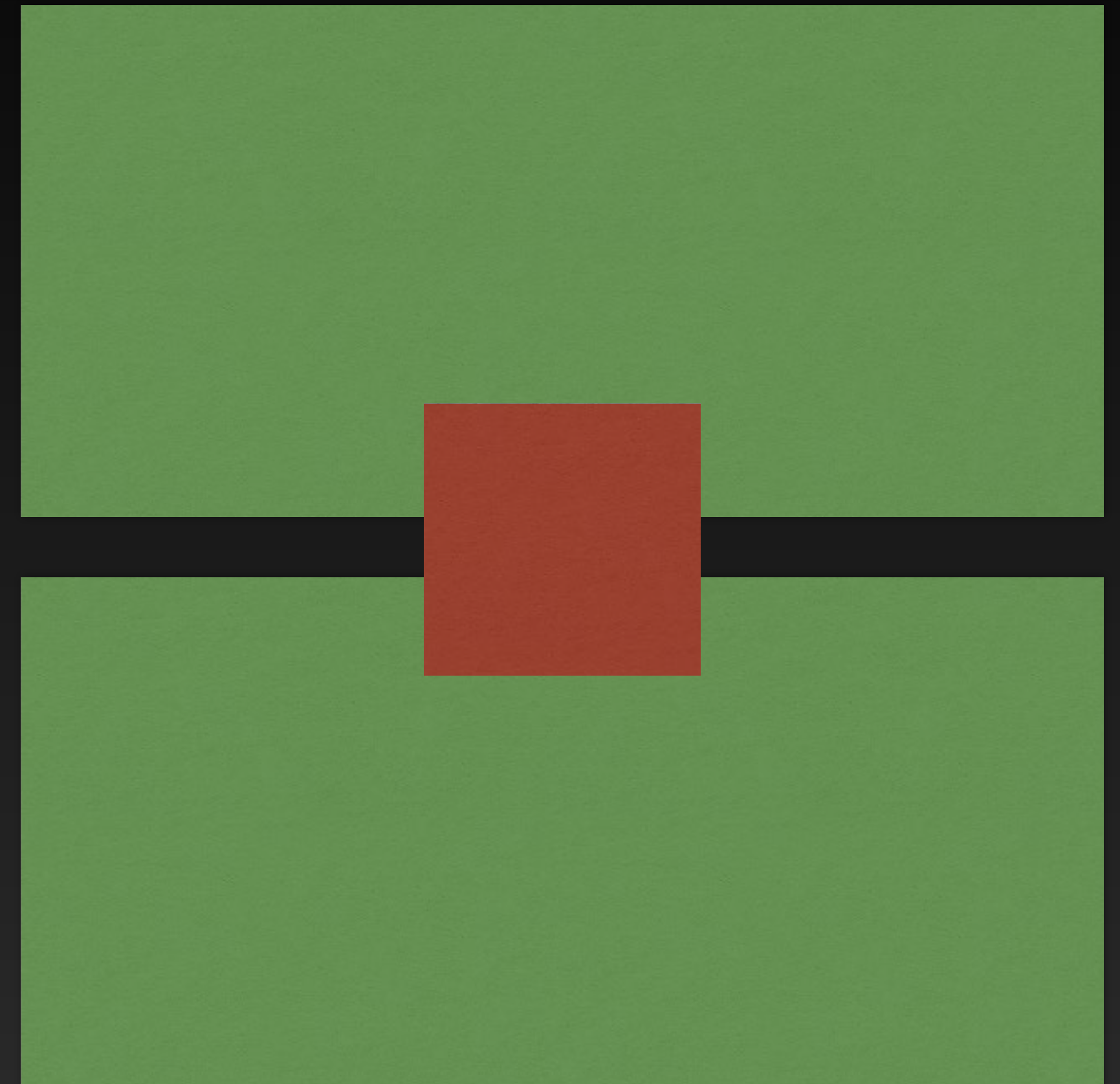
Theorist Conclusion #2:  
More Information is Needed

# The Morphology of the Signal

**INNER GALAXY**  
**GALACTIC CENTER**

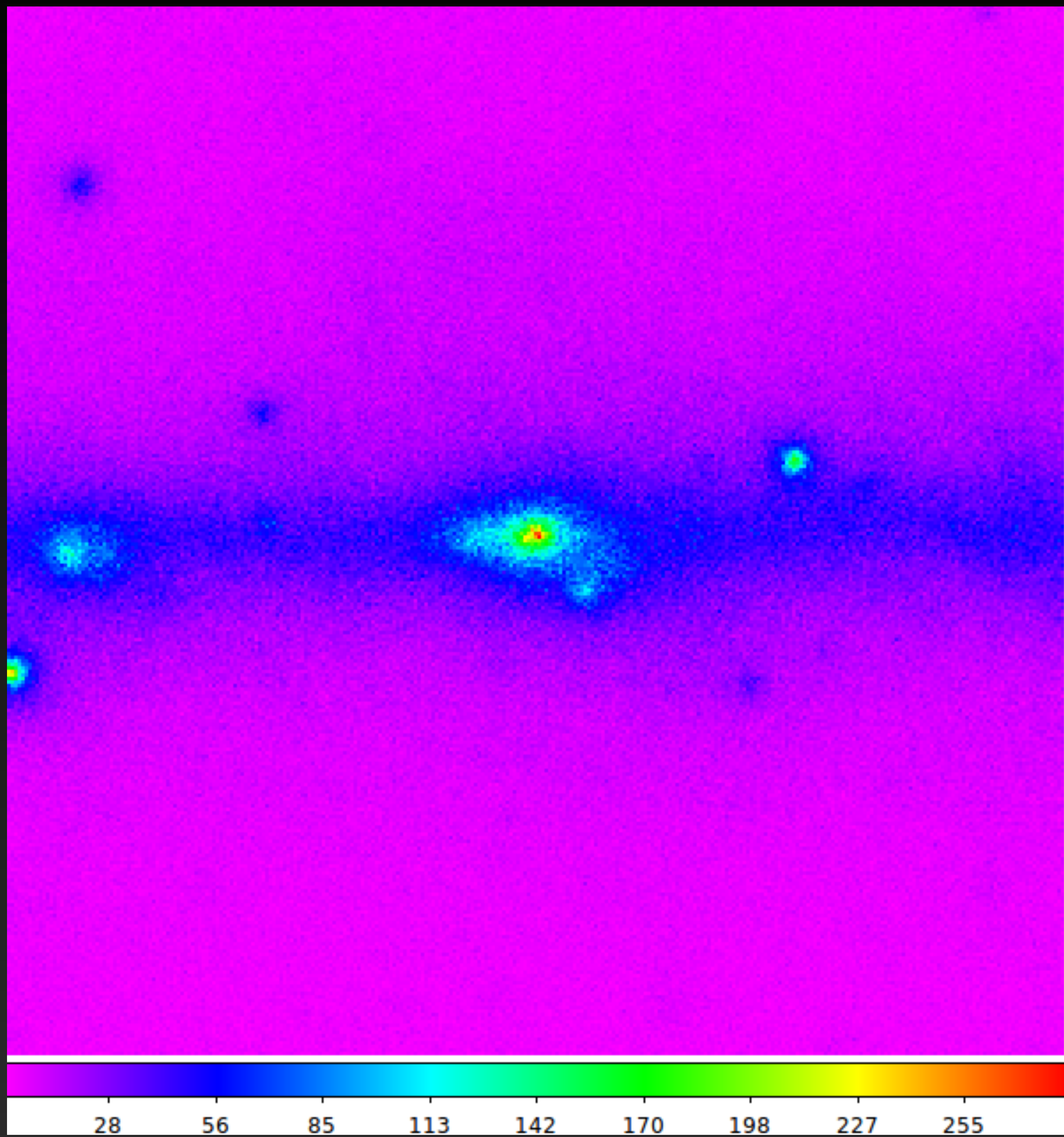
- Mask galactic plane (e.g.  $|b| > 1^\circ$ ), and consider  $40^\circ \times 40^\circ$  box
- Bright point sources masked at  $2^\circ$
- Background systematics controlled

- Box around the GC ( $10^\circ \times 10^\circ$ )
- Include and model all point sources
- Bright Signal



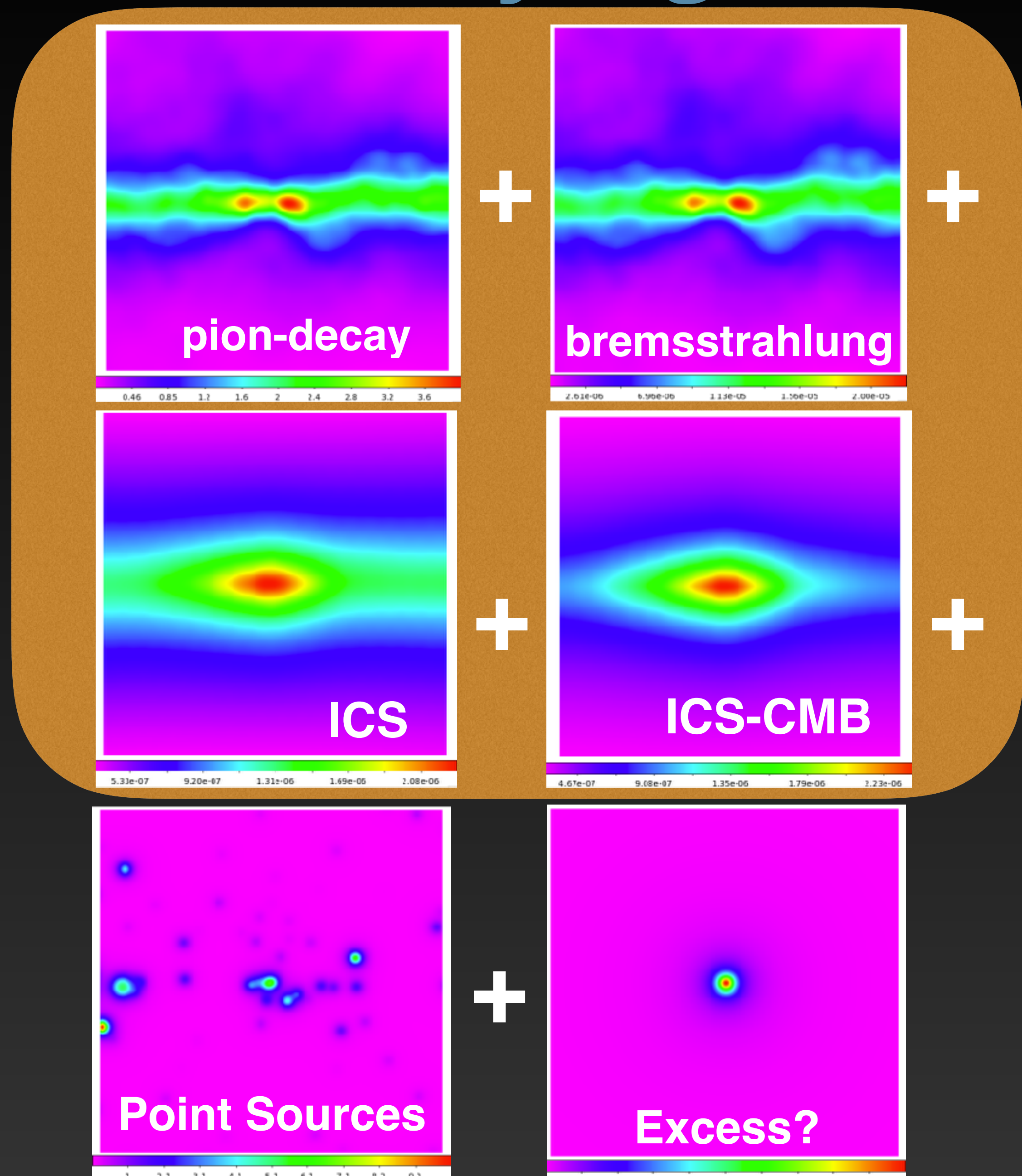
- **In Both Cases:** Use likelihood analysis to calculate the spectrum and intensity of each source.

# The Morphology of the Gamma-Ray Signal



Data  
> 1 GeV  
front-converting events  
10° x 10° ROI

=



# Fitting the Background Templates

In most recent analyses, fits are calculated independently in numerous energy bins spanning from  $\sim 100$  MeV -- 100 GeV:

$$\begin{aligned} \Phi_{\text{model}}(\ell, b, E) = & K_{\pi_0} \Phi_{\pi_0}(\ell, b, E) + K_{\text{brem}} \Phi_{\text{brem}}(\ell, b, E) + K_{\text{ICS}} \Phi_{\text{ICS}}(\ell, b, E) + \\ & + K_{\text{ICS,CMB}} \Phi_{\text{ICS,CMB}}(\ell, b, E) + K_{\text{EXS}} \Phi_{\text{EXS}}(\ell, b, E) + \sum_{\forall \text{PS}} K_{\text{PS},i} \Phi_{\text{PS},i}(\ell, b, E) \end{aligned}$$

$$\Phi_i(E) = K_i(E) \int_{\ell} \int_b \Phi_i(\ell, b, E) db d\ell$$

# Untuned Background Templates

## Option 1: Gas Model

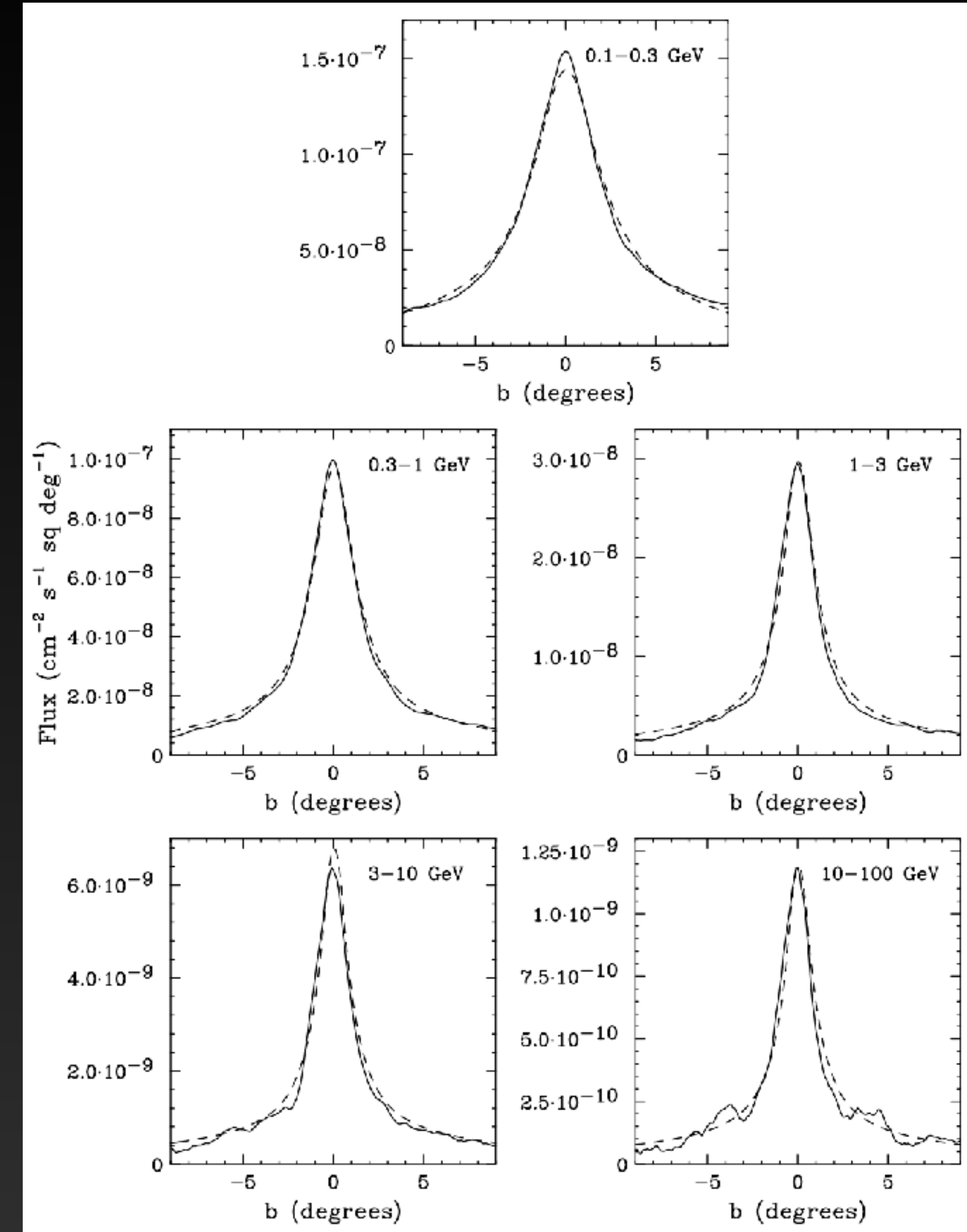
Use a simple model for the integrated gas density over the line of sight.

Completely independent of the gamma-ray data.

Hadronic interactions are the primary source of astrophysical gamma-rays

No sensitivity to a radially variable cosmic-ray density

Extremely rudimentary analytic model.



# Untuned Background Templates

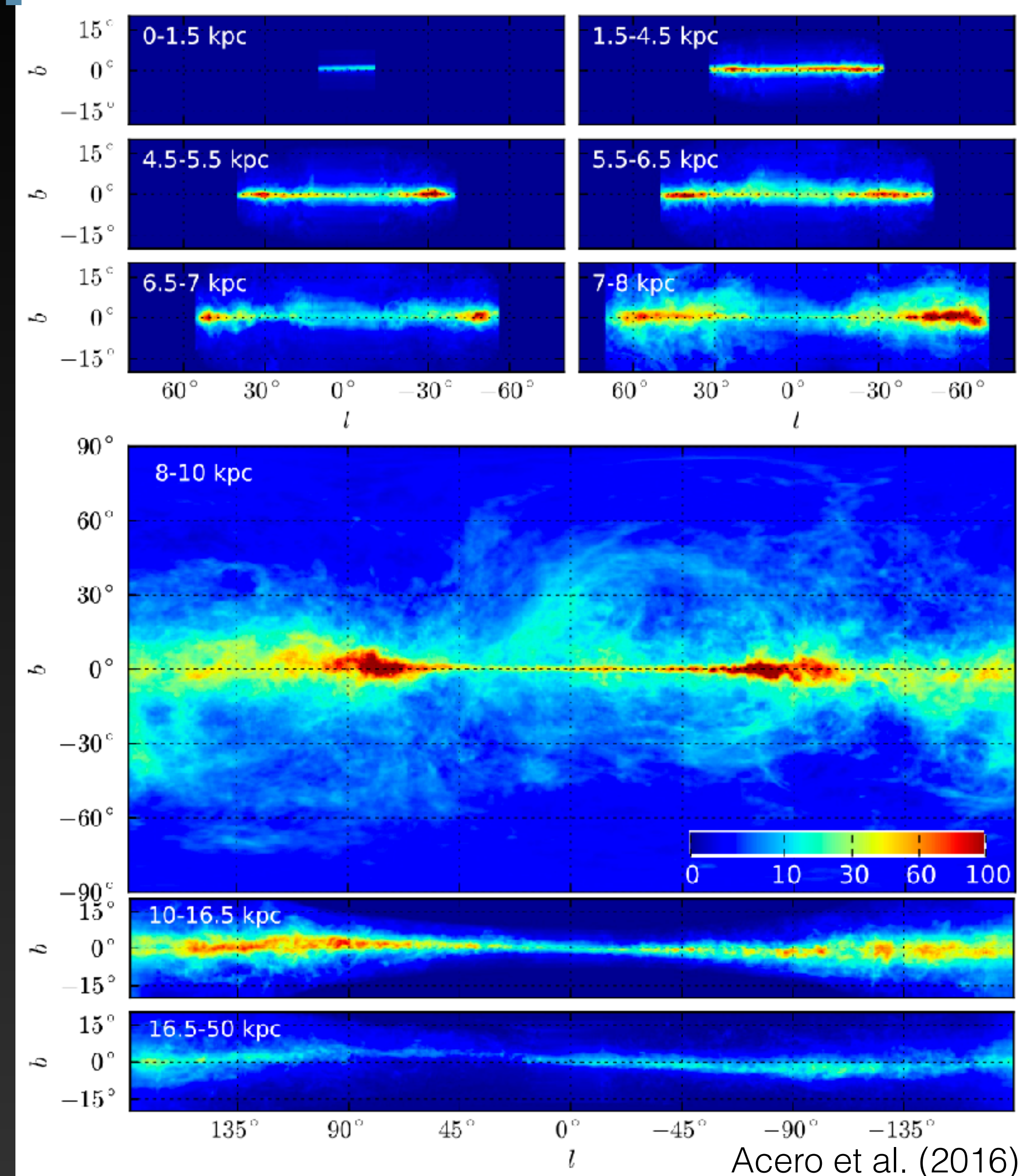
## Option 2: Fermi Diffuse Model

Template fit to the full sky, normalizing observed gas maps in cylindrical rings.

Diffuse model has been fit to the full sky, providing a nuanced statistical fit to the data.

Black box – Can not independently vary emission mechanisms in the fit.

Not calibrated for the Galactic center.



# Untuned Background Templates

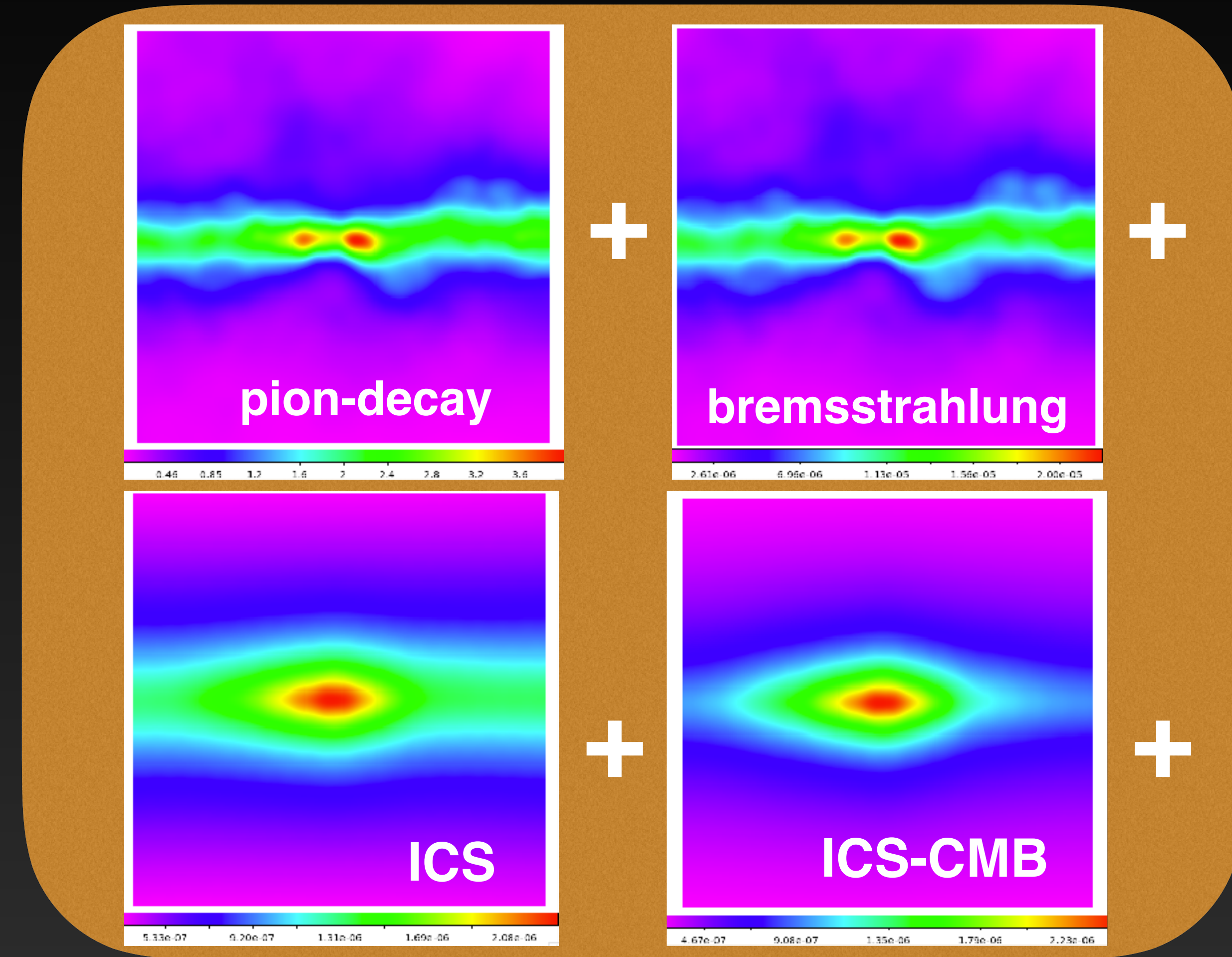
## Option 3: Galprop

Utilize computational tools to produce a physical model of the Galactic center, and compare to data.

Can easily customize model for the Galactic center.

Not clear what the physical parameters of Galactic center diffusion are.

Grids are necessarily coarse compared to data.

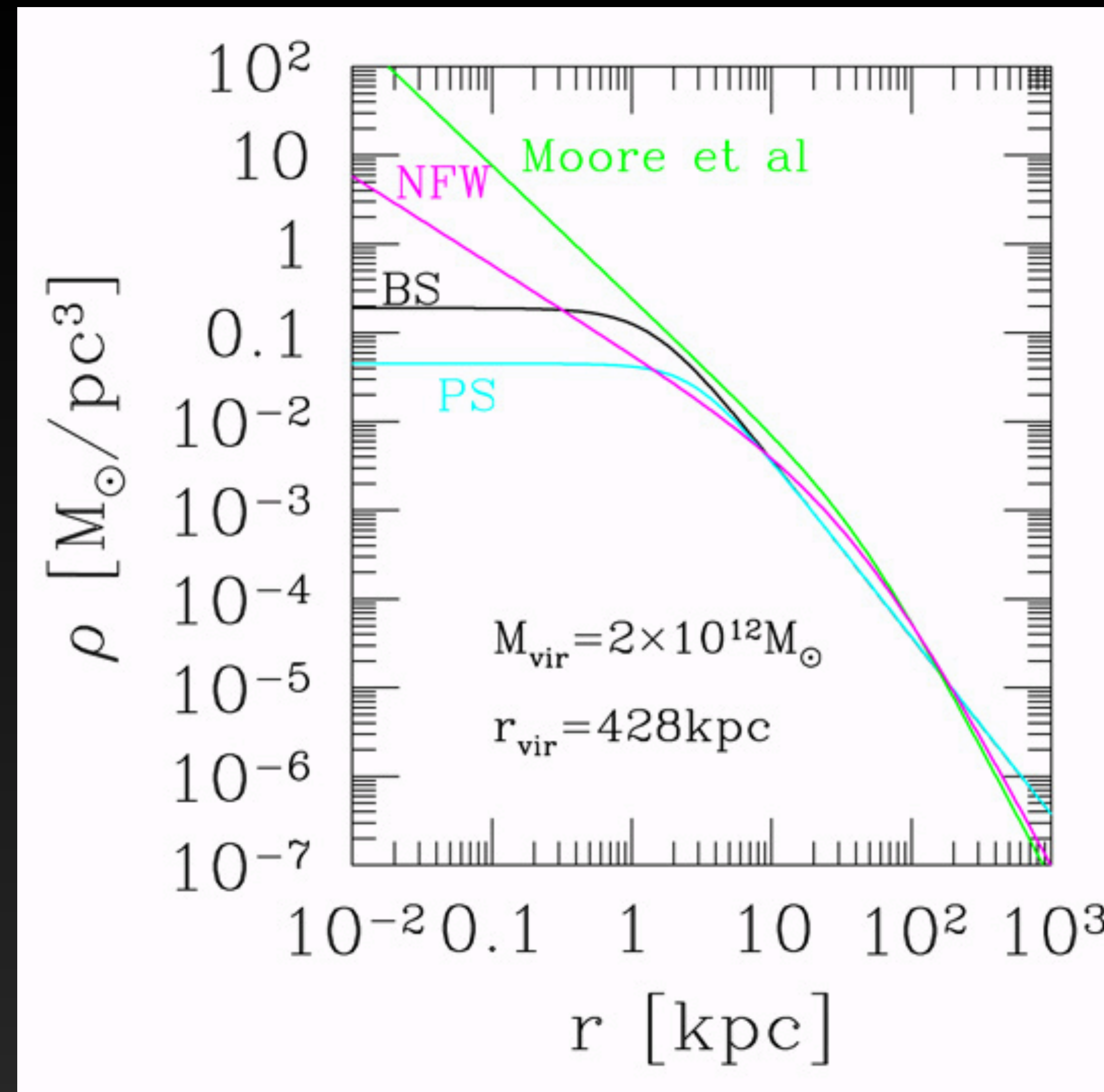


# Picking an Excess Model

$$\rho_{\text{NFW}} = \left( \frac{r}{r_s} \right)^{-\gamma} \left( 1 + \frac{r}{r_s} \right)^{-3+\gamma}$$

We employ an analytical model, known as the “generalized NFW Profile” which provides a fit to the observed dark matter density distribution.

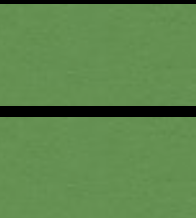
In the standard NFW scenario,  $\gamma = 1$



Brook & Di Cintio (2015)

Navarro, Frenk, White (1996)  
Springel et al. (2008, 0809.0898)

# Observational Results

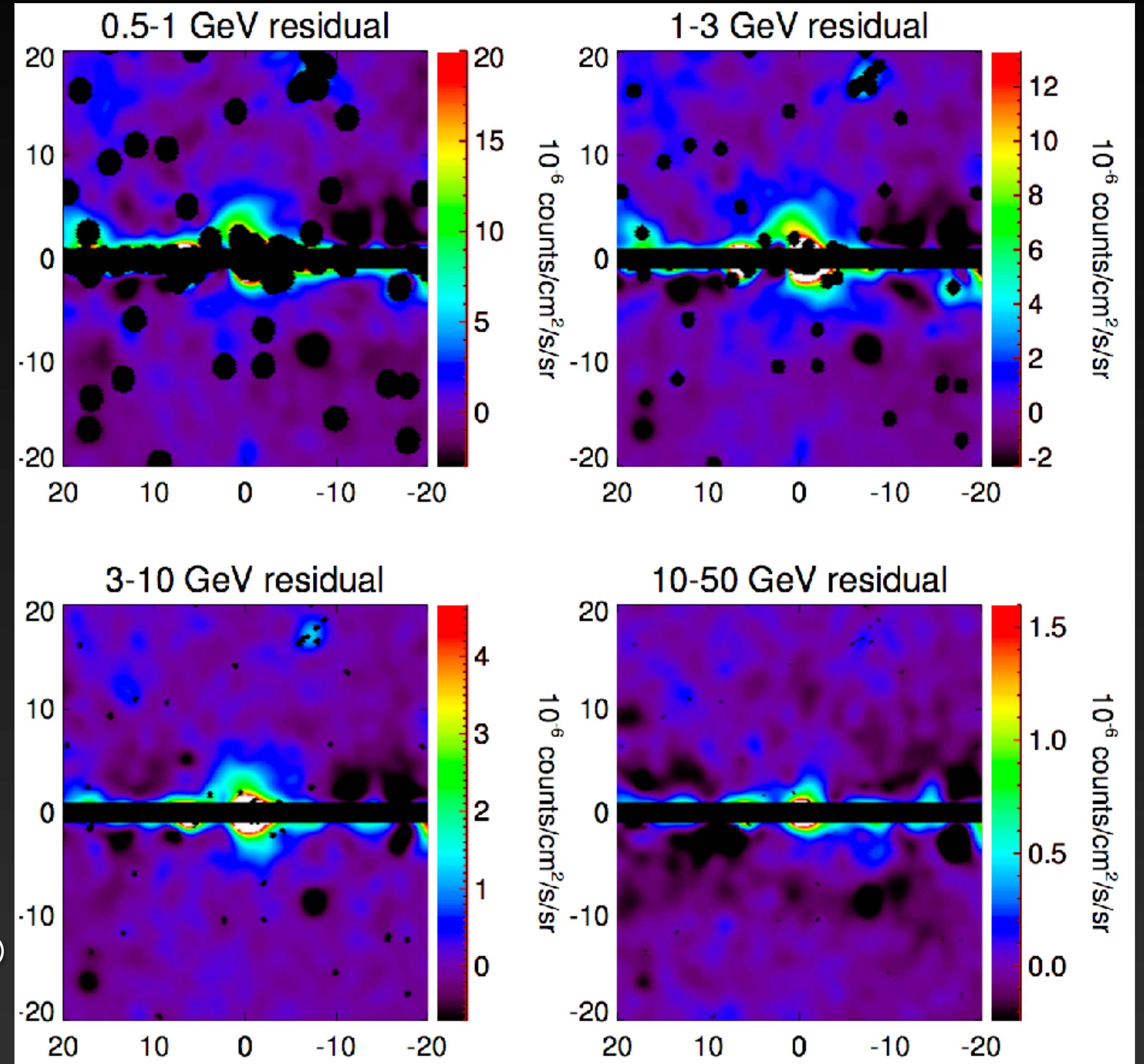


IG

Daylan et al. (2014)

Utilizing different models for removing astrophysical and point source foregrounds. Multiple studies have consistently observed a gamma-ray excess.

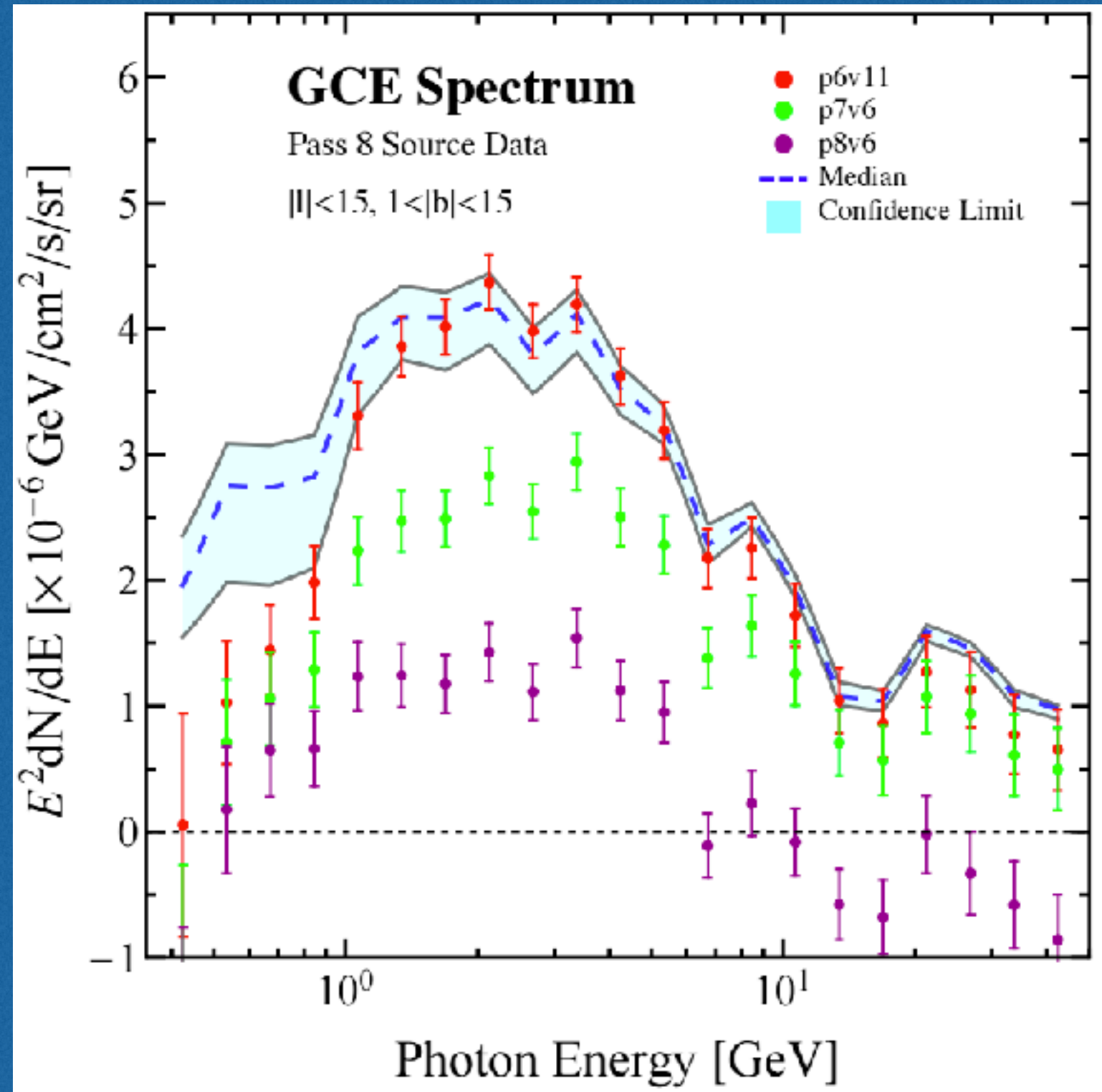
The statistical significance of the excess is  $\sim 30-60\sigma$ , depending on the ROI and photon selection employed.



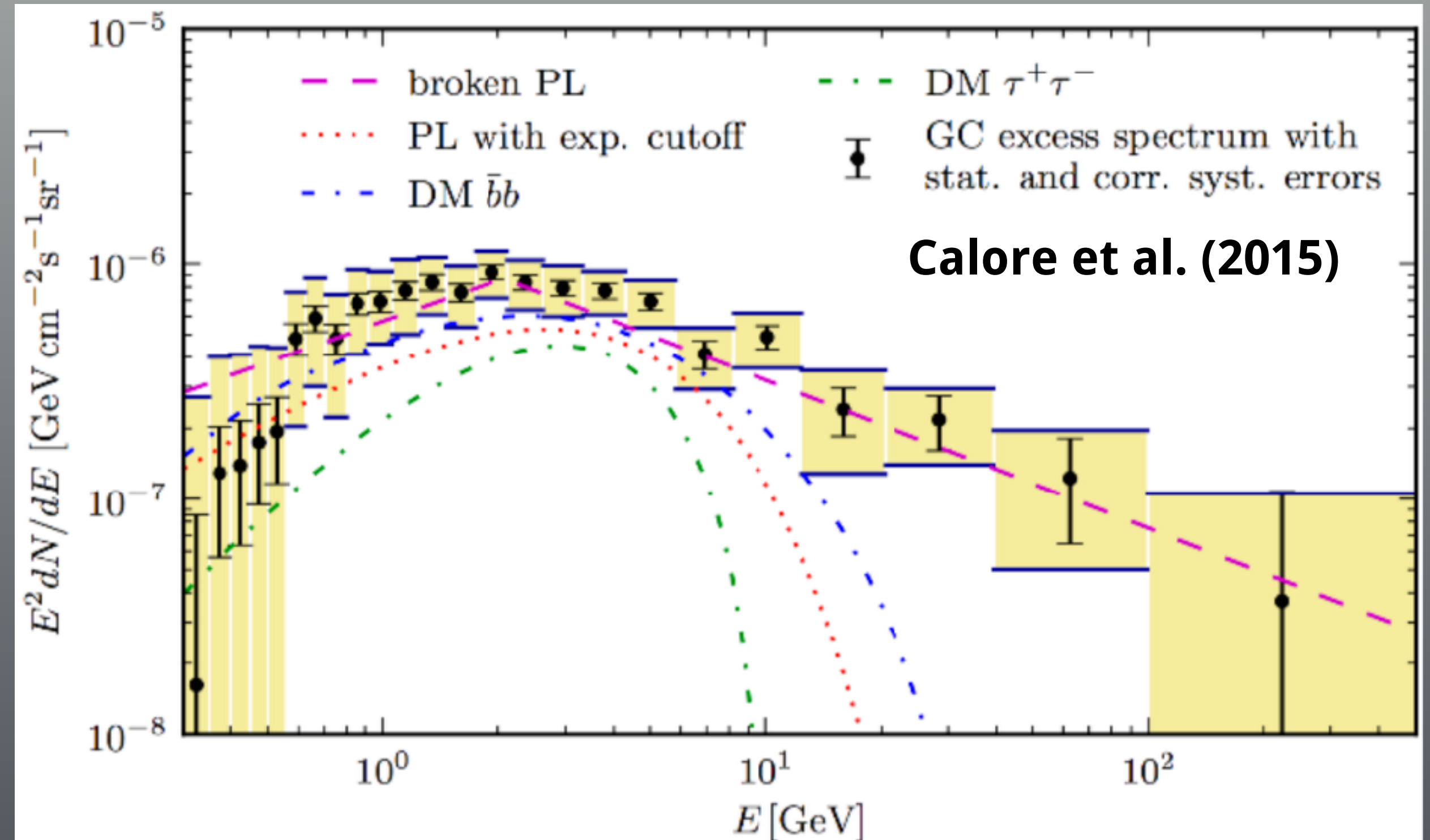
|  |  |
|--|--|
| Goodenough & Hooper (2009, 0910.2998)    | Abazajian et al. (2014, 1410.6168)             |
| Hooper & Goodenough (2010, 1010.2752)    | Bartels et al. (2015, 1506.05104)              |
| Hooper & Linden (2011, 1110.0006)        | Lee et al. (2015, 1506.05124 )                 |
| Abazajian & Kaplinghat (2012, 1207.6047) | Gaggero et al. (2015, 1507.06129)              |
| Gordon & Macias (2013, 1306.5725)        | Carlson et al. (2015, 1510.04698)              |
| Gordon & Macias (2013, 1312.6671)        | The Fermi-LAT Collaboration (2015, 1511.02938) |
| Abazajian et al. (2014, 1402.4090)       | Yang & Aharonian (2016, 1602.06764)            |
| Daylan et al. (2014, 1402.6703)          | Carlson et al. (2016, 1603.06584)              |
| Calore et al. (2014, 1409.0042)          | Linden et al. (2016, 1604.01026)               |
|  | Horiuchi et al. (2016, 1604.01402)             |

# Observational Results

## Fermi Diffuse Models



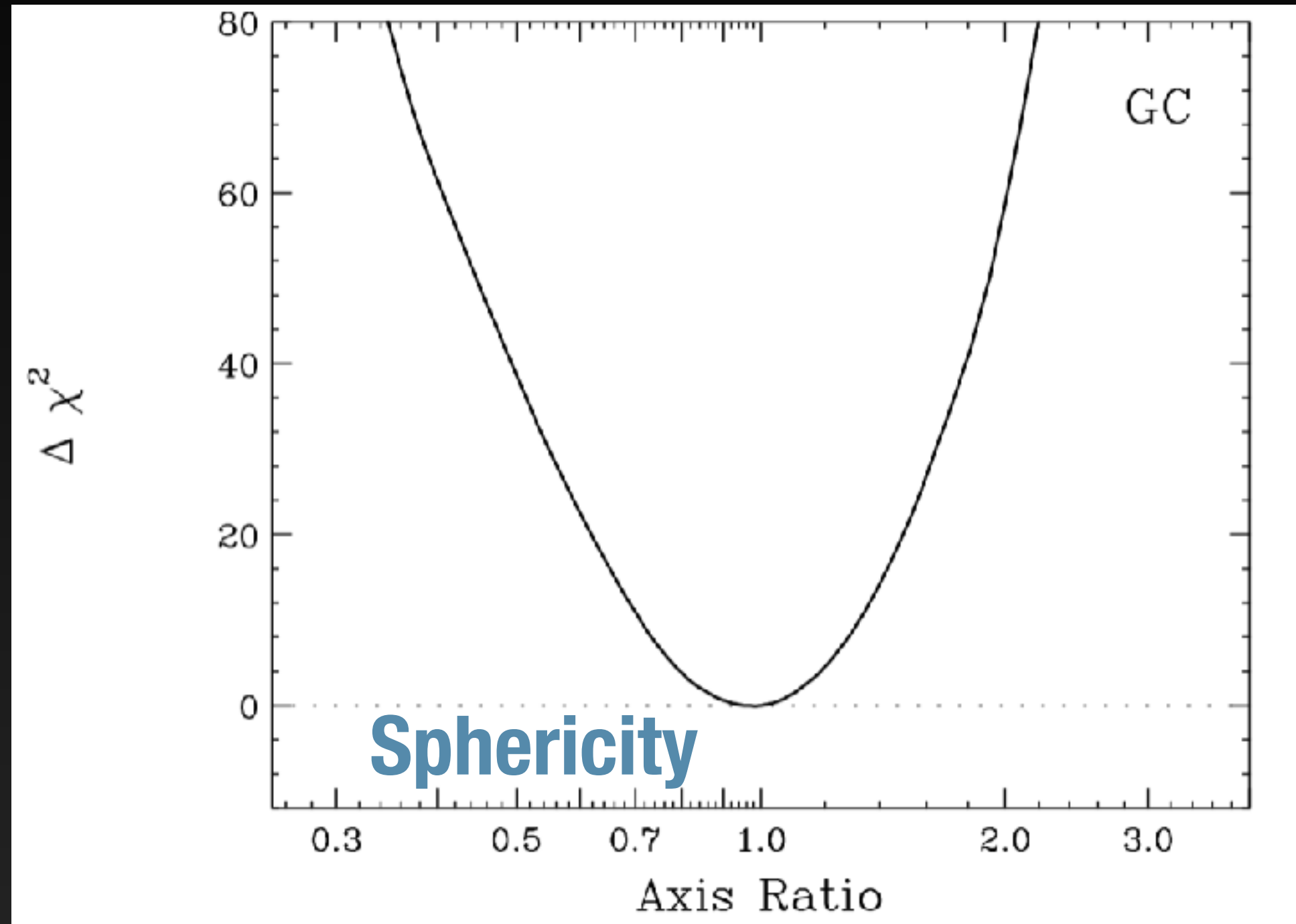
## Galprop Models



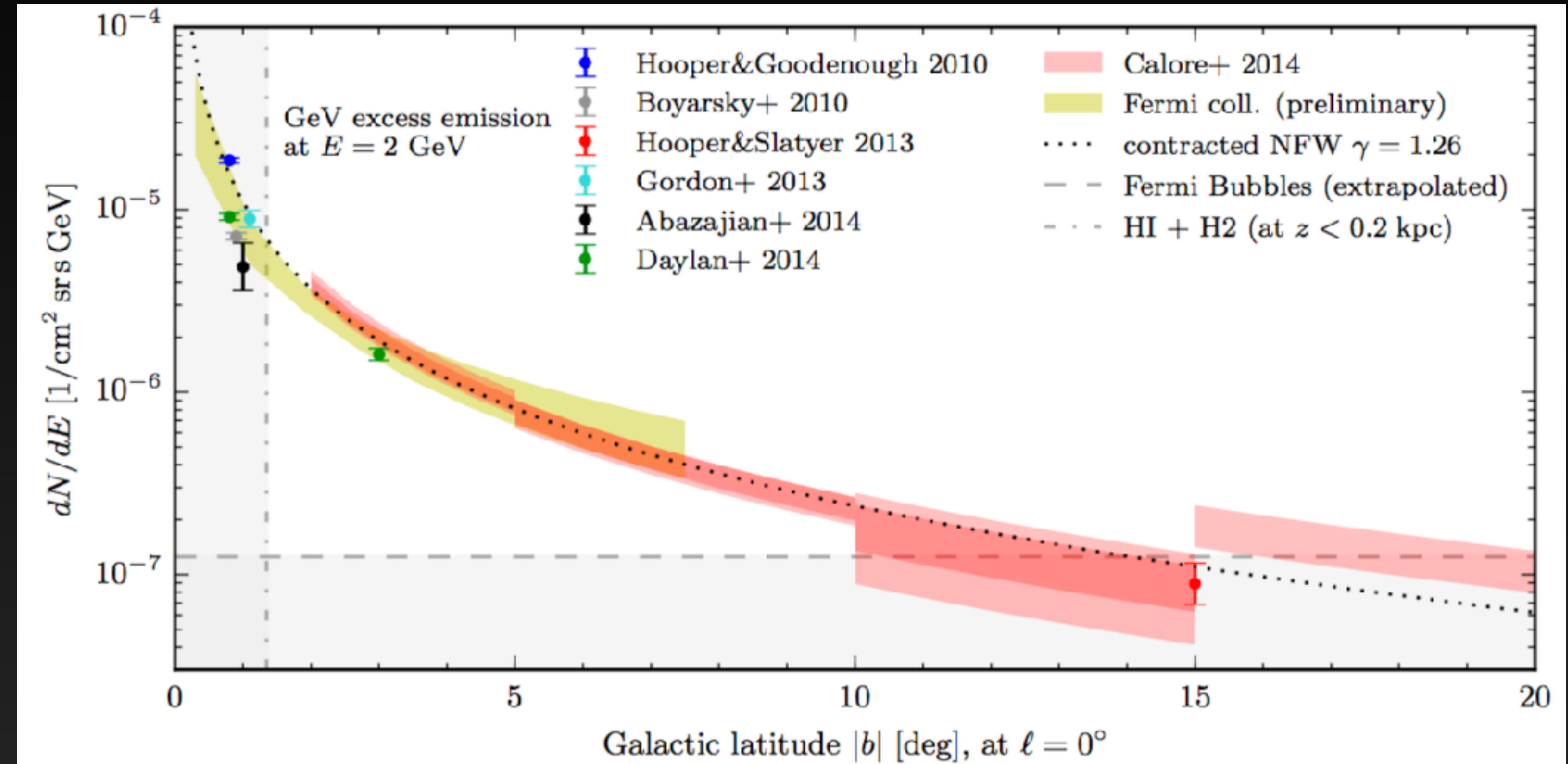
The excess has an unusual spectrum - highly peaked at an energy of  $\sim 2$  GeV.

This spectrum is significantly harder than expected from astrophysical diffuse emission.

# Observational Results



Daylan et al. (2014)



Calore et al. (2014b)

The GeV excess spherically symmetric, and is statistically significant from  $0.1^\circ - 10^\circ$  from the Galactic Center.

# Observational Results

These are the three resilient features of the GeV Excess:

- 1.) Hard Gamma-Ray Spectrum peaking at  $\sim 2$  GeV
- 2.) Spherically Symmetric Emission Morphology
- 3.) Extension to  $>10^\circ$  from the GC.

Upcoming Talks will Model this with:

- 1.) Dark Matter annihilation
- 2.) Millisecond Pulsars
- 3.) Leptonic Outbursts from Sgr A\*

# An Excess Compared to What?

In most recent analyses, fits are calculated independently in numerous energy bins spanning from  $\sim 100$  MeV -- 100 GeV:

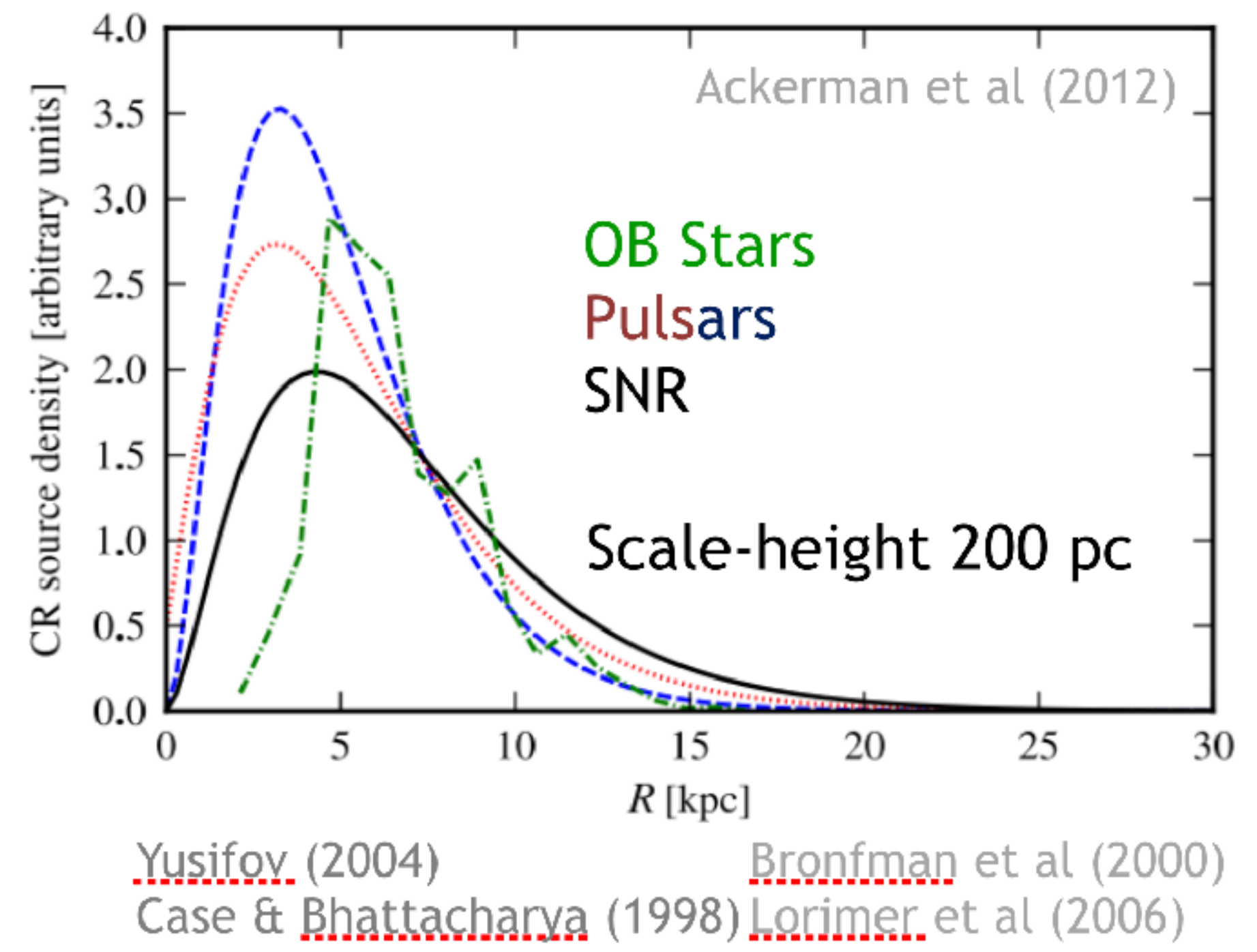
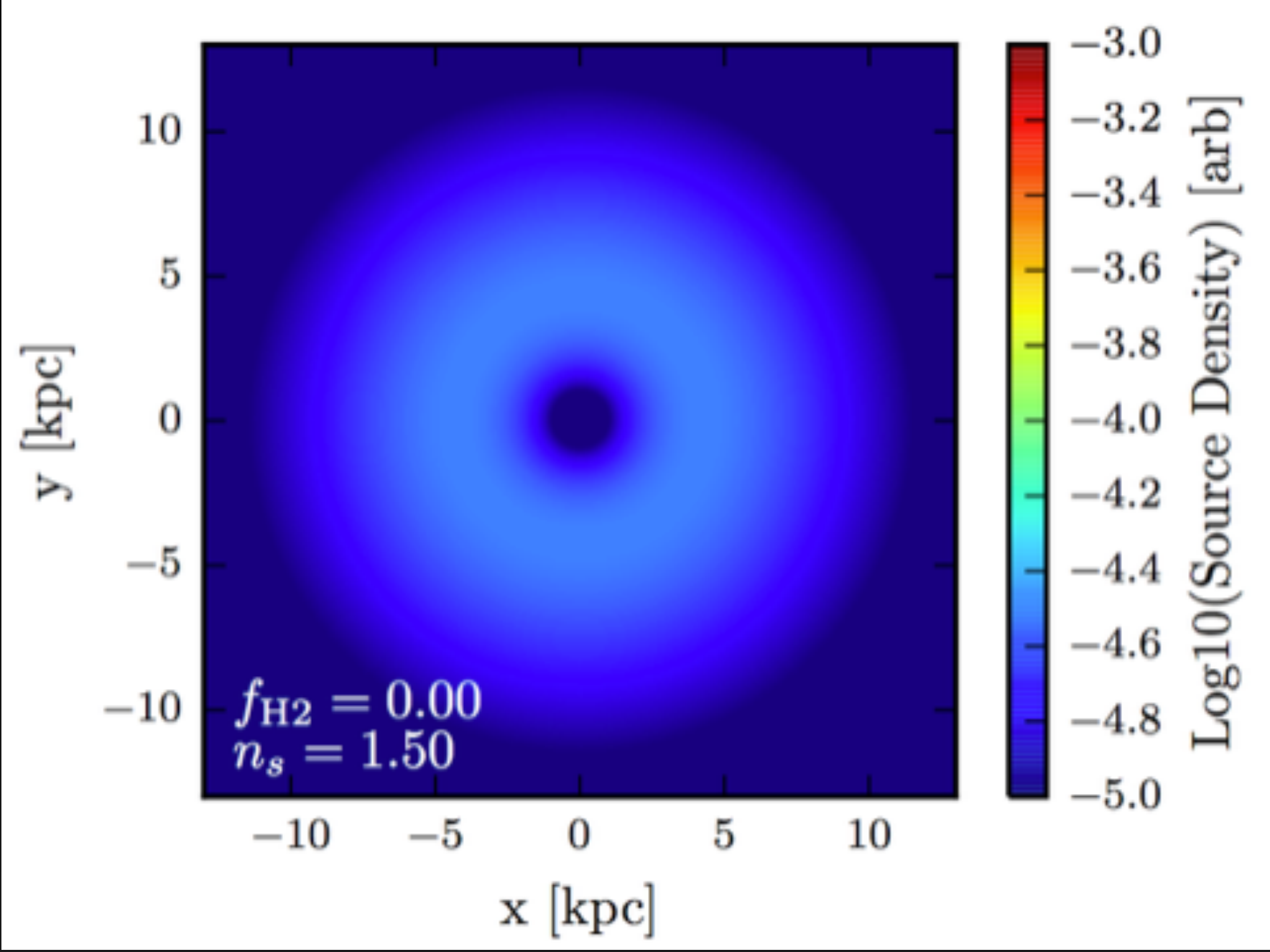
$$\begin{aligned} \Phi_{\text{model}}(\ell, b, E) = & K_{\pi_0} \Phi_{\pi_0}(\ell, b, E) + K_{\text{brem}} \Phi_{\text{brem}}(\ell, b, E) + K_{\text{ICS}} \Phi_{\text{ICS}}(\ell, b, E) + \\ & + K_{\text{ICS,CMB}} \Phi_{\text{ICS,CMB}}(\ell, b, E) + K_{\text{EXS}} \Phi_{\text{EXS}}(\ell, b, E) + \sum_{\forall \text{PS}} K_{\text{PS},i} \Phi_{\text{PS},i}(\ell, b, E) \end{aligned}$$

$$\Phi_i(E) = K_i(E) \int_{\ell} \int_b \Phi_i(\ell, b, E) db d\ell$$

# An Excess Compared to What?

Cosmic-Ray Propagation Codes (e.g. Galprop), generally utilize a cosmic-ray injection rate at the Galactic center that is identically 0.

These models were not produced to study the very center of the Galaxy!



Results from these cosmic-ray propagation codes are used in many analyses of the Galactic center region.

Carlson et al. (2016a, 2016b)  
1510.04698  
1603.06584

# The Solution

**Solution:** Add a new cosmic-ray injection morphology tracing the molecular gas density.

**Observationally Resilient:** Several tracers of molecular gas are sensitive to the galactic center region.

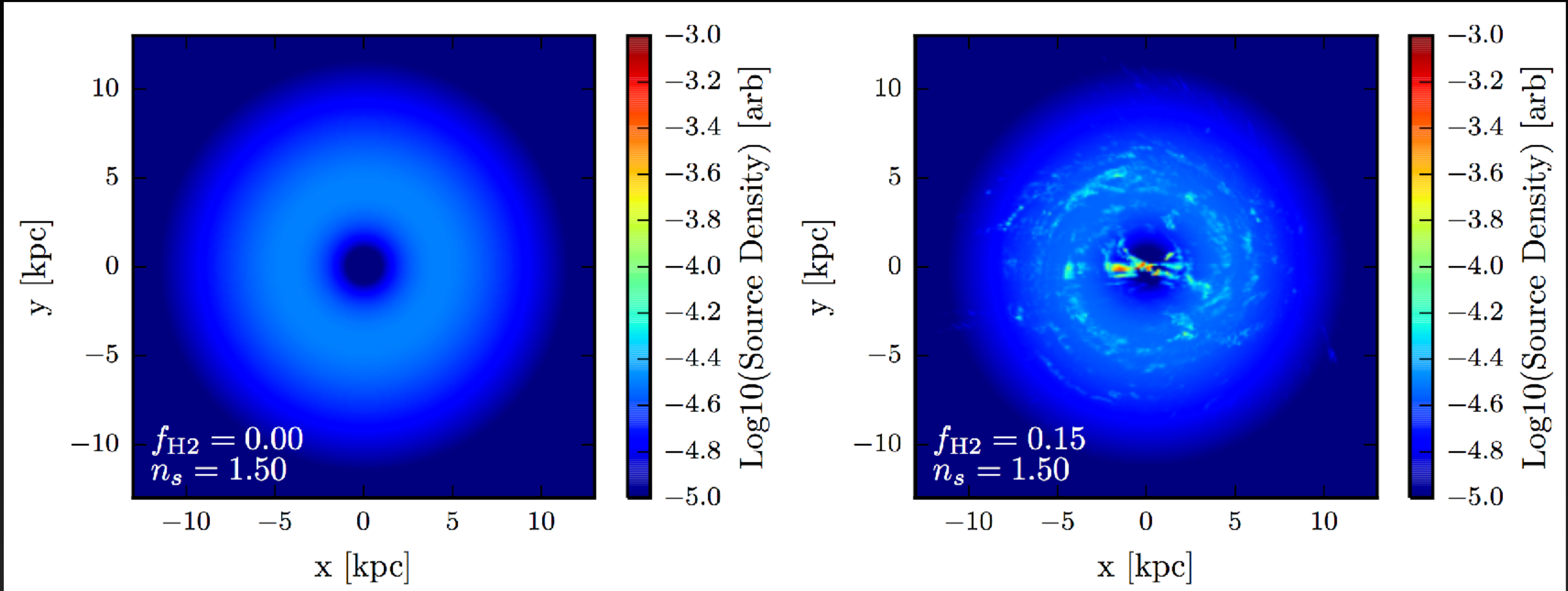
**Theoretically Motivated:** Molecular Gas is the seed of star formation, the Schmidt Law gives:

$$\Sigma_{\text{SFR}} \propto \Sigma_{\text{Gas}}^{1.4 \pm .15}$$

Specifically we inject a fraction of cosmic-rays ( $0 < f_{\text{H}_2} < 1$ ) following:

$$Q_{\text{CR}}(\vec{r}) \propto \begin{cases} 0 & \rho_{\text{H}_2} \leq \rho_s \\ \rho_{\text{H}_2}^{n_s} & \rho_{\text{H}_2} > \rho_s \end{cases}$$

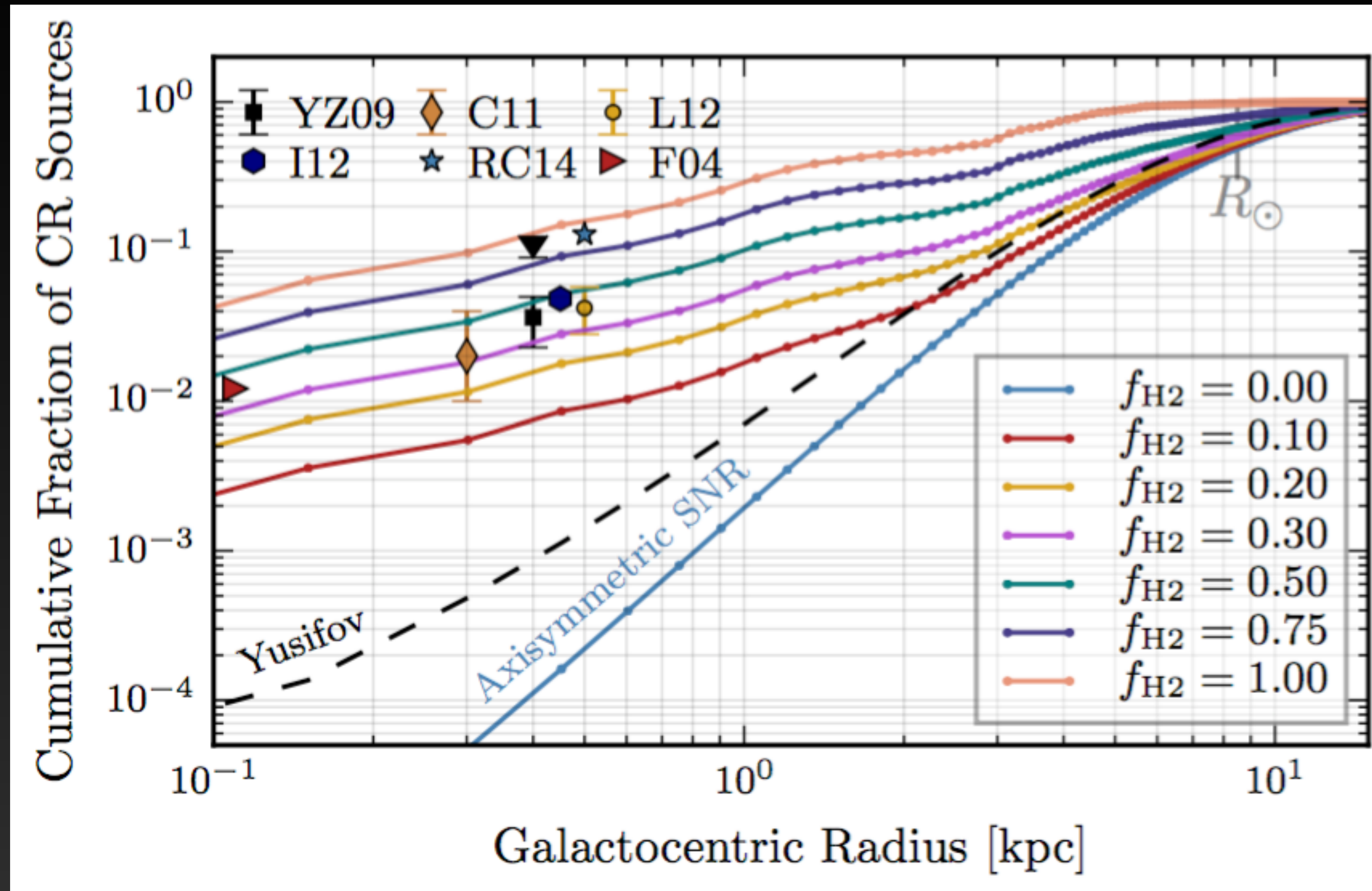
# The Solution



Two features leap out immediately:

- 1.) Spiral Arms
- 2.) A bright bar in the Galactic Center

# The Solution

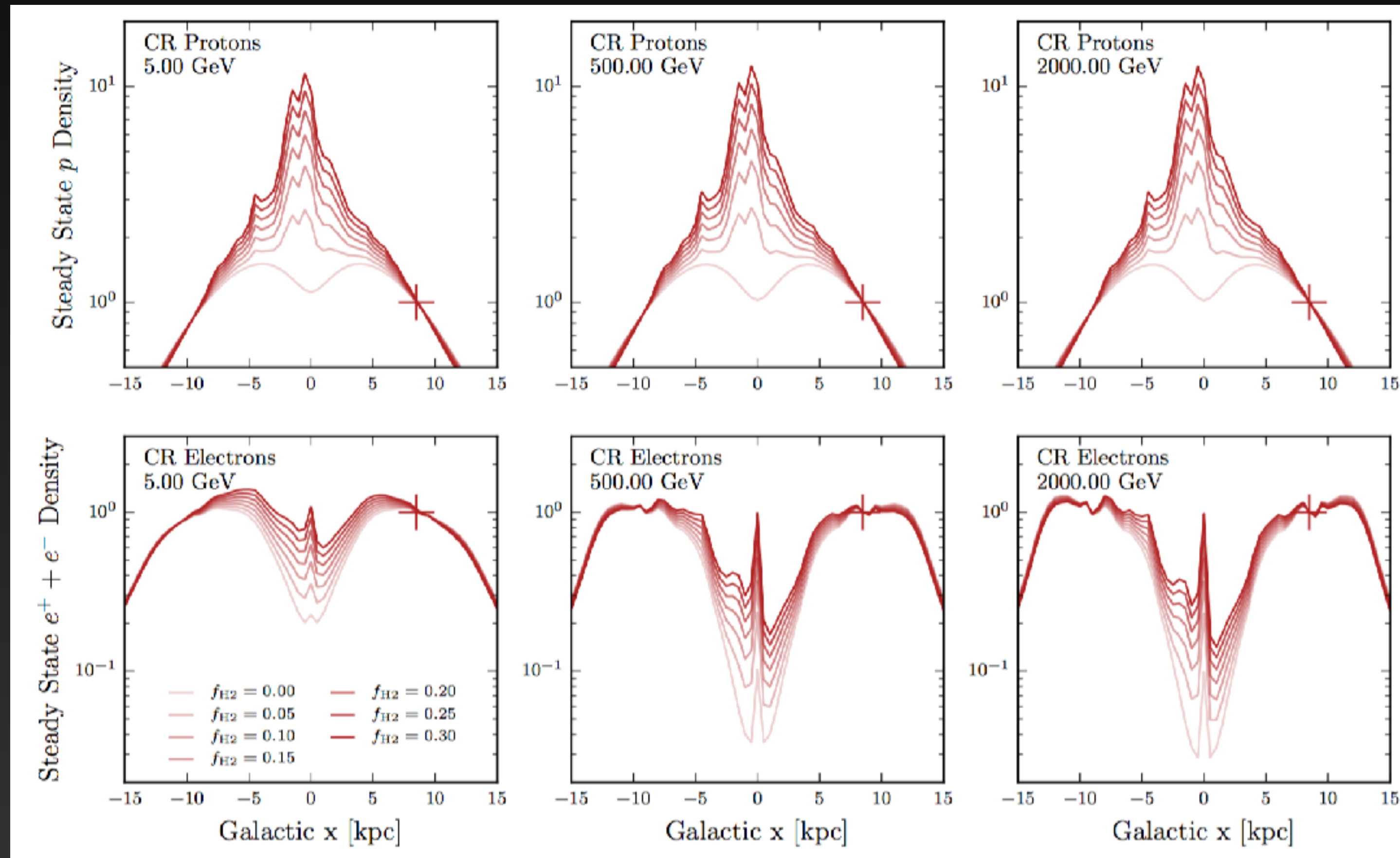


The cosmic-ray injection rate now matches observational constraints.

# Simulations!

Add the new cosmic-ray injection models into Galprop to produce a new steady-state cosmic-ray distribution.

| Parameter         | Units                              | Canonical            | Mod A                | Description   |
|-------------------|------------------------------------|----------------------|----------------------|---|
| $D_0$             | $\text{cm}^2 \text{s}^{-1}$        | $7.2 \times 10^{28}$ | $5.0 \times 10^{28}$ | Diffusion constant at $\mathcal{R} = 4 \text{ GV}$                |
| $\delta$          | –                                  | 0.33                 | 0.33                 | Index of diffusion constant energy dependence                     |
| $z_{\text{halo}}$ | kpc                                | 3                    | 4                    | Half-height of diffusion halo                                     |
| $R_{\text{halo}}$ | kpc                                | 20                   | 20                   | Radius diffusion halo   |
| $v_a$             | $\text{km s}^{-1}$                 | 35                   | 32.7                 | Alfvén velocity   |
| $dv/dz$           | $\text{km s}^{-1} \text{kpc}^{-1}$ | 0                    | 50                   | Vertical convection gradient                                      |
| $\alpha_p$        | –                                  | 1.88 (2.39)          | 1.88 (2.47)          | $p$ injection index below (above) $\mathcal{R} = 11.5 \text{ GV}$ |
| $\alpha_e$        | –                                  | 1.6 (2.42)           | 1.6 (2.43)           | $e^-$ injection index below (above) $\mathcal{R} = 2 \text{ GV}$  |
| Source            | –                                  | SNR                  | SNR                  | Distribution of $(1 - f_{\text{H}2})$ primary sources*            |
| $f_{\text{H}2}$   | –                                  | .20                  | N/A                  | Fraction of sources in star formation model*                      |
| $n_s$             | –                                  | 1.5                  | N/A                  | Schmidt Index*  |
| $\rho_c$          | $\text{cm}^{-3}$                   | 0.1                  | N/A                  | Critical $\text{H}_2$ density for star formation*                 |
| $B_0$             | $\mu\text{G}$                      | 7.2                  | 9.0                  | Local ( $r = R_\odot$ ) magnetic field strength                   |
| $r_B, z_B$        | kpc                                | 5, 1                 | 5, 2                 | Scaling radius and height for magnetic field                      |
| ISRF              | –                                  | (1.0,.86,.86)        | (1.0,.86,.86)        | Relative CMB, Optical, FIR density                                |
| $dx, dy$          | kpc                                | 0.5, 0.5             | 1 (2D)               | $x, y$ (3D) or radial (2D) cosmic-ray grid spacing                |
| $dz$              | kpc                                | 0.125                | .1                   | $z$ -axis cosmic-ray grid spacing                                 |



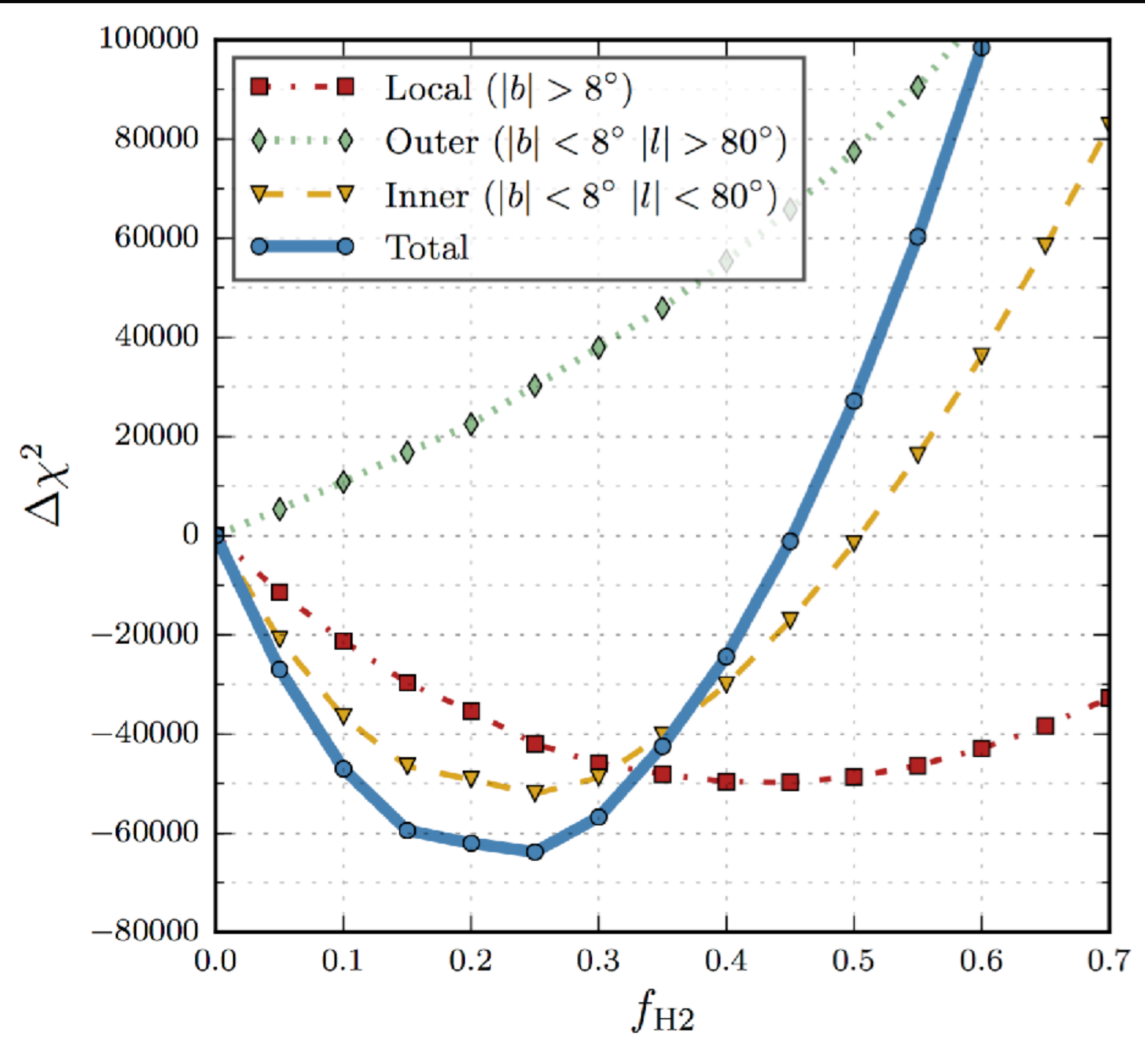
New cosmic ray *injection* distribution produces a sharply peaked *steady state* cosmic-ray density

# A Better fit to the Gamma-Ray Sky

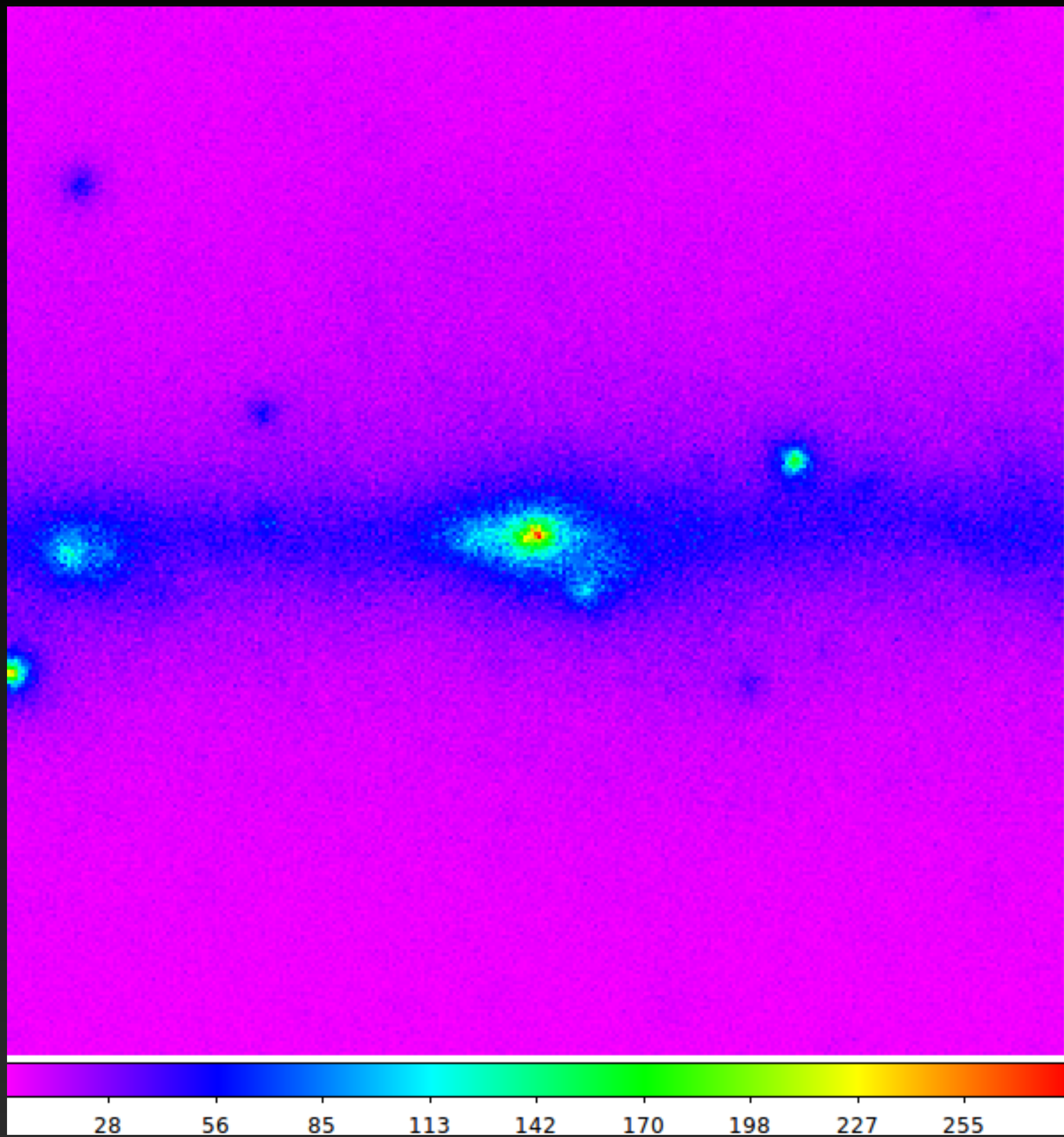
1.) Adding a cosmic-ray injection component tracing  $f_{\text{H}_2}$  improves the full-sky fit to the gamma-ray data.

2.) The best fit value over the full sky is  $f_{\text{H}_2} = 0.25$

3.) Technique will become more powerful with the introduction of 3D gas and dust maps in the near future.

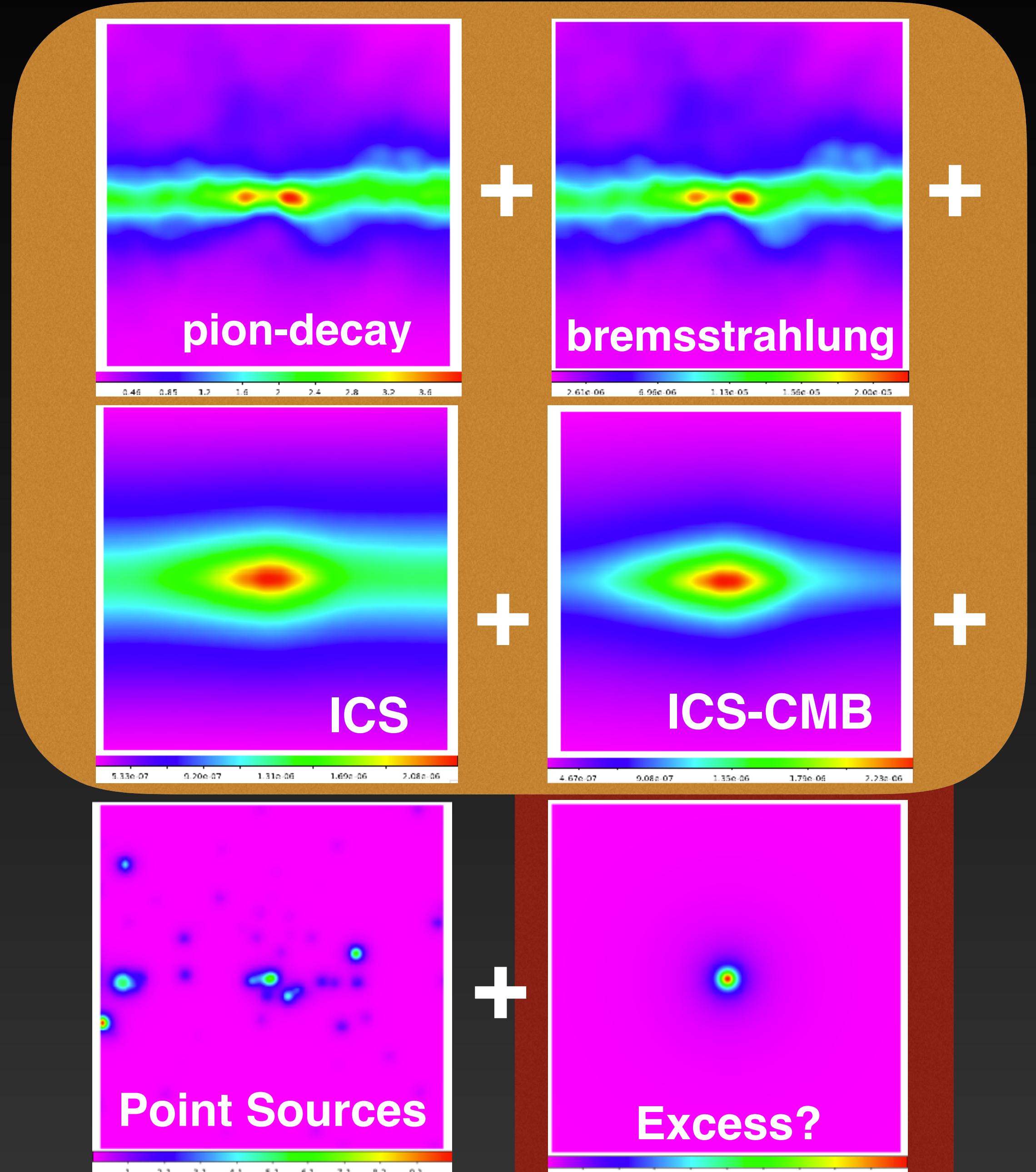


# Application to the Galactic Center

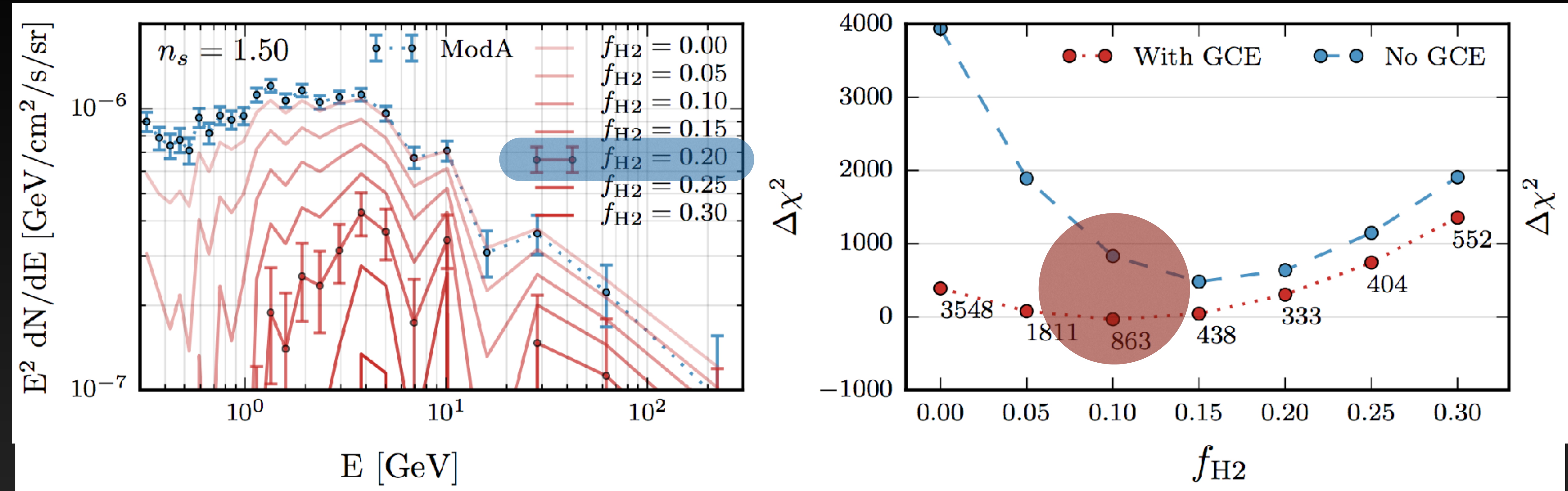


Data  
> 1 GeV  
front-converting events  
10° x 10° ROI

=



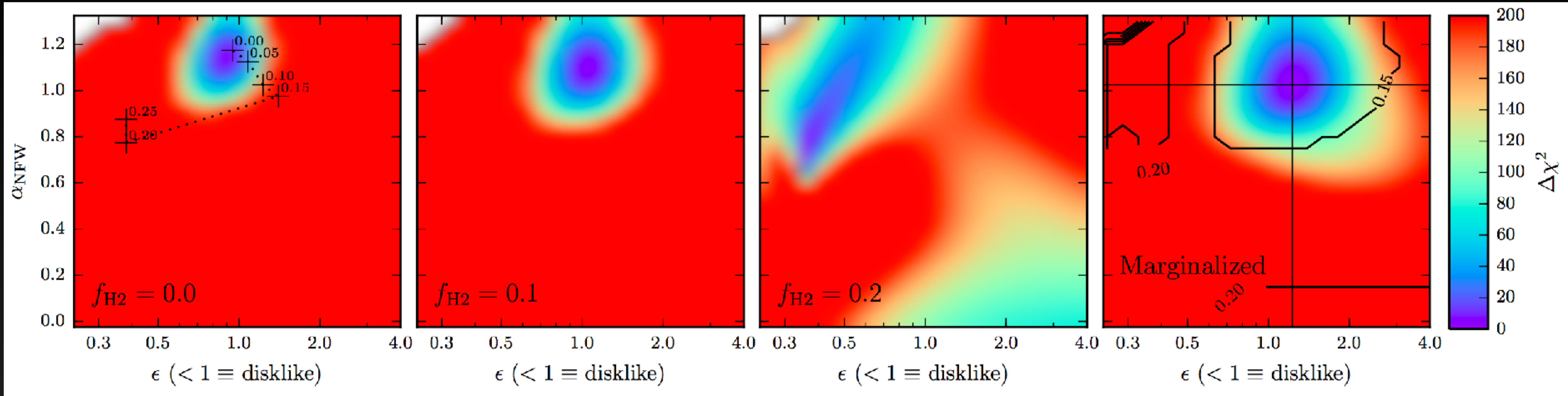
# Effect on the GC Excess



Increasing the value of  $f_{H2}$  decreases the intensity of the gamma-ray excess.

However, the best global fit is  $f_{H2} = 0.1$ , with a GC excess intensity that decreases by only ~30%.

# Effect on the Excess Morphology



The morphology of the excess is also degenerate with  $f_{\text{H}_2}$ .

As  $f_{\text{H}_2}$  is increased, the best-fit morphology becomes stretched perpendicular to the galactic plane.

However, marginalized over all values of  $f_{\text{H}_2}$ , the standard NFW template is still consistent with the data.

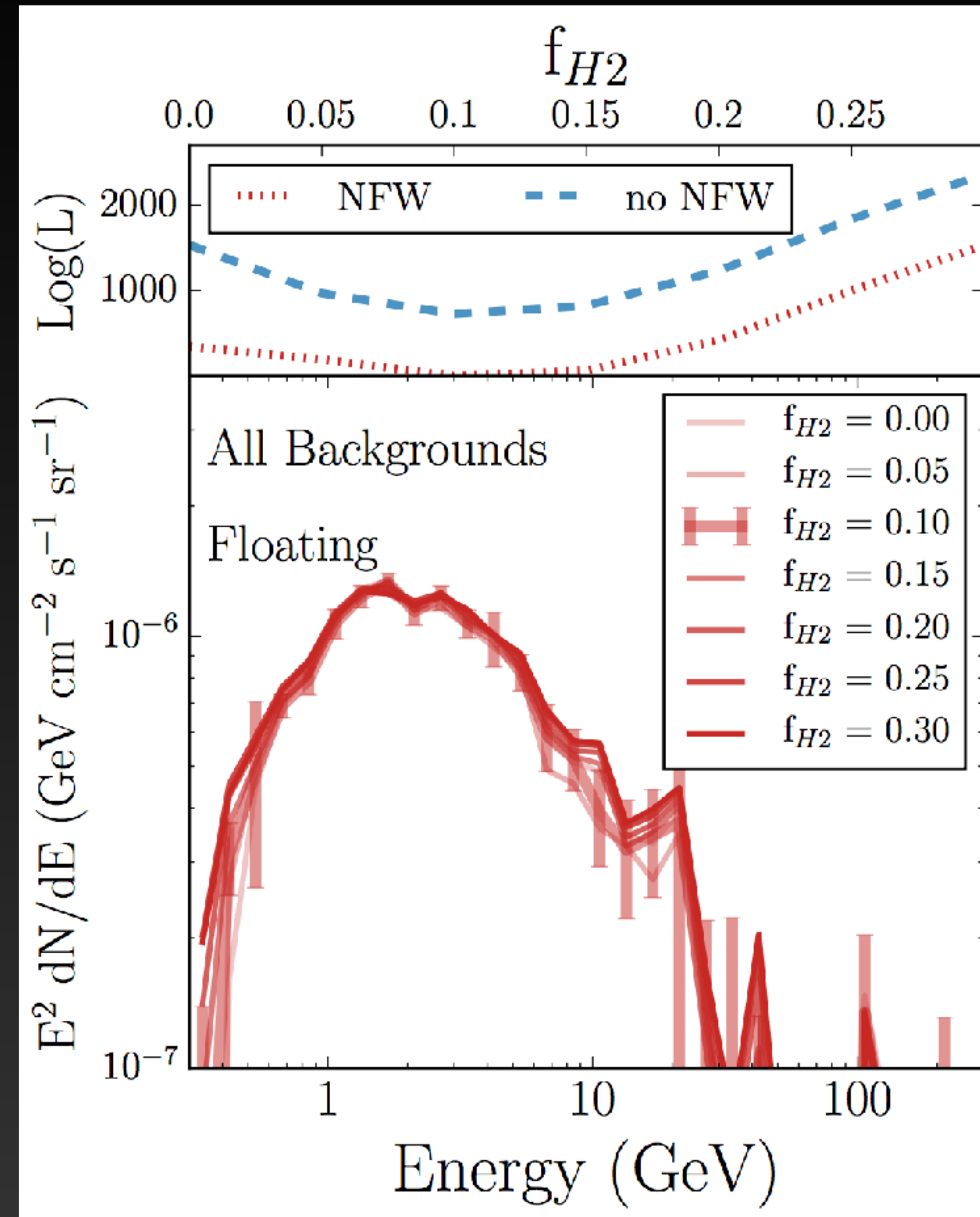
# Analysis in the Galactic Center



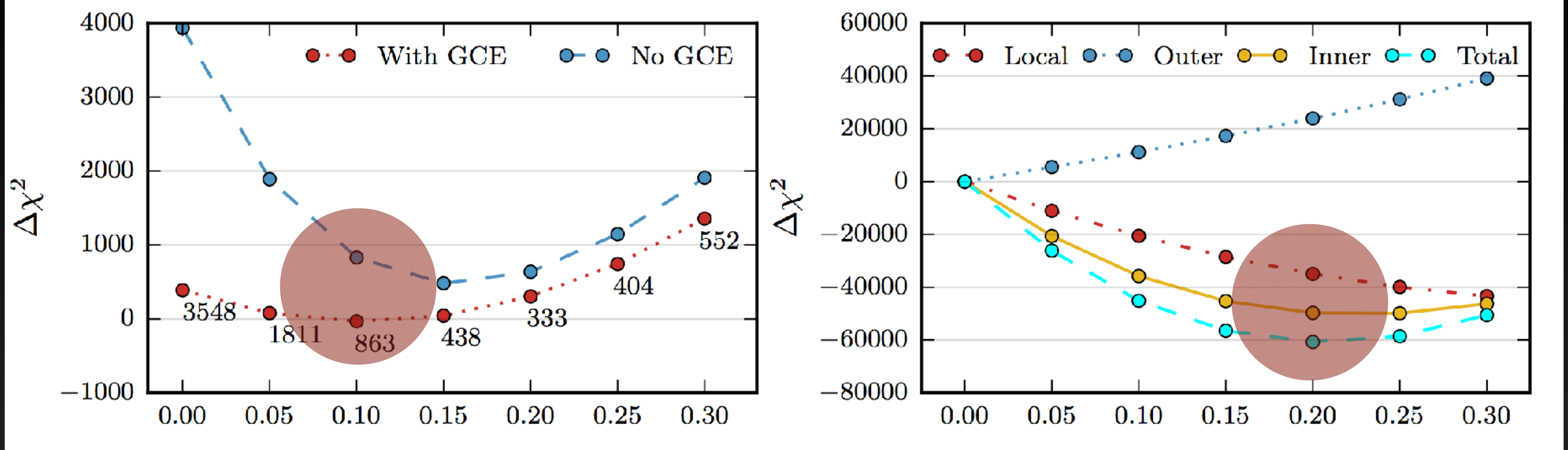
In this smaller region, the excess remains resilient to changes in the diffuse emission modeling.

The removal of the large side-bands in the ROI is more important than the inclusion of the GC.

$f_{H2} = 0.15$  still favored by the data, especially in the case of no NFW component.

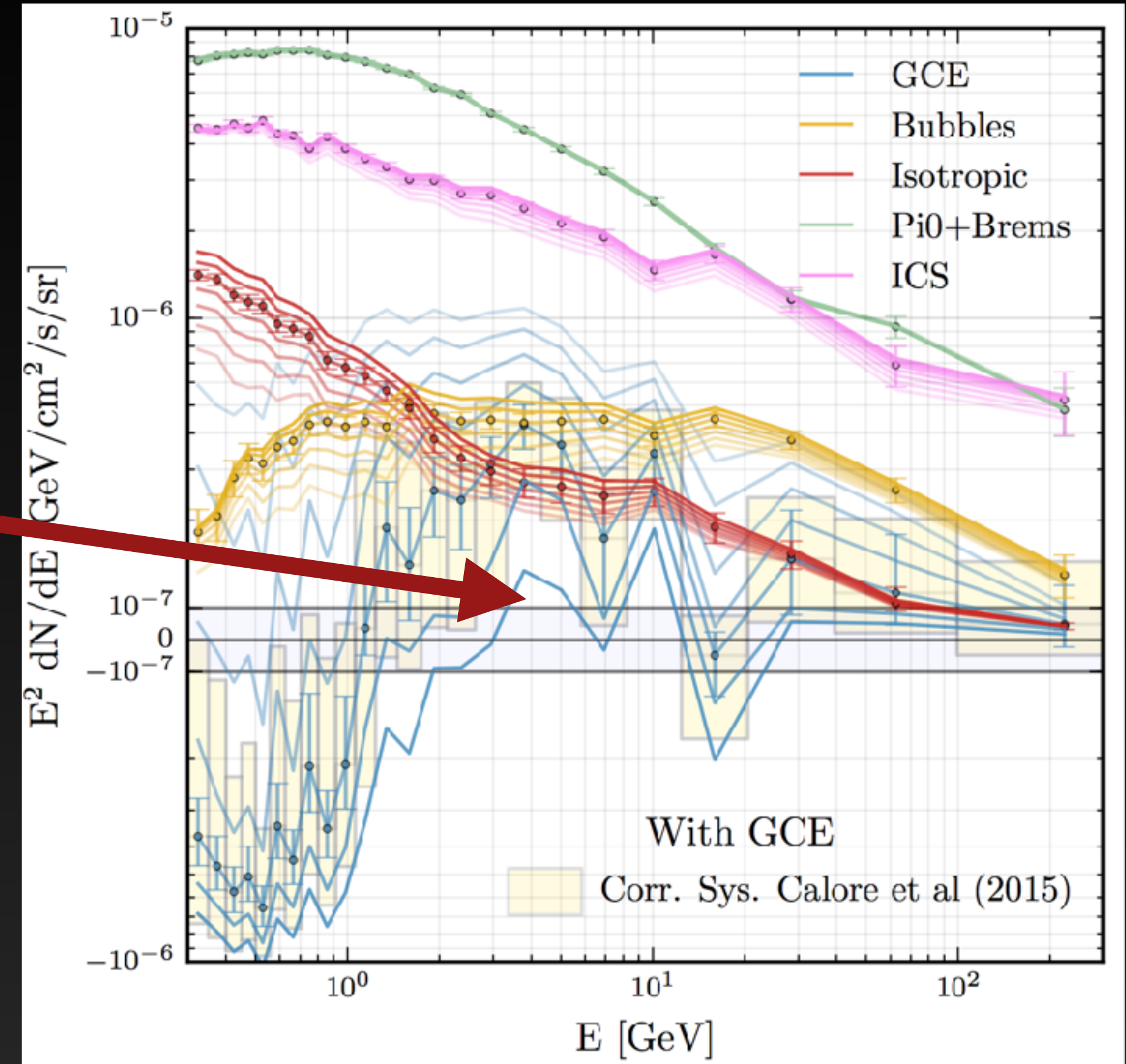
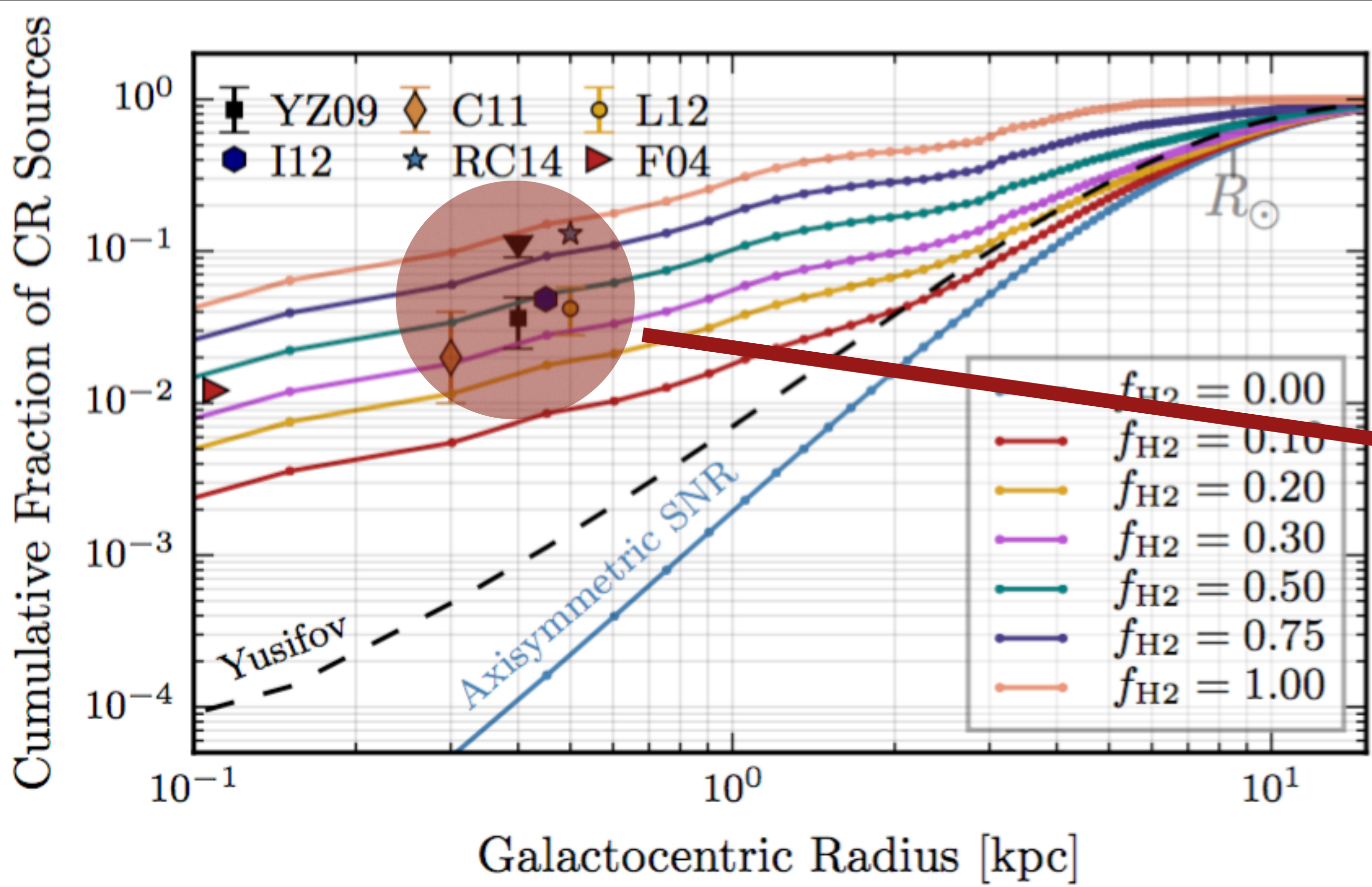


# The Galactic Center Deficit?



The best-fit value of  $f_{H_2}$  is smaller in the Galactic center, compared to its best fit value in the Milky Way....

# The Galactic Center Deficit?



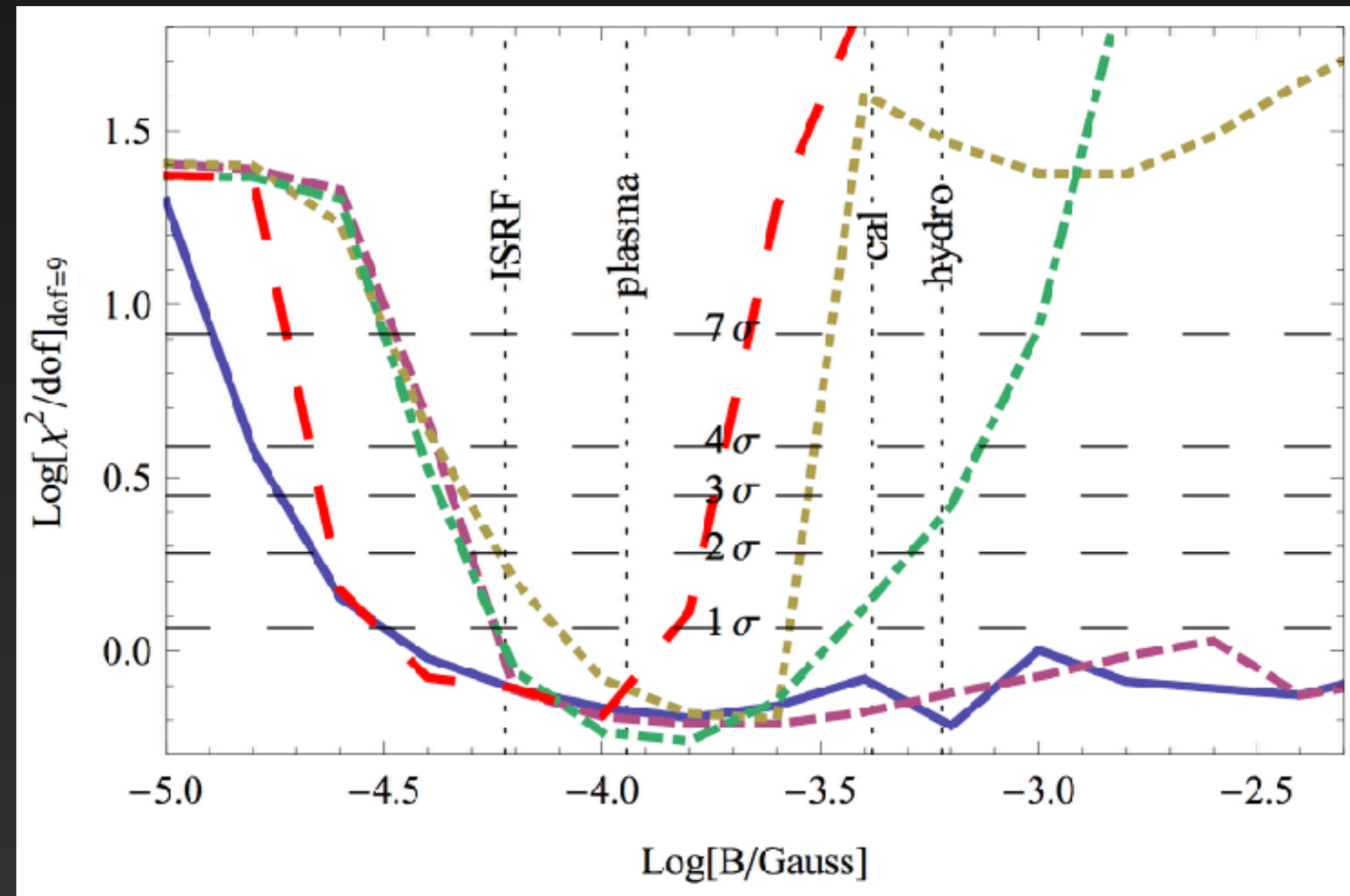
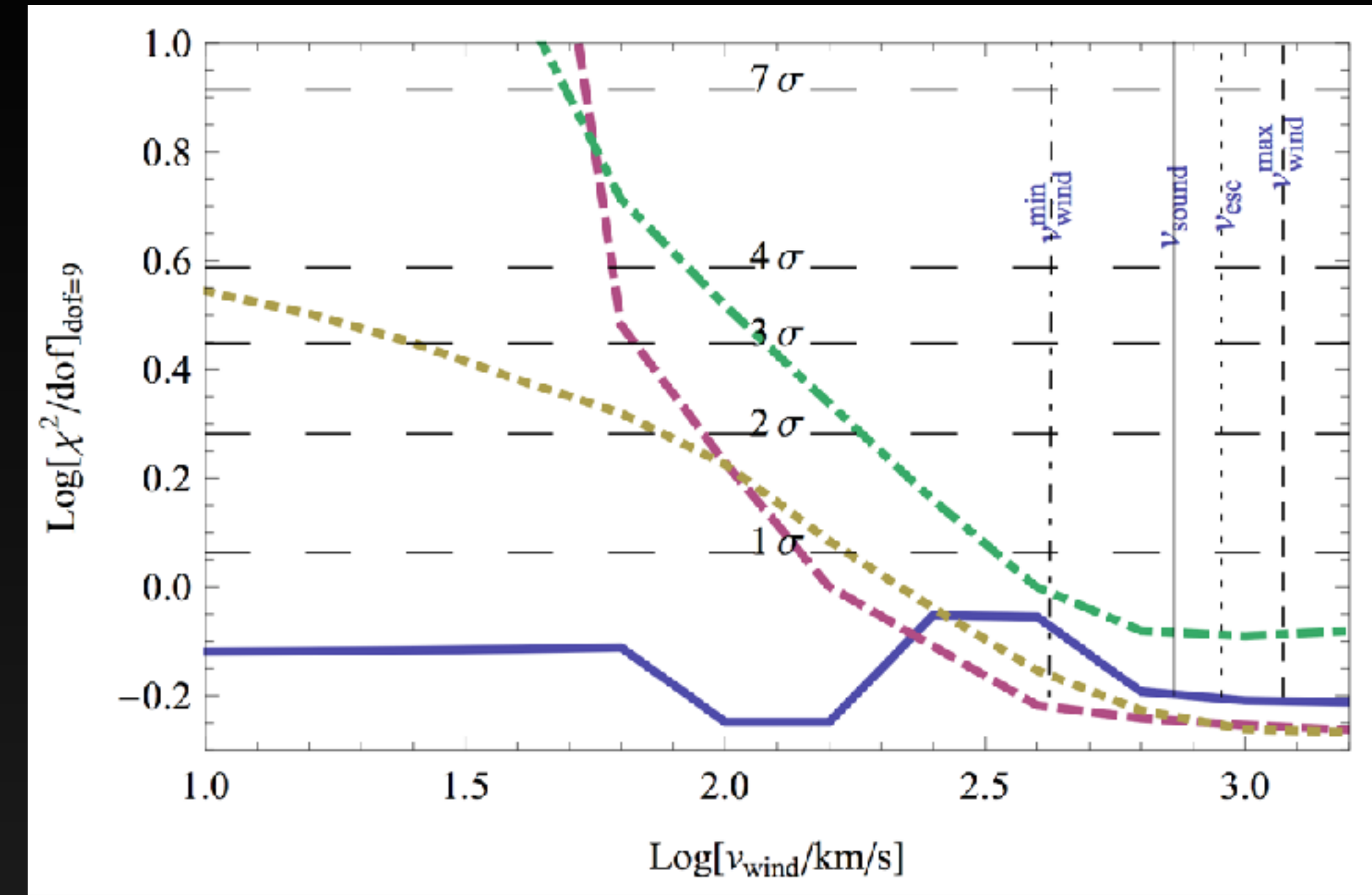
Forcing the value of  $f_{H2}$  to fit the best-fit value from the full galaxy leads to an excess template which is negative at low energies.

# Advection and Convection in the Galactic Center

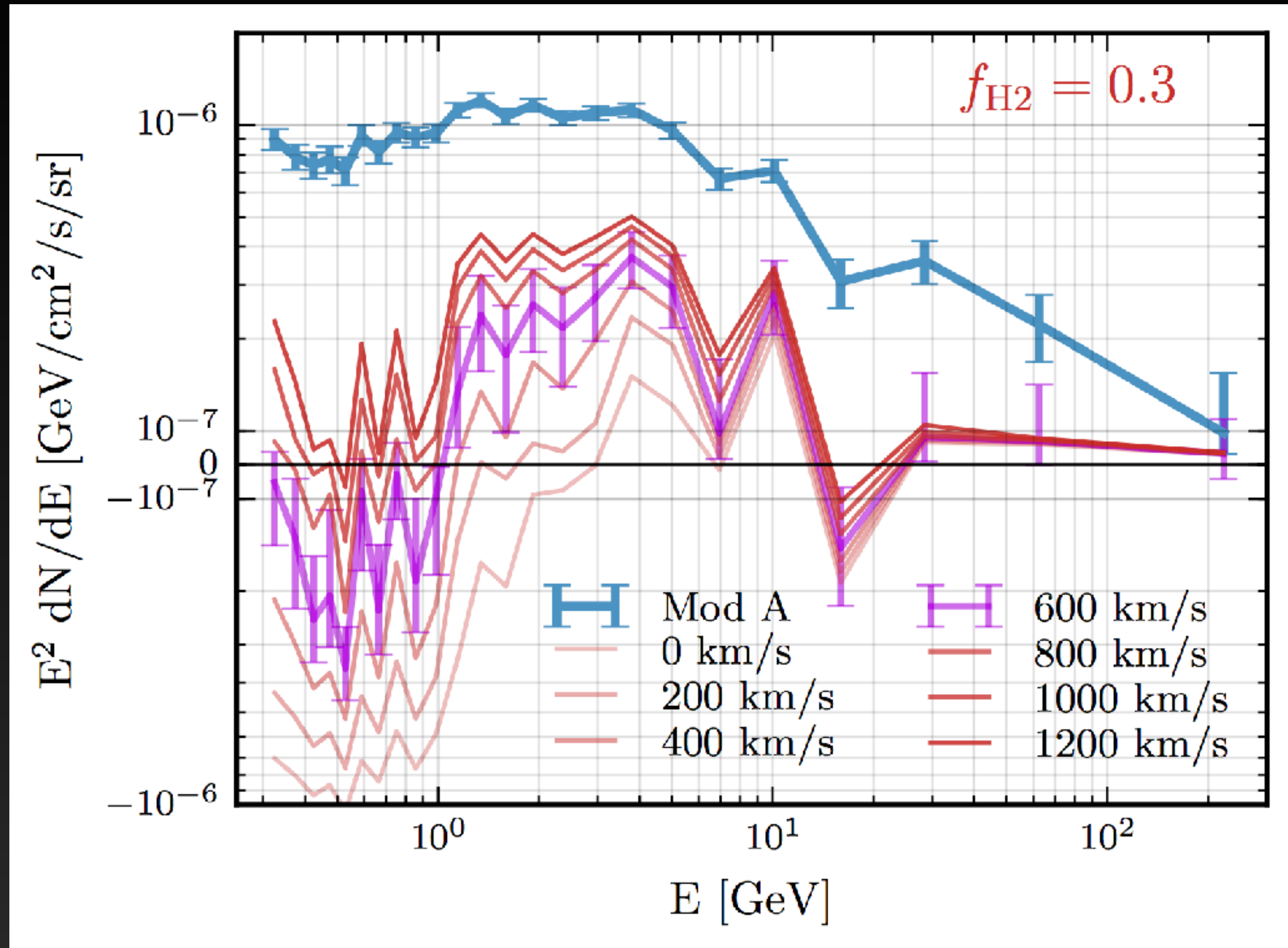
Crocker et al. (2011) demonstrated that the break in the GC synchrotron spectrum is best fit in the regime with:

- a.) Large Magnetic Fields
- b.) Large Convective Winds

Very different from typical Galprop diffusion scenario.



# The Low Energy Spectrum



Applying strong convective winds to the diffuse emission model fixes the low-energy over subtraction.

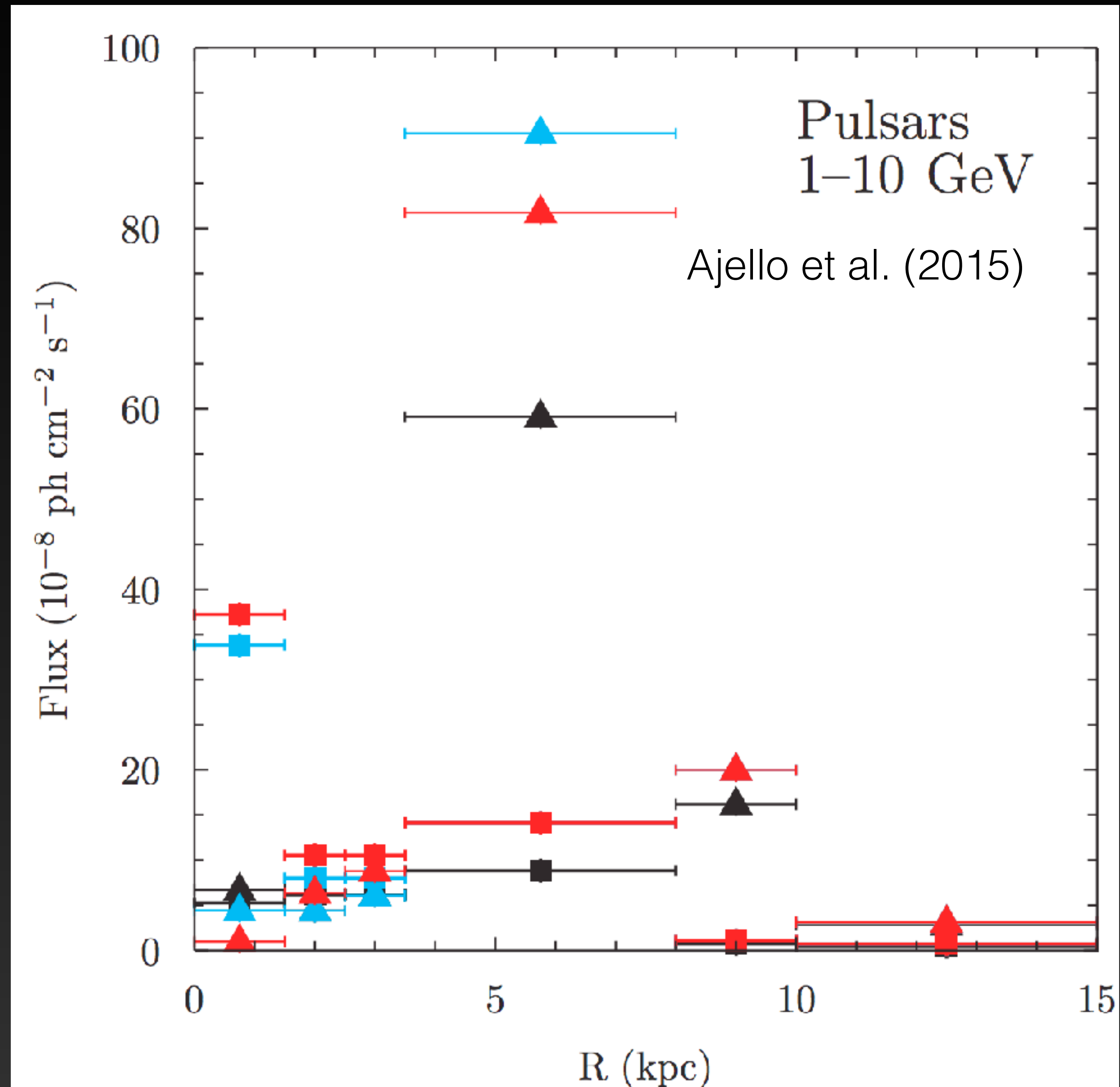
The intensity of the excess near the spectral peak also increases, up to ~50% of its nominal value.

The model produces a significantly better fit to the gamma-ray sky dataset - and also coincides better with multi wavelength data.

# A Similar Result with Different Techniques

Several recent papers have come to similar conclusions:

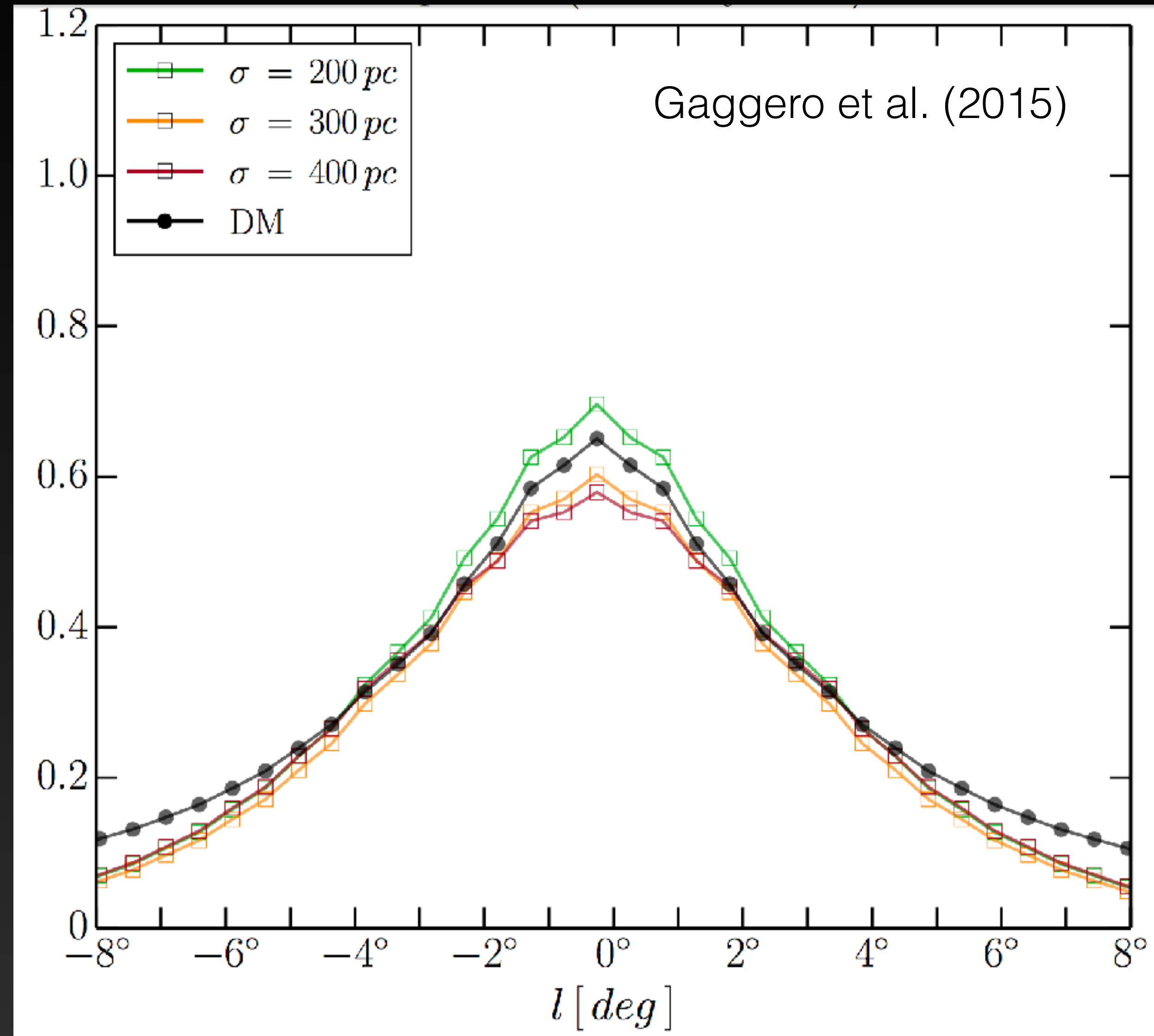
Ajello et al. (2015) find that the gamma-ray data near the galactic center is fit when the normalization of the inverse-Compton scattering component is highly peaked in the inner kpc.



# A Similar Result with Different Techniques

Several recent papers have come to similar conclusions:

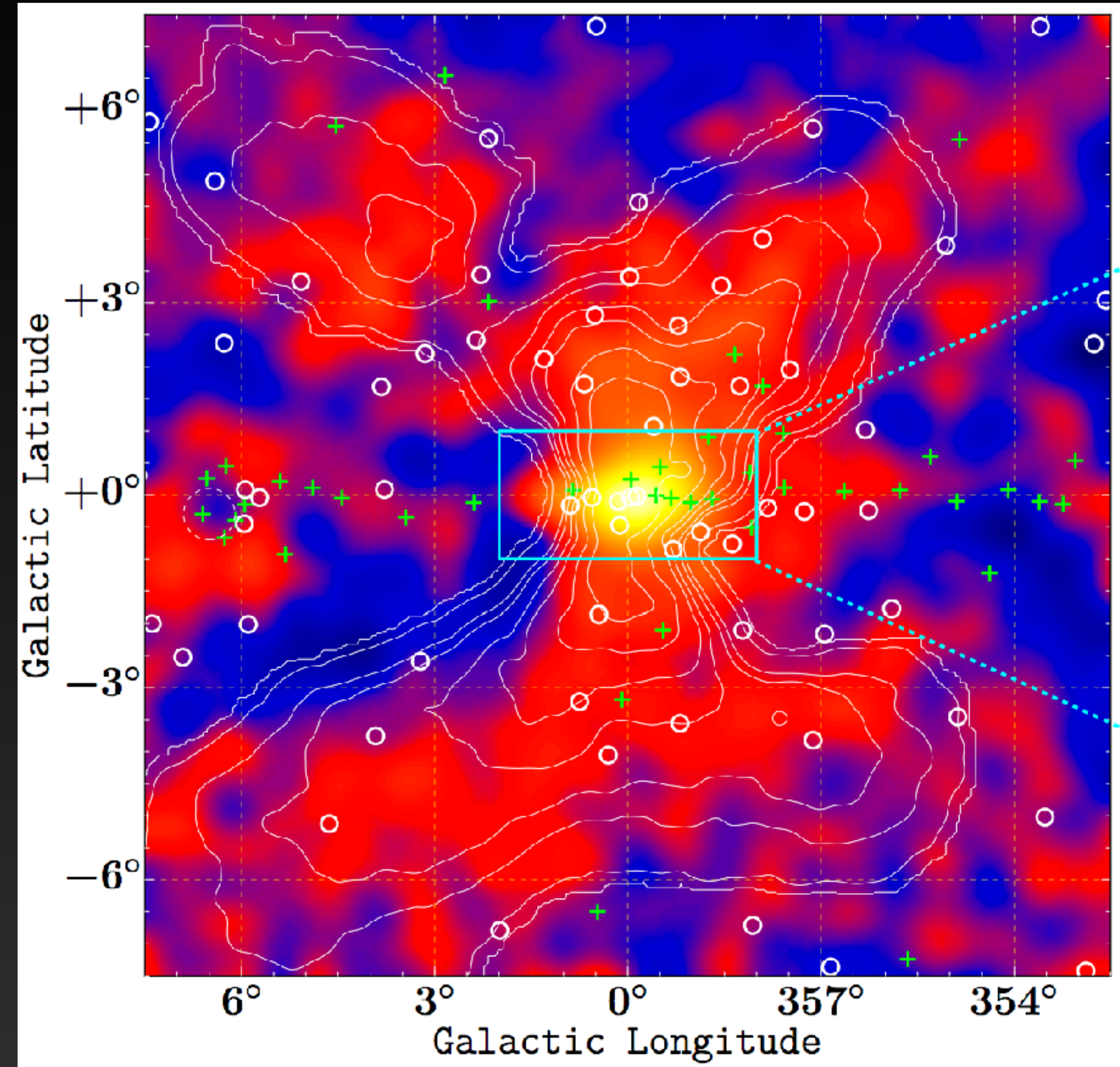
Gaggero et al. (2015) find that the gamma-ray data is better fit when a spherically symmetric gaussian flux is added to the gamma-ray data near the Galactic center.



# A Similar Result with Different Techniques

Several recent papers have come to similar conclusions:

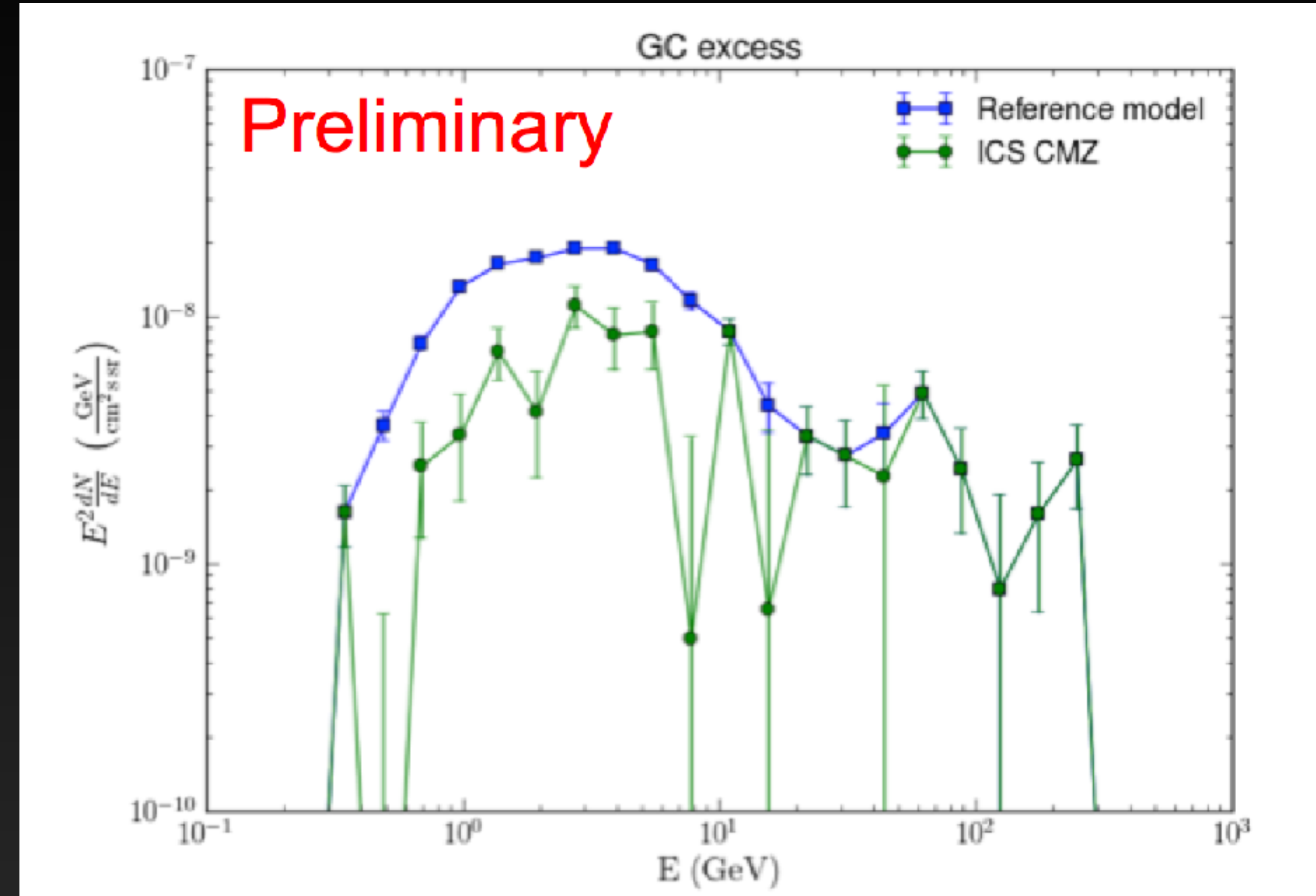
Macias et al. (2016) find that the gamma-ray data is better fit when a template tracing the nuclear stellar bulge is added into the gamma-ray model.



# A Similar Result with Different Techniques

Several recent papers have come to similar conclusions:

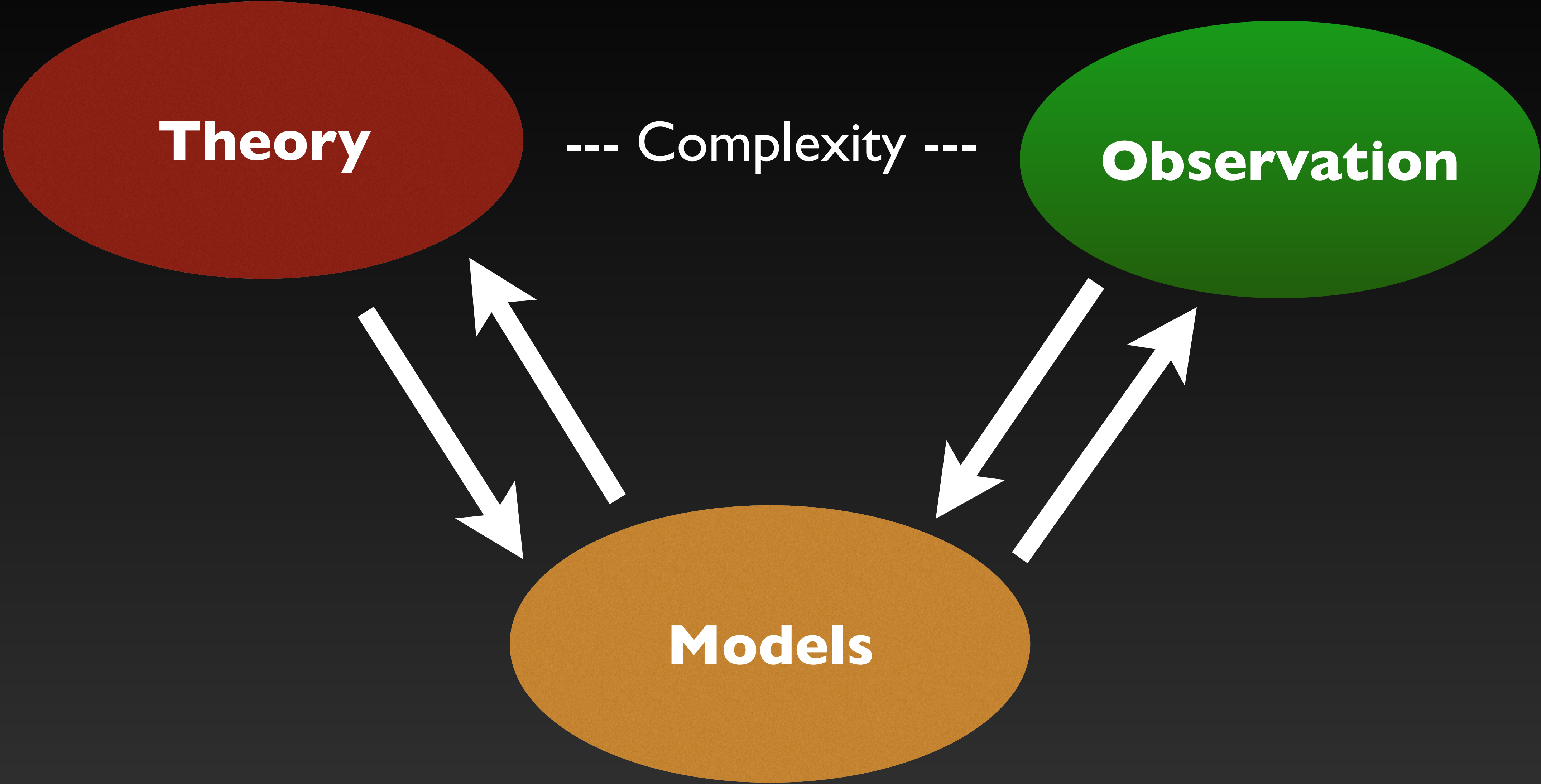
The Fermi-LAT collaboration has shown that the gamma-ray data is better fit when a new ICS component tracing the CMZ is added to the gamma-ray data.



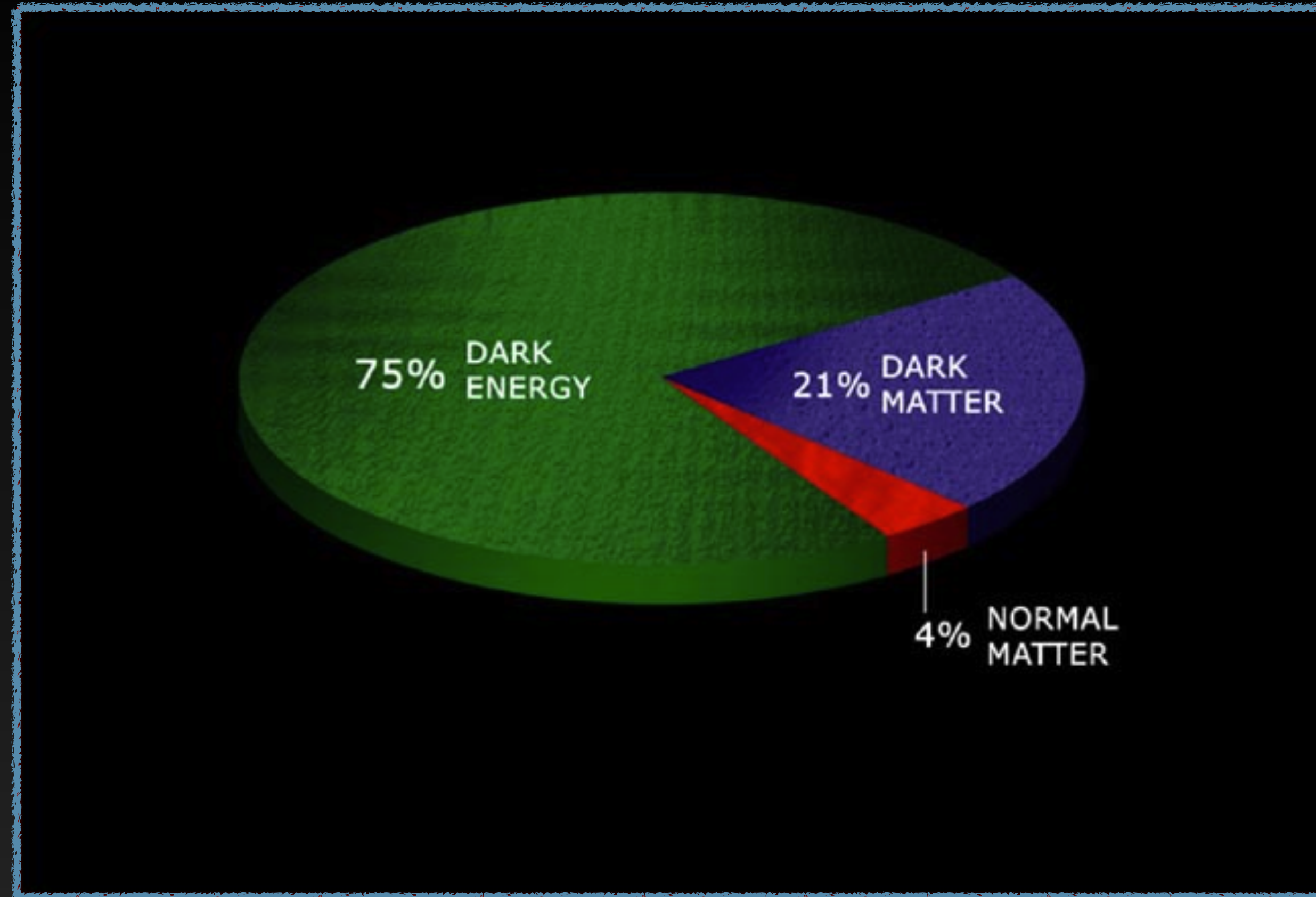
# A Similar Result with Different Techniques

The majority of these analyses (with the exception of Macias et al.) still find a galactic center excess template (following an NFW profile) to provide a statistically significant improvement in the fit to the gamma-ray data.

The remainder of the talks in this session will discuss interpretations of this excess.



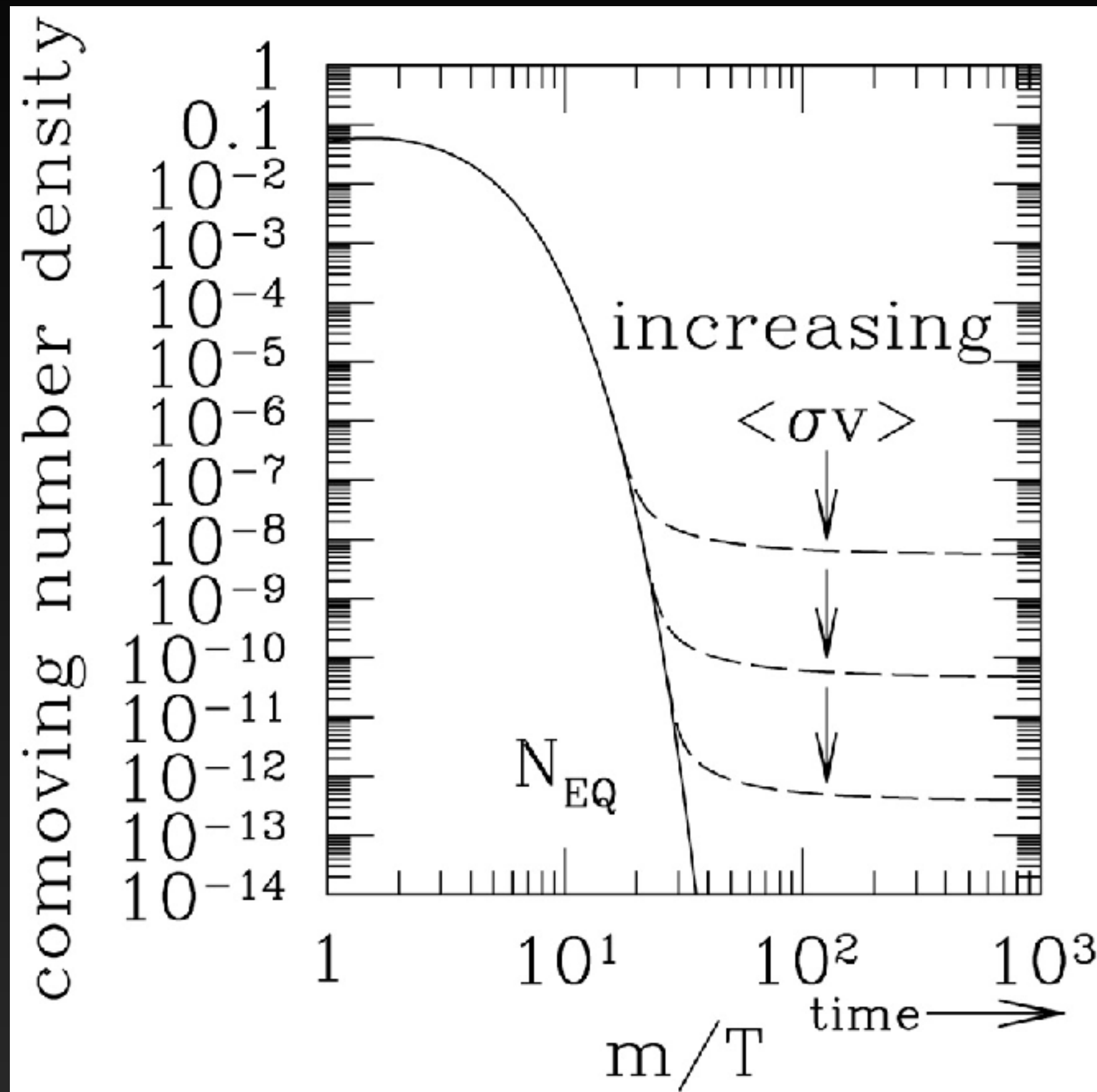
# The Implications for WIMP Dark Matter



**The Density of Dark Matter is similar to the density of protons in our universe.**

**This requires either significant fine tuning, or a dynamical interaction - which in QFT must correspond to some force.**

# WIMPS in Thermal Equilibrium



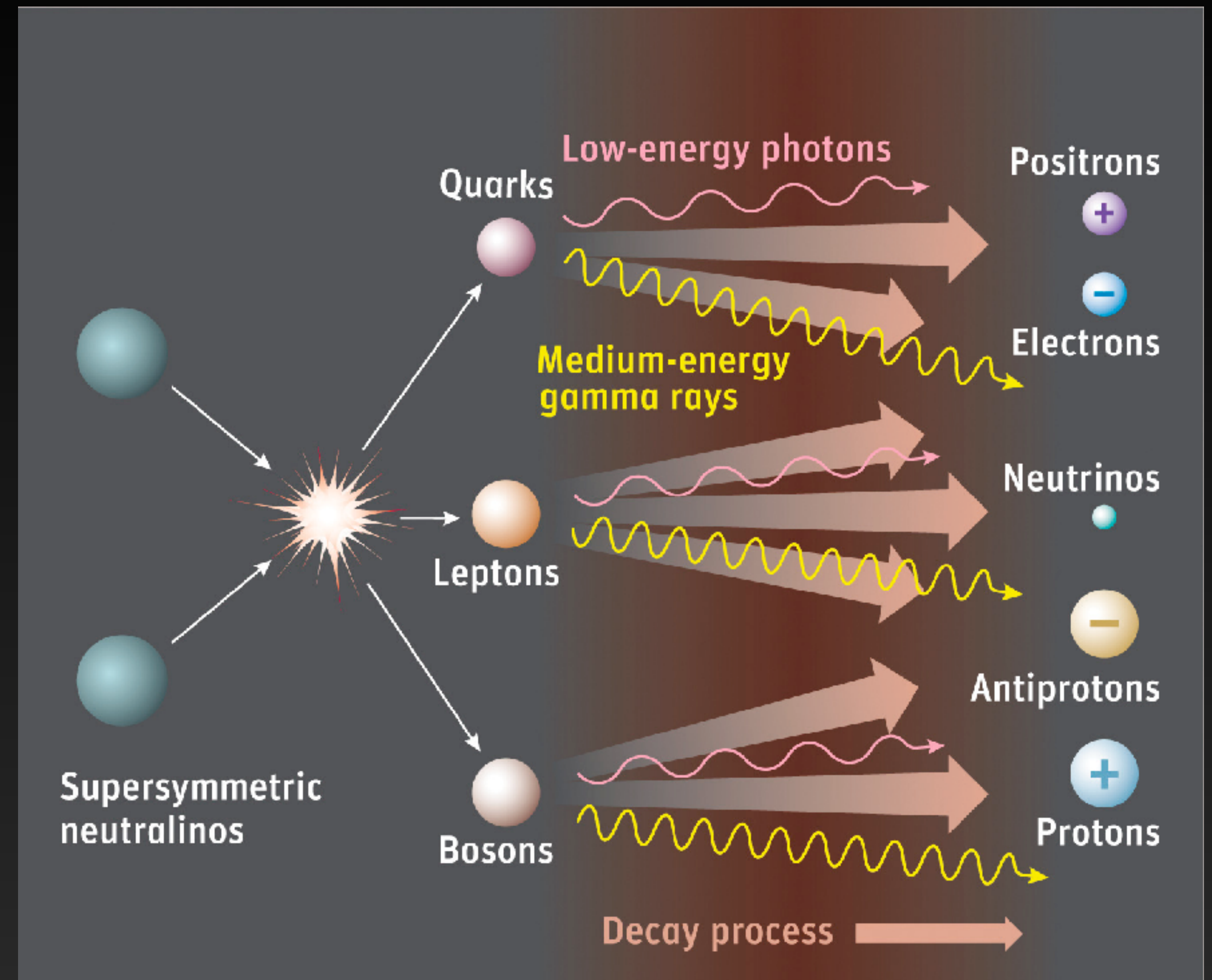
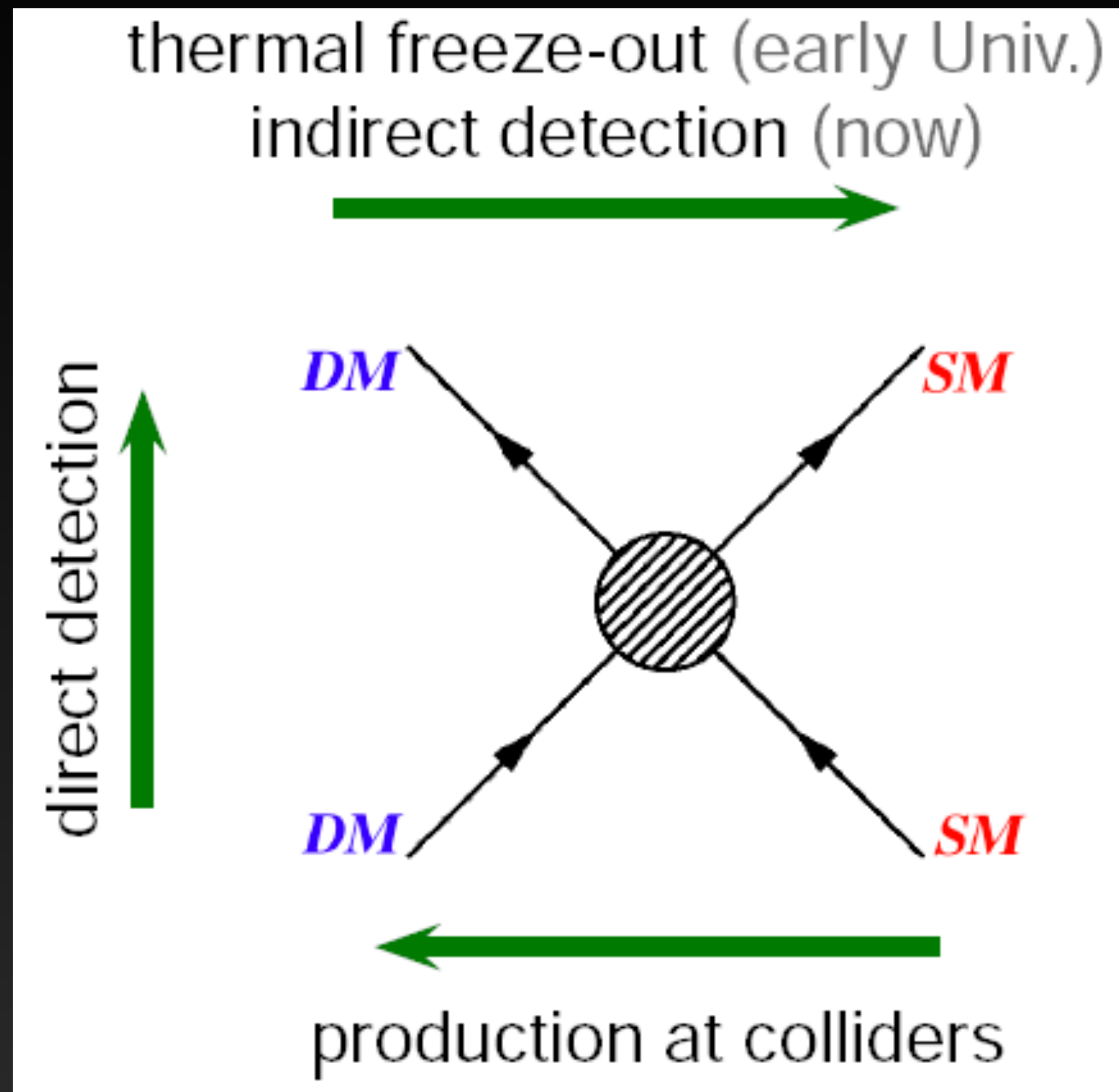
A particle with a weak interaction cross-section and a mass on the weak scale naturally obtains the correct relic abundance through thermal freeze-out in the Early Universe.

$$\left( \frac{\Omega_\chi}{0.2} \right) \simeq \frac{x_{\text{f.o.}}}{20} \left( \frac{10^{-8} \text{ GeV}^{-2}}{\sigma} \right)$$

$$\langle \sigma v \rangle \sim 10^{-8} \text{ GeV}^{-2} (3 \times 10^{-28} \text{ GeV}^2 \text{ cm}^2) 10^{10} \frac{\text{cm}}{\text{s}} = 3 \times 10^{-26} \frac{\text{cm}^3}{\text{s}}$$

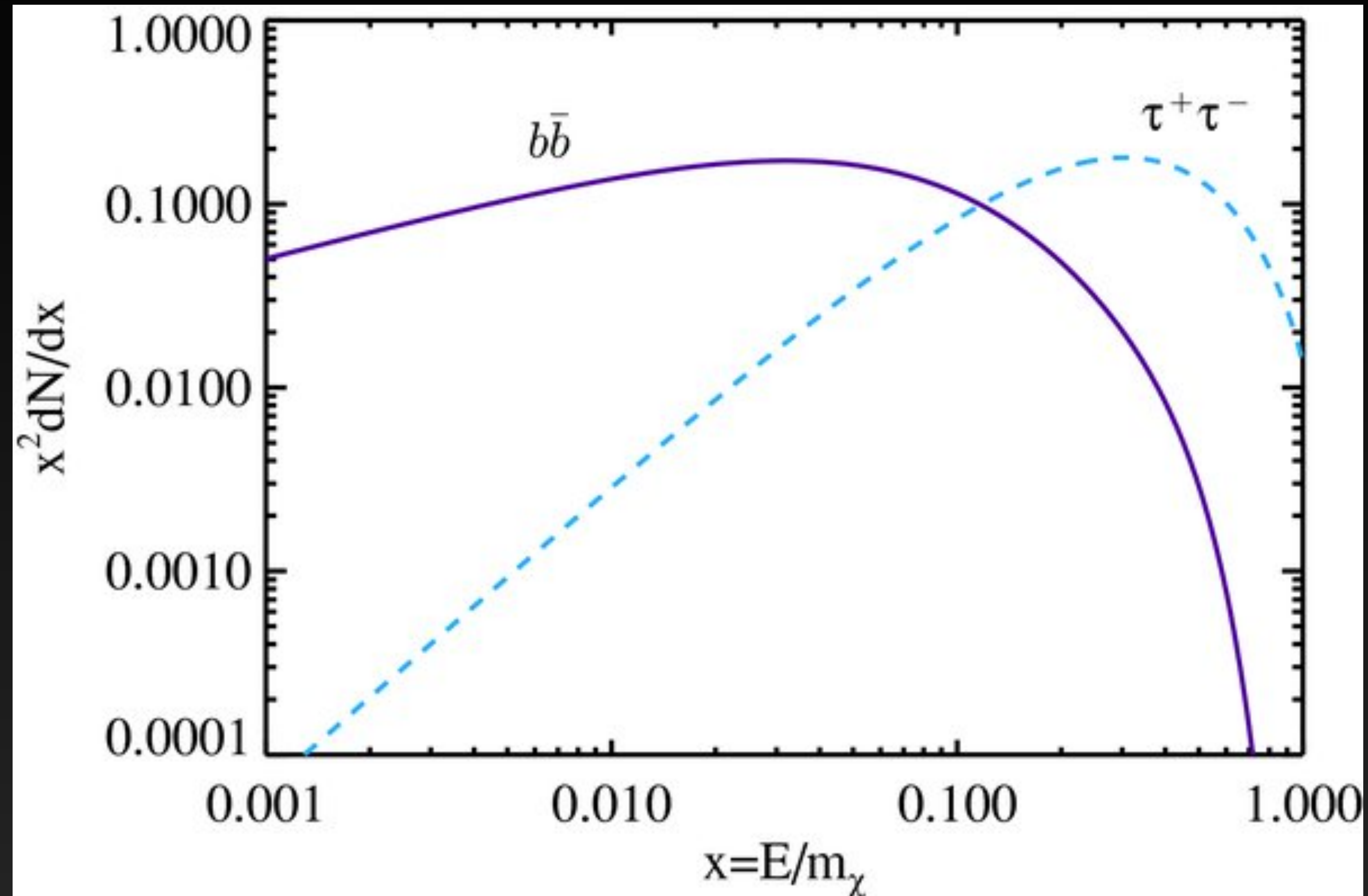
This guaranteed cross-section is unique to indirect detection.

# Gamma-Rays from WIMPs



If dark matter had a thermal cross-section in the early universe, it should still have an observable cross-section today.

# Gamma-Rays from WIMPs



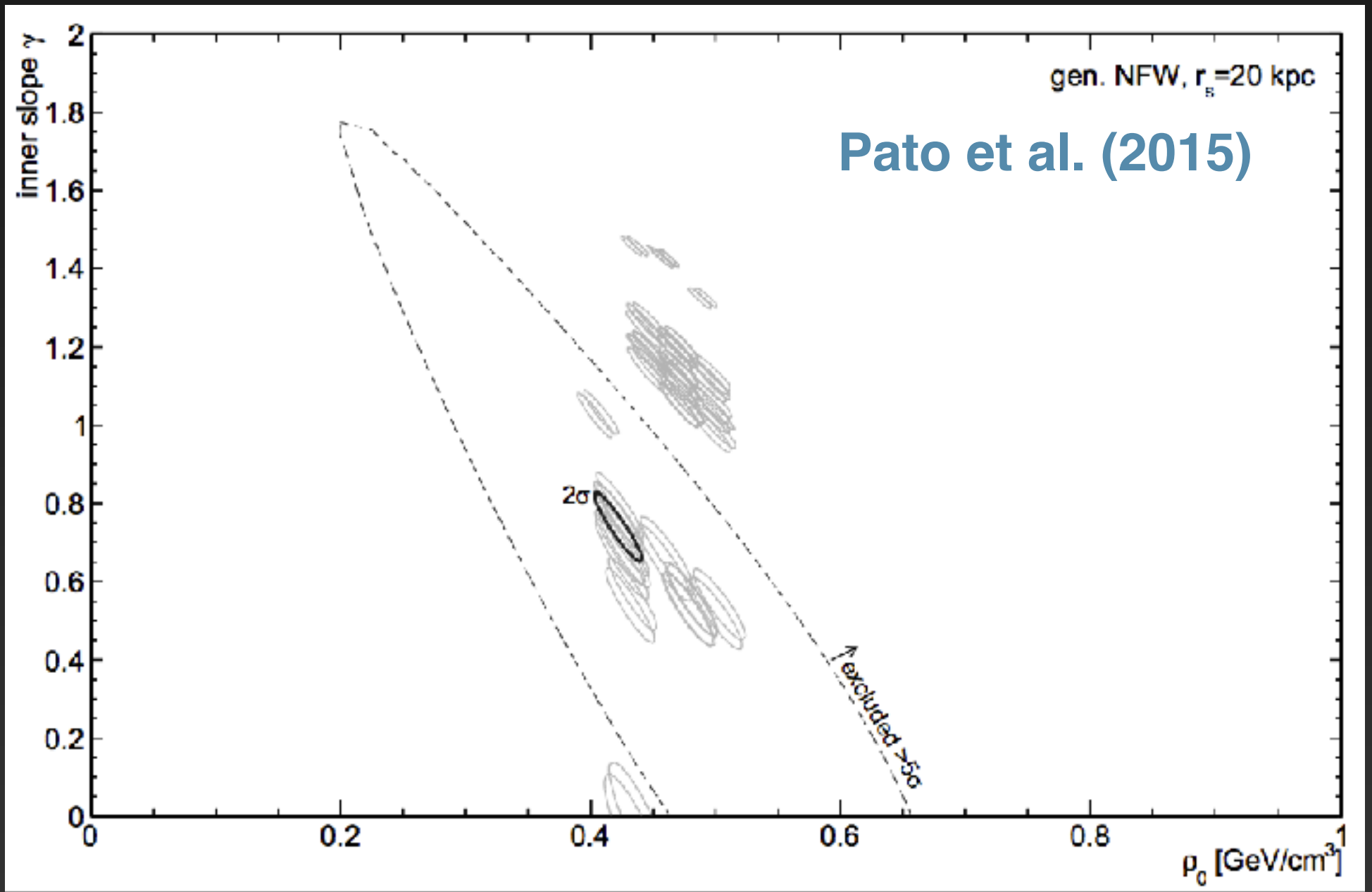
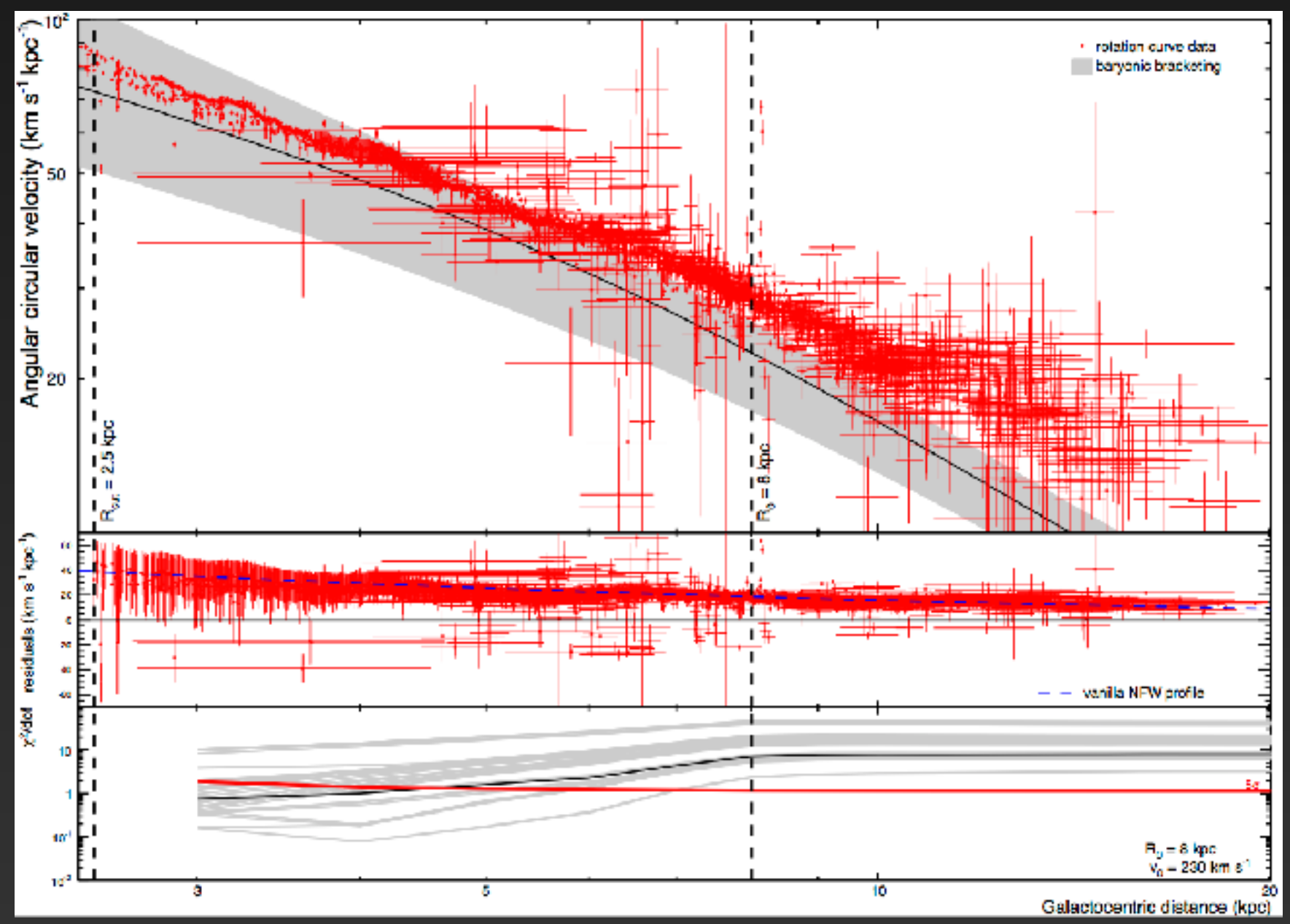
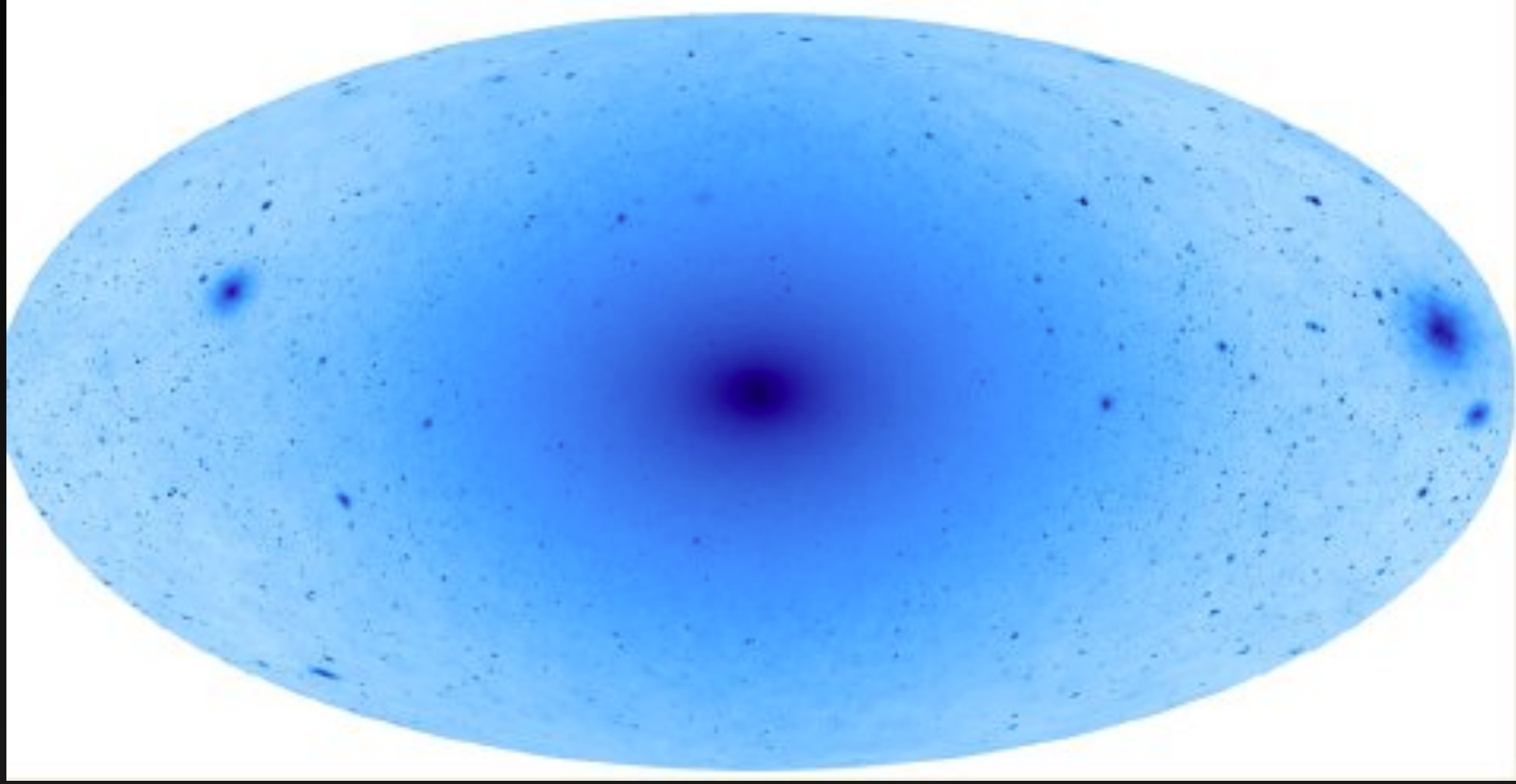
Once a standard model final state is selected, the resulting photon spectrum can be calculated from known physics.

For WIMP scale dark matter, photon energy peaks in the GeV range.

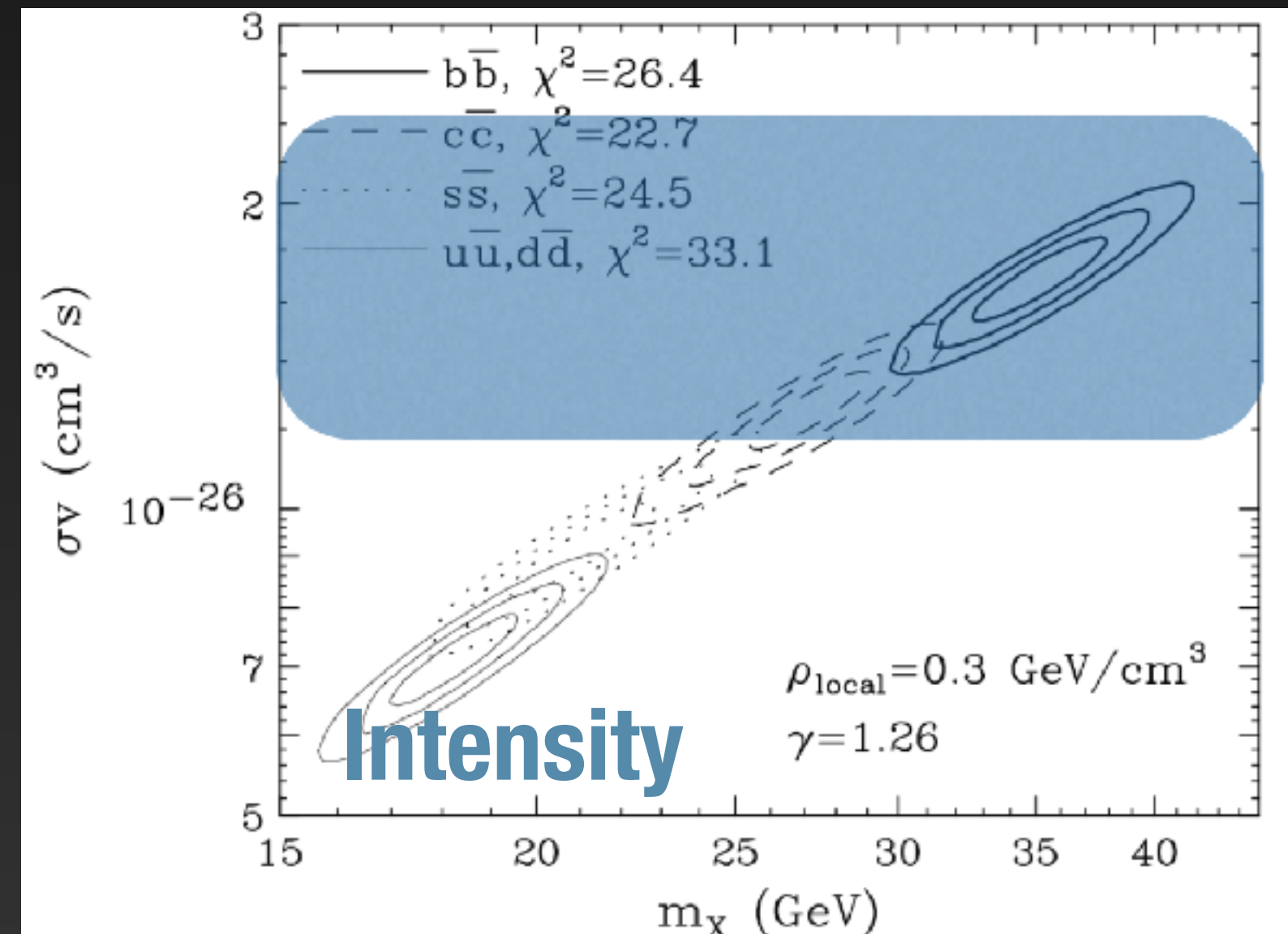
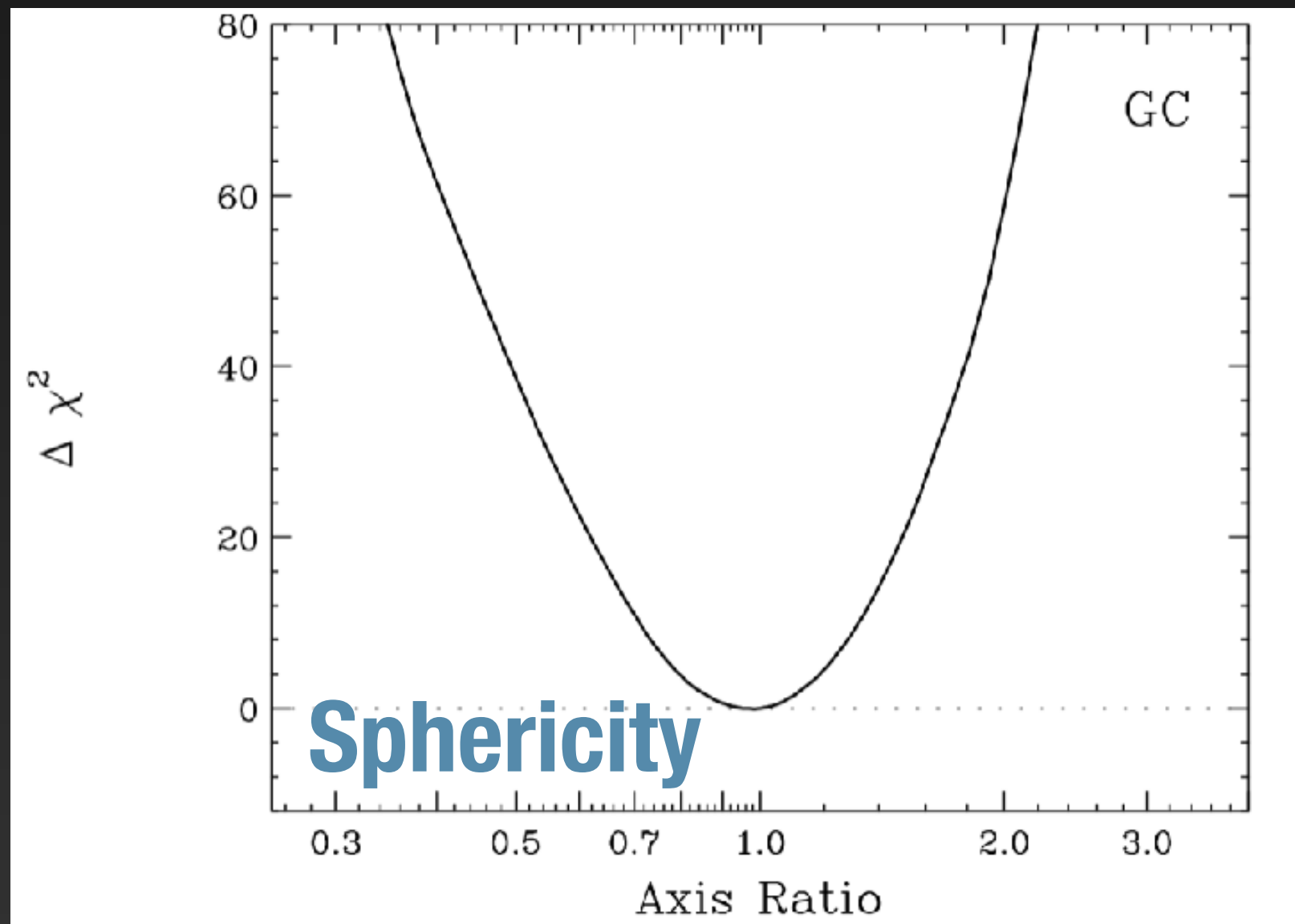
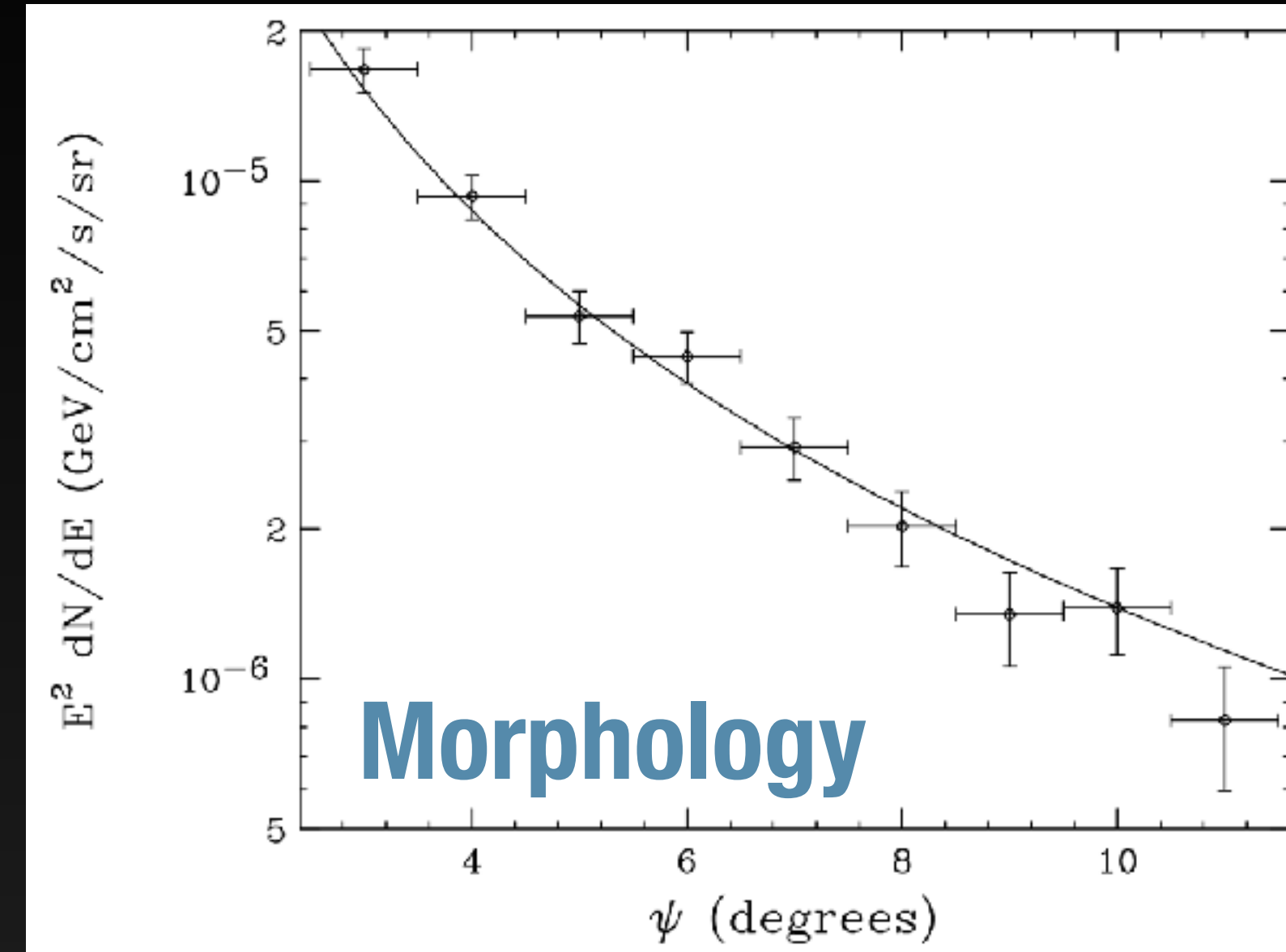
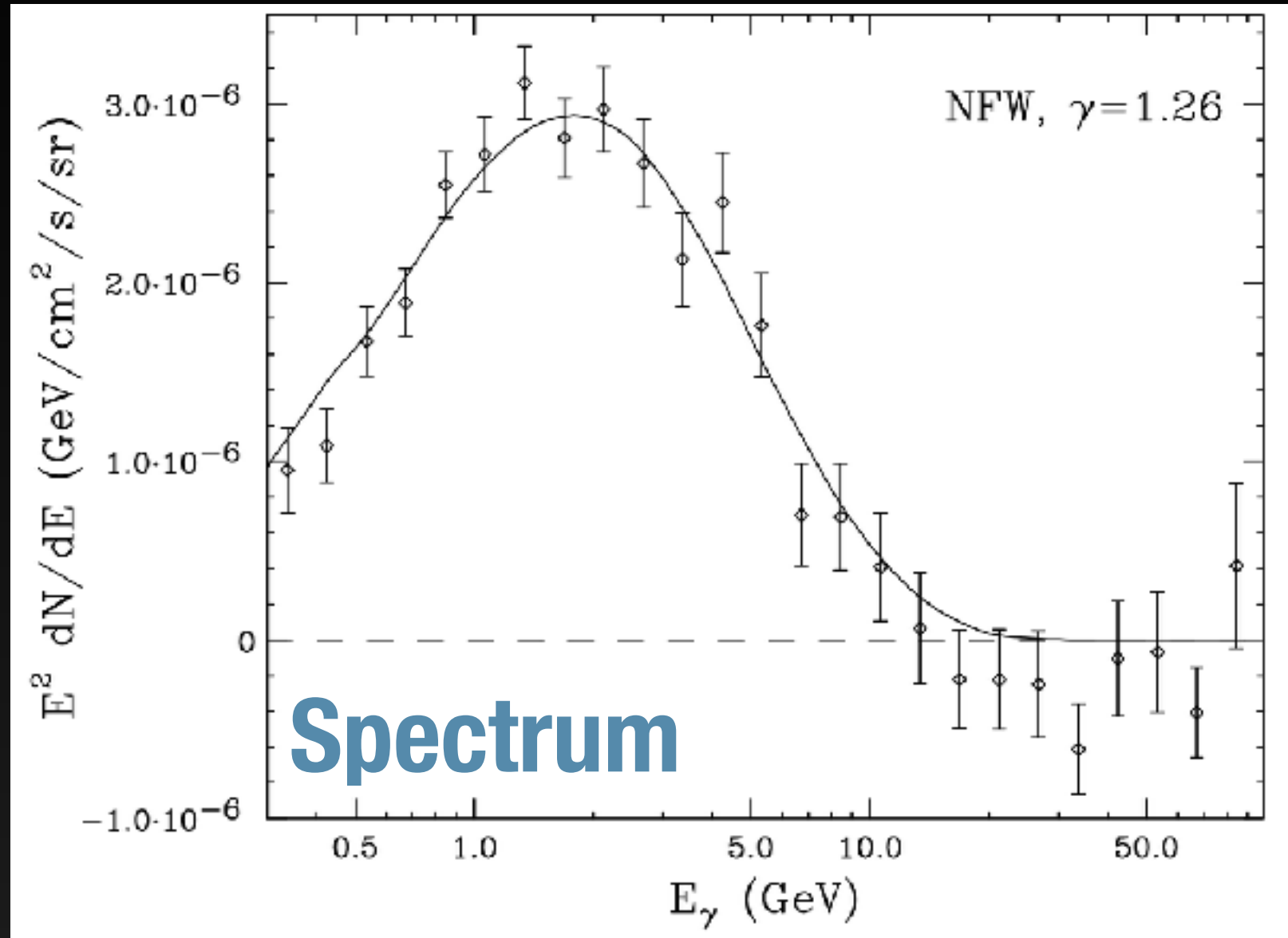
# The Galactic Center as an Indirect Detection Target

Both observational data and simulations indicate that the Galactic Center should produce the highest flux of dark matter annihilation products of any location in the sky.

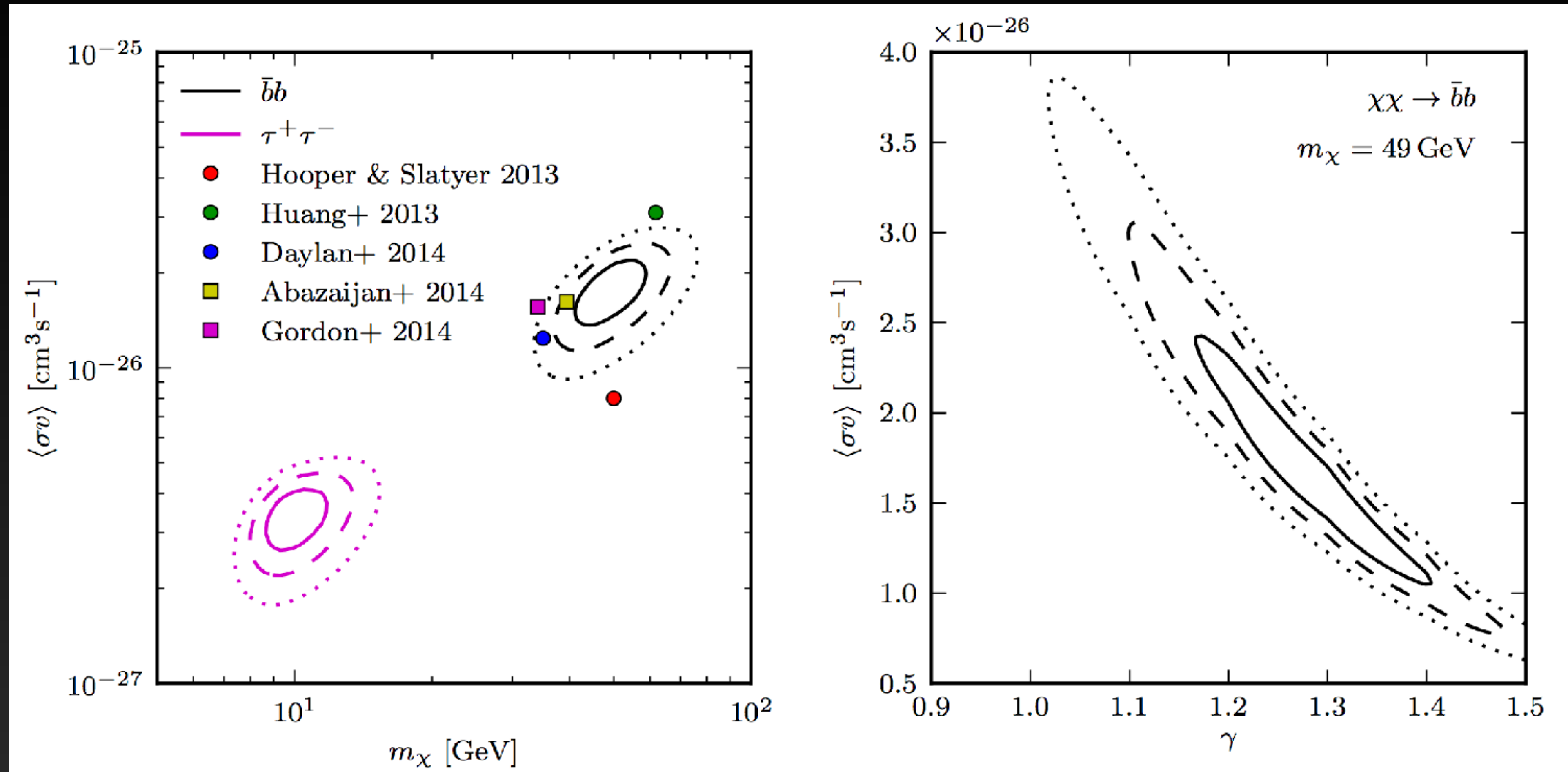
Recent work has provided the first direct evidence for dark matter within the Milky Way solar circle.



# The WIMP Interpretation of the Galactic Center Excess



# The WIMP Interpretation of the Galactic Center Excess



And intriguingly, the necessary dark matter cross-section is similar to the necessary thermal relic cross-section.

# Particle Physics Models Exist...

Chan (1607.02246)  
Jia (1607.00737)  
Barrau et al. (1606.08031)  
Huang et al. (1605.09018)  
Cui et al. (1605.08138)  
Krauss et al. (1605.05327 )  
Kumar et al. (1605.00611)  
Biswas et al. (1604.06566)  
Sage et al. (1604.04589 )  
Choquette et al. (1604.01039)  
Cuoco et al. (1603.08228)  
Chao et al. (1602.05192)  
Horiuchi et al. (1602.04788)  
Hektor et al. (1602.00004)  
Freytsis et al. (1601.07556)  
Kim et al. (1601.05089)  
Huang et al. (1512.08992)  
Kulkarni et al. (1512.06836)  
Tang et al. (1512.02899)  
Cox et al. (1512.00471)  
Cai et al. (1511.09247)  
Agrawal et al. (1511.06293)  
Duerr et al. (1510.07562)  
Drozd et al. (1510.07053)  
Arcadi et al. (1510.02297)  
Williams (1510.00714)  
Cai & Spray (1509.08481)  
Freese et al. (1509.05076)  
Bhattacharya et al. (1509.03665)  
Algeri et al. (1509.01010)  
Fox & Tucker-Smith (1509.00499)  
Dutta et al. (1509.05989)  
Liu et al. (1508.05716)  
Berlin et al. (1508.05390)  
Fan et al. (1507.06993)  
Hektor et al. (1507.05096)  
Achterbeg et al. (1507.04644)  
Biswas et al. (1507.04543)

Butter et al. (1507.02288)  
Mondal et al. (1507.01793)  
Cao et al. (1506.06471)  
Banik et al. (1506.05665)  
Ipek (1505.07826)  
Buchmueller et al. (1505.07826)  
Balazs et al. (1505.06758)  
Medina (1505.05565)  
Kim et al. (1505.04620)  
Ko et al. (1504.06944)  
Ko & Tang (1504.03908)  
Ghorbani & Ghorbani (1504.03610)  
Fortes et al. (1503.08220)  
Cline et al. (1503.08213)  
Rajaraman et al. (1503.05919)  
Bi et al. (1503.03749)  
Kopp et al. (1503.02669)  
Elor et al. (1503.01773)  
Gherghetta et al. (1502.07173)  
Berlin et al. (1502.06000)  
Achterberg et al. (1502.05703)  
Modak et al. (1502.05682)  
Guo et al. (1502.00508)  
Chen & Nomura (1501.07413)  
Kozaczuk & Martin (1501.07275)  
Berlin et al. (1501.03496)  
Kaplinghat et al. (1501.03507)  
Alves et al. (1501.03490)  
Biswas et al. (1501.02666)  
Biswas et al. (1501.02666)  
Ghorbani & Ghorbani (1501.00206)  
Cerdeno et al. (1501.01296)  
Liu et al. (1412.1485)  
Hooper (1411.4079)  
Arcadi et al. (1411.2985)  
Cheung et al. (1411.2619)  
Agrawal et al. (1411.2592)  
Kile et al. (1411.1407)

Buckley et al. (1410.6497)  
Heikinheimo & Spethmann (1410.4842)  
Freytsis et al. (1410.3818)  
Yu et al. (1410.3347)  
Cao et al. (1410.3239)  
Guo et al. (1409.7864)  
Yu (1409.3227)  
Cahill-Rowley et al. (1409.1573)  
Banik & Majumdar (1408.5795)  
Bell et al. (1408.5142)  
Ghorbani (1408.4929)  
Okada & Seto (1408.2583)  
Frank & Mondal (1408.2223)  
Baek et al. (1407.6588)  
Tang (1407.5492)  
Balazs & Li (1407.0174)  
Huang et al. (1407.0038)  
McDermott (1406.6408)  
Cheung et al. (1406.6372)  
Arina et al. (1406.5542)  
Chang & Ng (1406.4601)  
Wang & Han (1406.3598)  
Cline et al. (1405.7691)  
Berlin et al. (1405.5204)  
Mondal & Basak (1405.4877)  
Martin et al. (1405.0272)  
Ghosh et al. (1405.0206)  
Abdullah et al. (1404.5503)  
Park & Tang (1404.5257)  
Cerdeno et al. (1404.2572)  
Izaguirre et al. (1404.2018)  
Agrawal et al. (1404.1373)  
Berlin et al. (1404.0022)  
Alves et al. (1403.5027)  
Finkbeiner & Weiner (1402.6671)  
Boehm et al. (1401.6458)  
Kopp et al. (1401.6457)  
Modak et al. (1312.7488)  
Alves et al. (1312.5281)

Alves et al. (1312.5281)  
Fortes et al. (1312.2837)  
Banik et al. (1311.0126)  
Arhrib et al. (1310.0358)  
Kelso et al. (1308.6630)  
Kozaczuk et al. (1308.5705)  
Kumar (1308.4513)  
Demir et al. (1308.1203)  
Buckley et al. (1307.3561)  
Cline et al. (1306.4710)  
Cannoni et al. (1205.1709)  
An et al. (1110.1366)  
Buckley et al. (1106.3583)  
Boucenna et al. (1106.3368)  
Ellis et al. (1106.0768)  
Cheung et al. (1104.5329)  
Marshall et al. (1102.0492)  
Abada et al. (1101.0365 )  
Tytgat (1012.0576)  
Logan (1010.4214)  
Barger et al. (1008.1796)  
Raklev et al. (0911.1986)

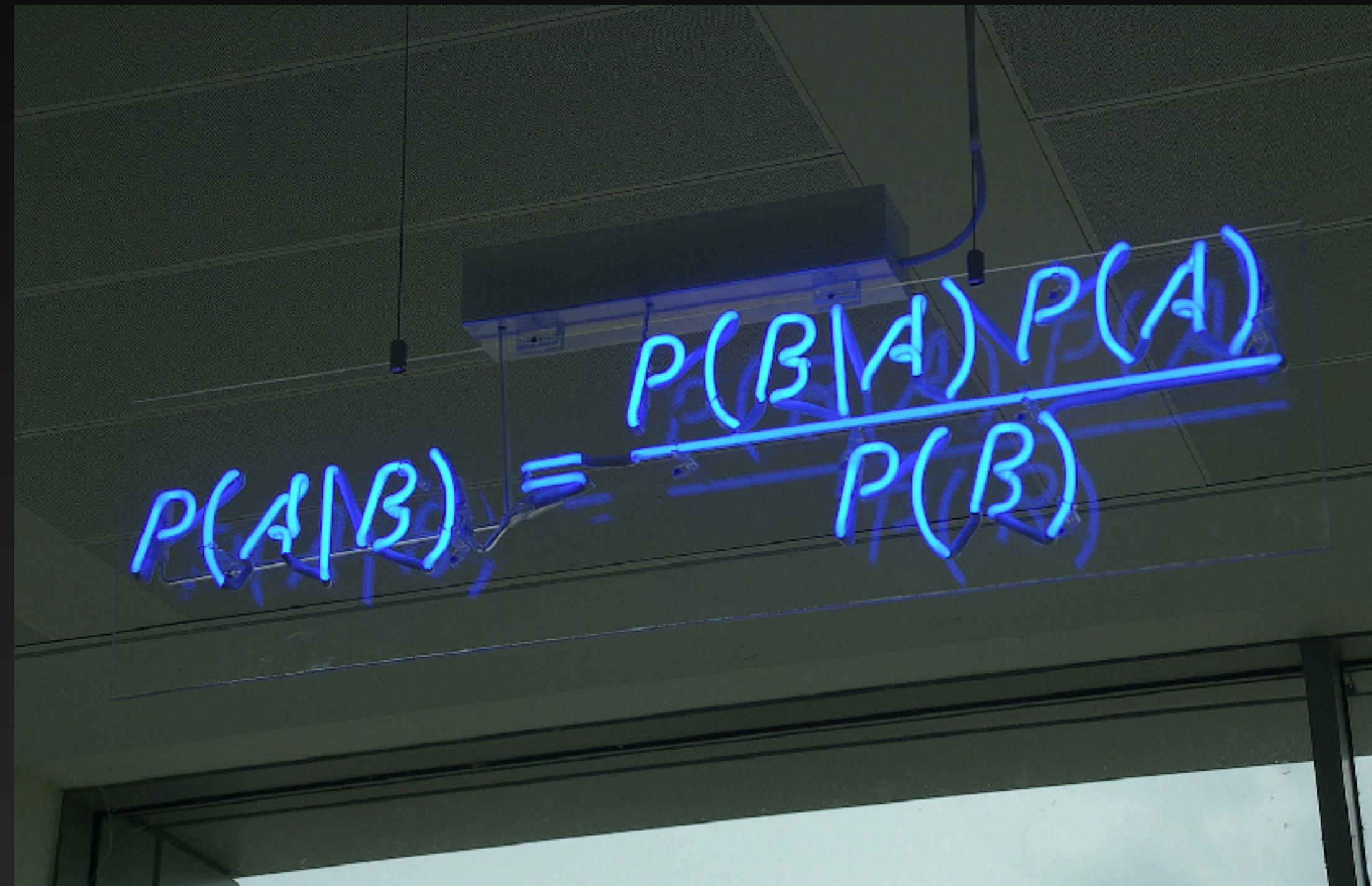
# Simple Particle Physics Models Also Work

| <i>Model Number</i> | <i>DM</i>        | <i>Mediator</i>           | <i>Interactions</i>  | <i>Elastic Scattering</i>  | <i>Near Future Reach?</i> |            |
|---------------------|------------------|---------------------------|--|--|---------------------------|------------|
|                     |                  |                           |  |  | <i>Direct</i>             | <i>LHC</i> |
| 1                   | Dirac Fermion    | Spin-0                    | $\bar{\chi}\gamma^5\chi, \bar{f}f$                             | $\sigma_{\text{SI}} \sim (q/2m_\chi)^2$ (scalar)                                   | No                        | Maybe      |
| 1                   | Majorana Fermion | Spin-0                    | $\bar{\chi}\gamma^5\chi, \bar{f}f$                             | $\sigma_{\text{SI}} \sim (q/2m_\chi)^2$ (scalar)                                   | No                        | Maybe      |
| 2                   | Dirac Fermion    | Spin-0                    | $\bar{\chi}\gamma^5\chi, \bar{f}\gamma^5f$                     | $\sigma_{\text{SD}} \sim (q^2/4m_n m_\chi)^2$                                      | Never                     | Maybe      |
| 2                   | Majorana Fermion | Spin-0                    | $\bar{\chi}\gamma^5\chi, \bar{f}\gamma^5f$                     | $\sigma_{\text{SD}} \sim (q^2/4m_n m_\chi)^2$                                      | Never                     | Maybe      |
| 3                   | Dirac Fermion    | Spin-1                    | $\bar{\chi}\gamma^\mu\chi, \bar{b}\gamma_\mu b$                | $\sigma_{\text{SI}} \sim \text{loop (vector)}$                                     | Yes                       | Maybe      |
| 4                   | Dirac Fermion    | Spin-1                    | $\bar{\chi}\gamma^\mu\chi, \bar{f}\gamma_\mu\gamma^5f$         | $\sigma_{\text{SD}} \sim (q/2m_n)^2$ or<br>$\sigma_{\text{SD}} \sim (q/2m_\chi)^2$ | Never                     | Maybe      |
| 5                   | Dirac Fermion    | Spin-1                    | $\bar{\chi}\gamma^\mu\gamma^5\chi, \bar{f}\gamma_\mu\gamma^5f$ | $\sigma_{\text{SD}} \sim 1$  | Yes                       | Maybe      |
| 5                   | Majorana Fermion | Spin-1                    | $\bar{\chi}\gamma^\mu\gamma^5\chi, \bar{f}\gamma_\mu\gamma^5f$ | $\sigma_{\text{SD}} \sim 1$  | Yes                       | Maybe      |
| 6                   | Complex Scalar   | Spin-0                    | $\phi^\dagger\phi, \bar{f}\gamma^5f$                           | $\sigma_{\text{SD}} \sim (q/2m_n)^2$   | No                        | Maybe      |
| 6                   | Real Scalar      | Spin-0                    | $\phi^2, \bar{f}\gamma^5f$                                     | $\sigma_{\text{SD}} \sim (q/2m_n)^2$   | No                        | Maybe      |
| 6                   | Complex Vector   | Spin-0                    | $B_\mu^\dagger B^\mu, \bar{f}\gamma^5f$                        | $\sigma_{\text{SD}} \sim (q/2m_n)^2$   | No                        | Maybe      |
| 6                   | Real Vector      | Spin-0                    | $B_\mu B^\mu, \bar{f}\gamma^5f$                                | $\sigma_{\text{SD}} \sim (q/2m_n)^2$   | No                        | Maybe      |
| 7                   | Dirac Fermion    | Spin-0 ( <i>t</i> -ch.)   | $\bar{\chi}(1 \pm \gamma^5)b$                                  | $\sigma_{\text{SI}} \sim \text{loop (vector)}$                                     | Yes                       | Yes        |
| 7                   | Dirac Fermion    | Spin-1 ( <i>t</i> -ch.)   | $\bar{\chi}\gamma^\mu(1 \pm \gamma^5)b$                        | $\sigma_{\text{SI}} \sim \text{loop (vector)}$                                     | Yes                       | Yes        |
| 8                   | Complex Vector   | Spin-1/2 ( <i>t</i> -ch.) | $X_\mu^\dagger\gamma^\mu(1 \pm \gamma^5)b$                     | $\sigma_{\text{SI}} \sim \text{loop (vector)}$                                     | Yes                       | Yes        |
| 8                   | Real Vector      | Spin-1/2 ( <i>t</i> -ch.) | $X_\mu\gamma^\mu(1 \pm \gamma^5)b$                             | $\sigma_{\text{SI}} \sim \text{loop (vector)}$                                     | Yes                       | Yes        |

About 2/3 of the simple tree level diagrams compatible with the excess have not yet been ruled out by other experiments...

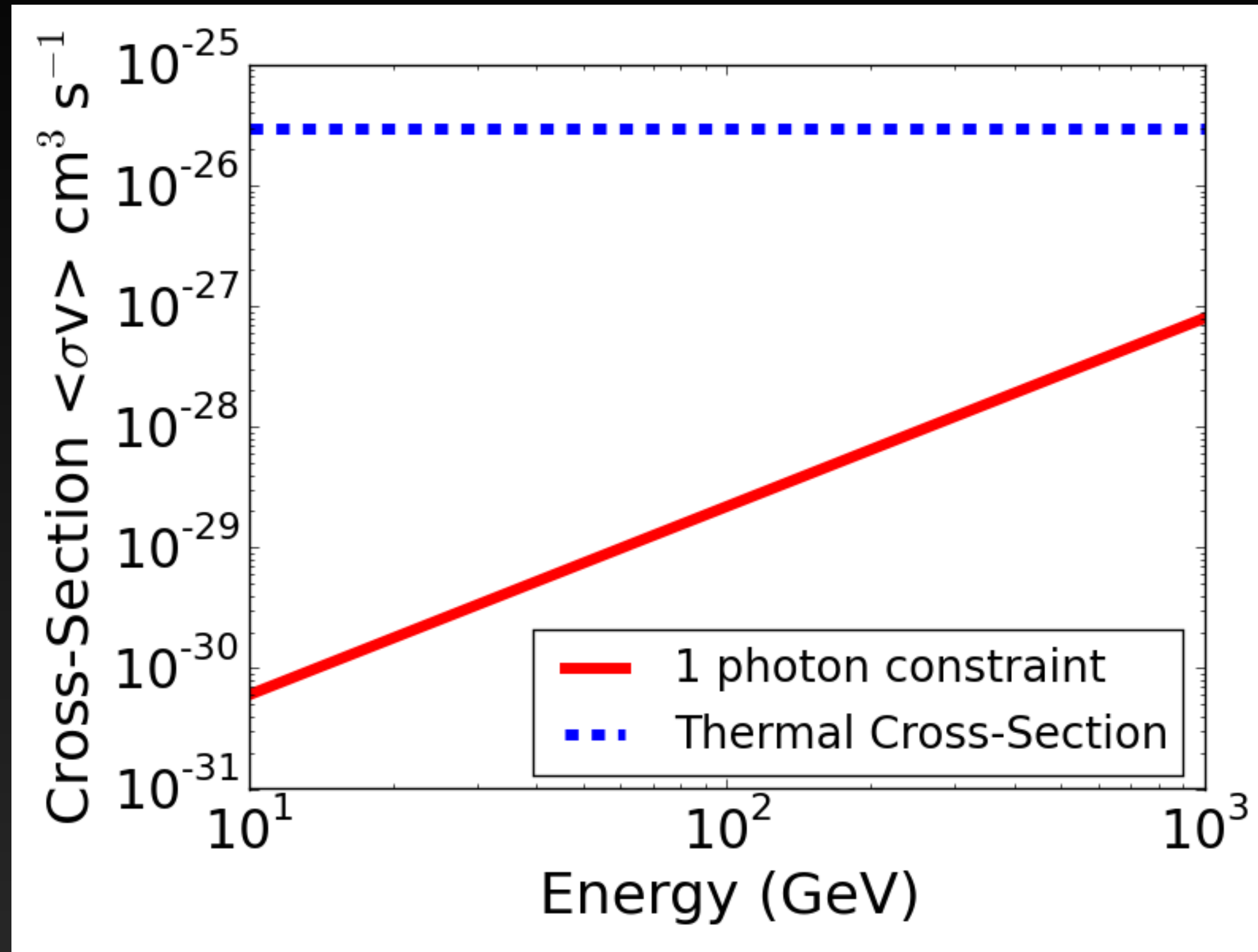
# Priors for a Dark Matter Discovery

Myriad Evidence Suggests Dark Matter exists, and should have non-gravitational interactions:

A photograph of a whiteboard with a blue marker equation. The equation is  $P(A|B) = \frac{P(B|A)P(A)}{P(B)}$ . The whiteboard is mounted on a wall, and the equation is written in blue marker. The background is a plain wall with a light-colored ceiling.
$$P(A|B) = \frac{P(B|A)P(A)}{P(B)}$$

We shouldn't think of dark matter searches as a "needle in a haystack". Our theoretical priors should lead us to bet that particle dark matter can be feasibly observed.

# Conversely, as a pessimist....



If astrophysical models were proven to produce the entirety of the Galactic center signal, nearly the full WIMP parameter space could be ruled out.

# Not a Conclusion Yet...

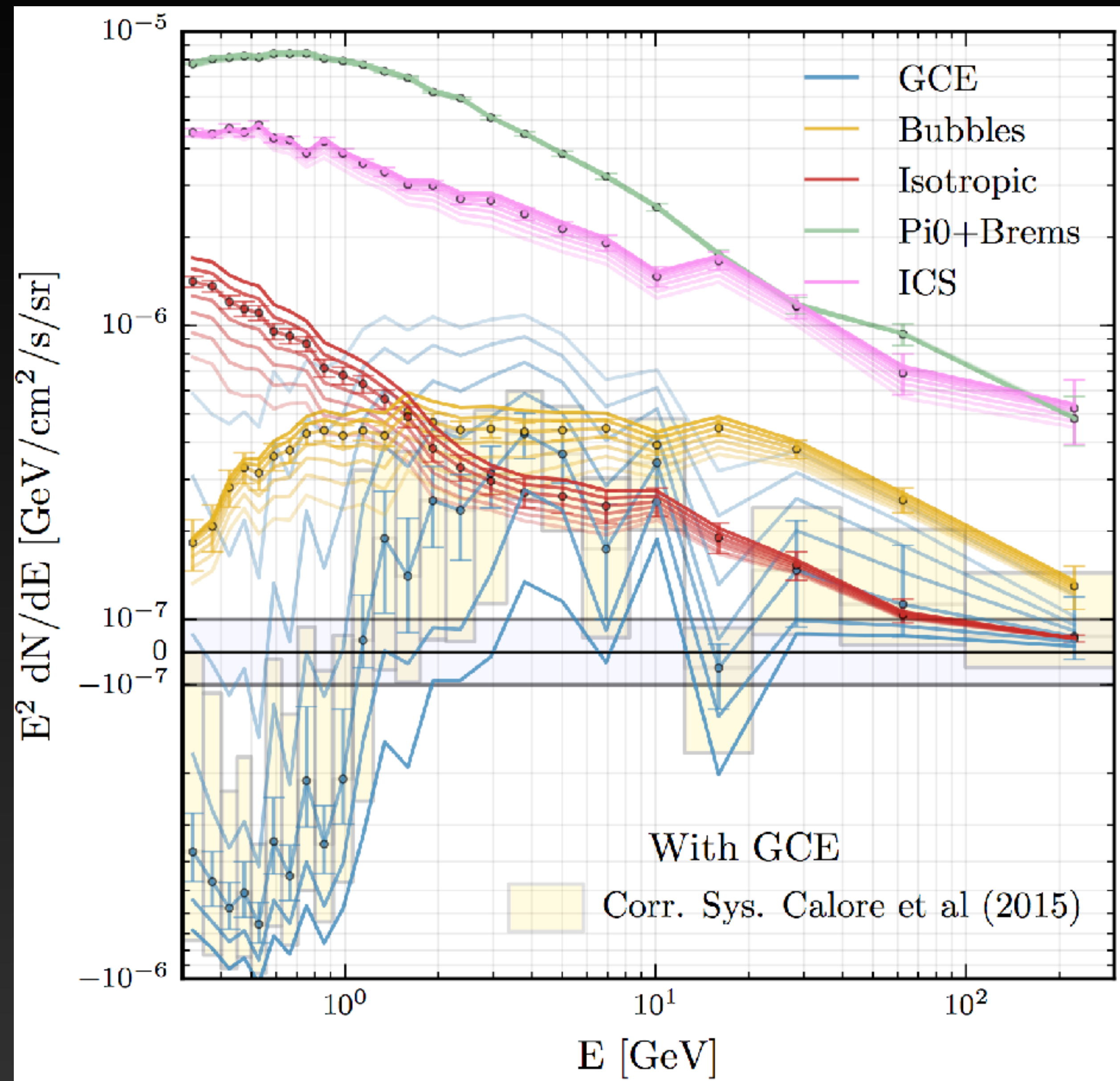
- 1.) The Galactic Center is a complex, but exciting environment. Several significant excesses are tied to the dynamics of the Galactic center environment.**
- 2.) The GeV excess is a robust component of the Galactic center emission profile. At present, no models have successfully eliminated the excess.**
- 3.) Improving our diffuse emission modeling is imperative to understanding the properties of the excess.**

Extra Slides

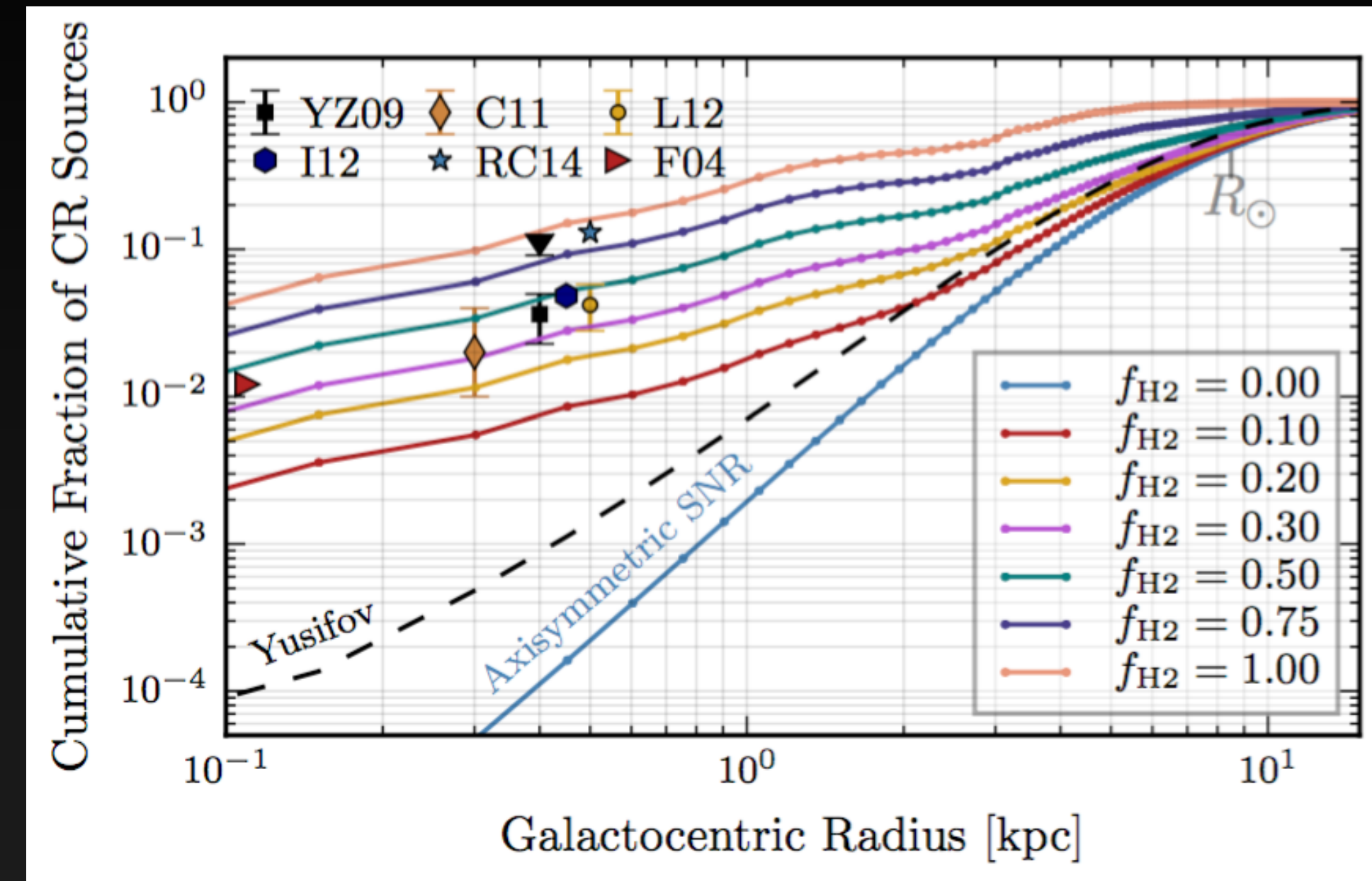
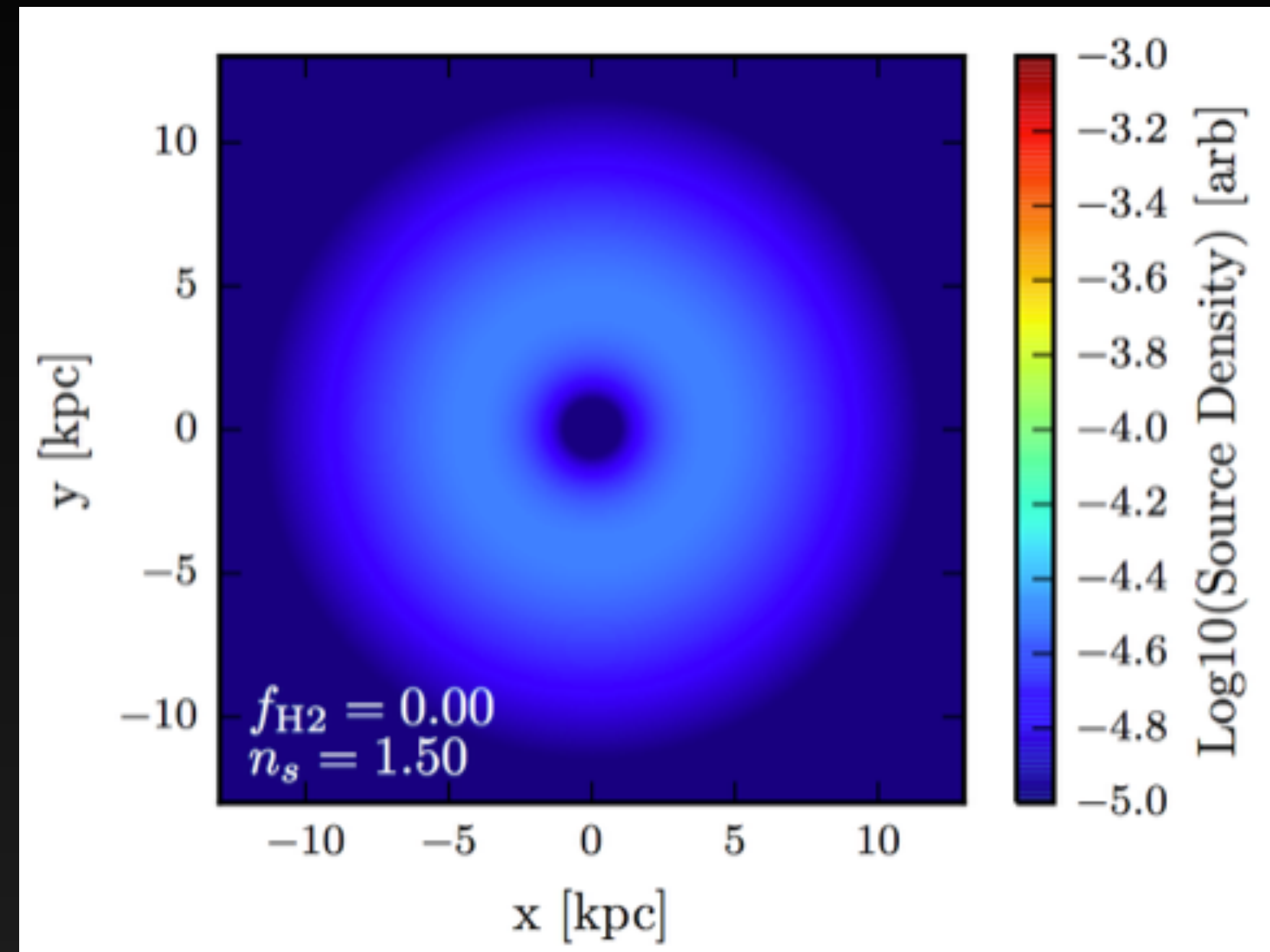
# Effect on the Excess Spectrum

Changing the background model has a significant effect on the spectrum of the gamma-ray excess.

The spectrum becomes extremely hard as  $f_{\text{H}_2}$  is increased, most likely indicating that the GCE template is picking up mismodeling of some residual.



# Waxing Philosophical.....

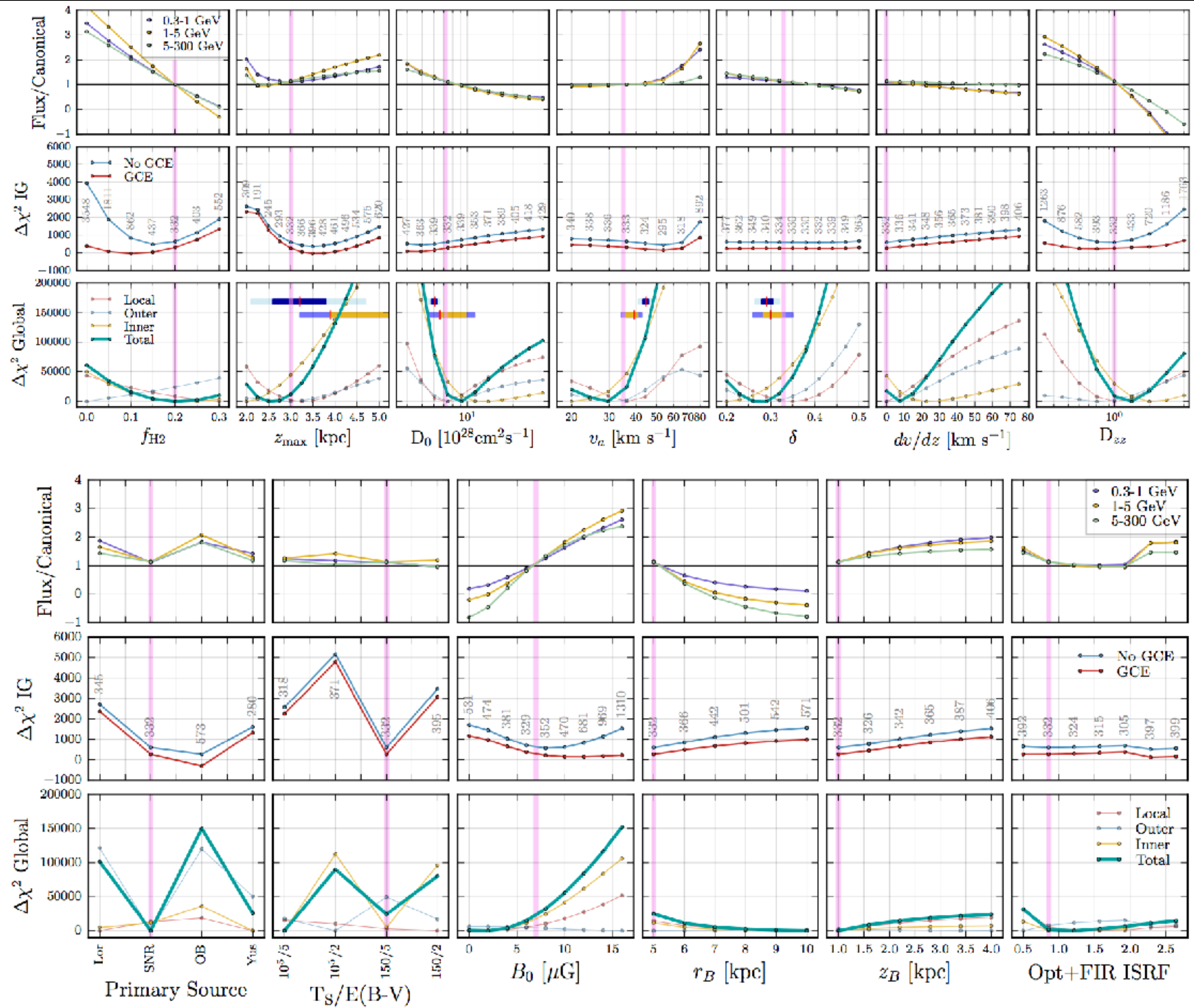


The lack of cosmic-ray injection in the GC should still be slightly disturbing. Especially when we try to answer the question: “excess compared to what?”

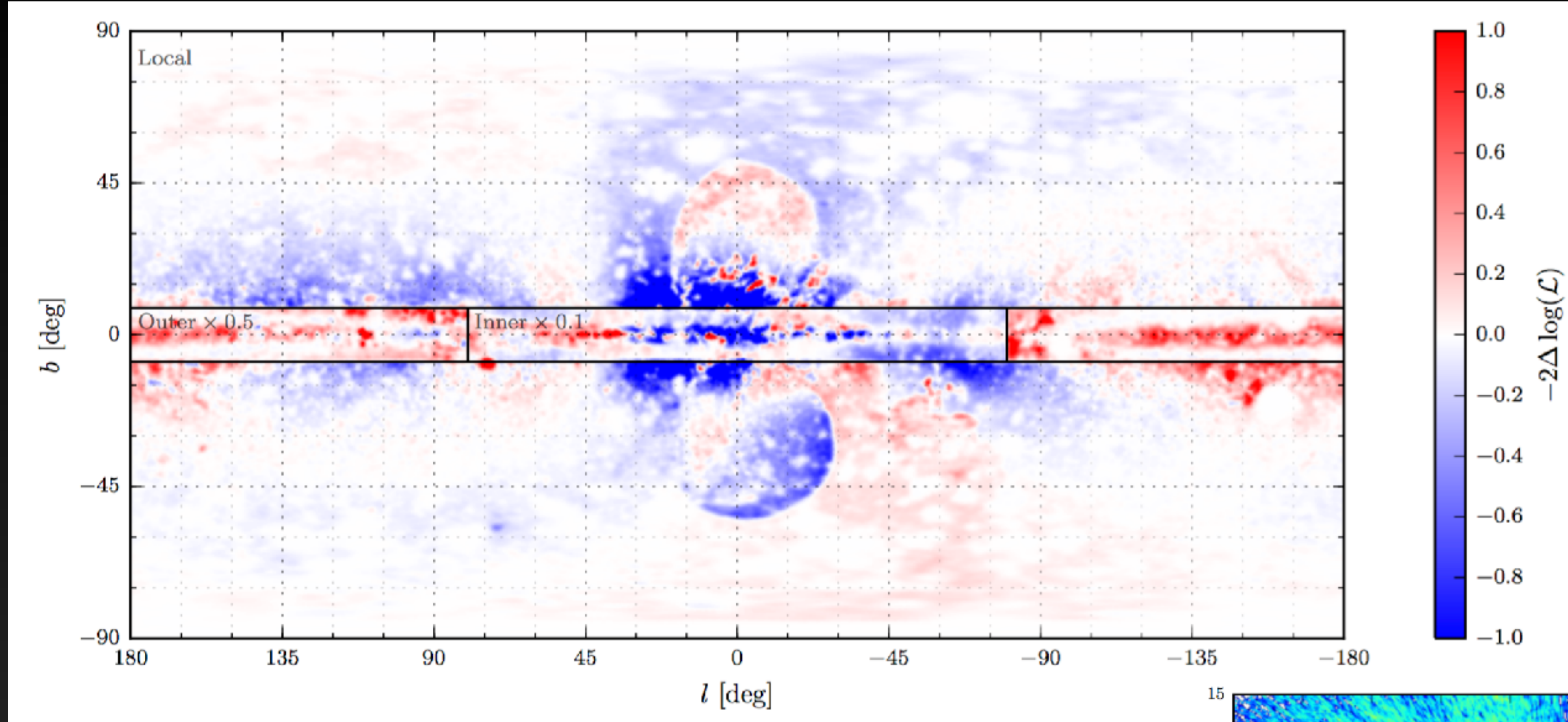
Our models indicate a degeneracy between cosmic-ray injection and the Galactic center excess template tracing an NFW profile. However, at present the best fit models still include a significant NFW component.

# Galactic center excess is resilient...

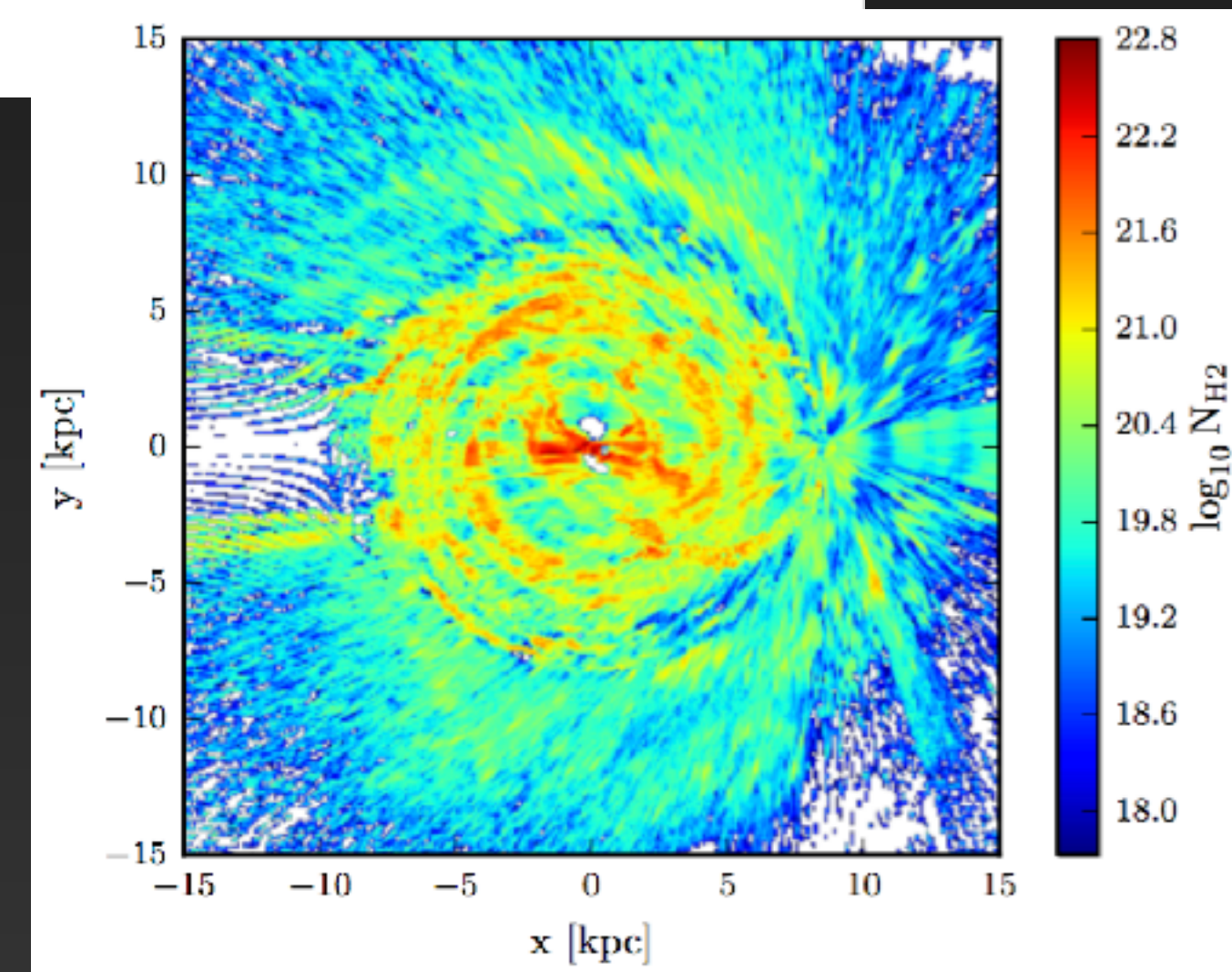
IG



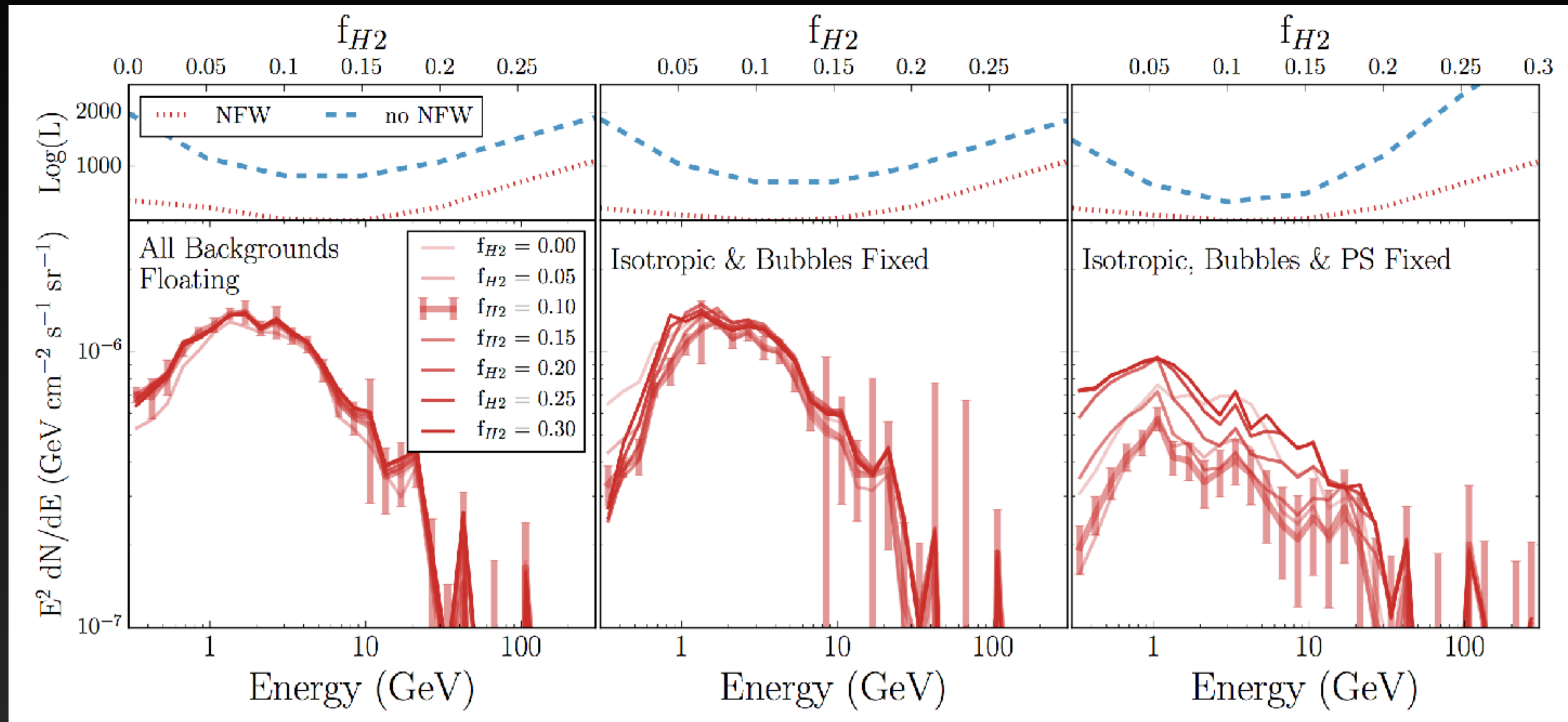
# A Better fit to the Gamma-Ray Sky



Fits are significantly improved, in particular in regions near the Galactic Center where there is significant kinematic gas information.

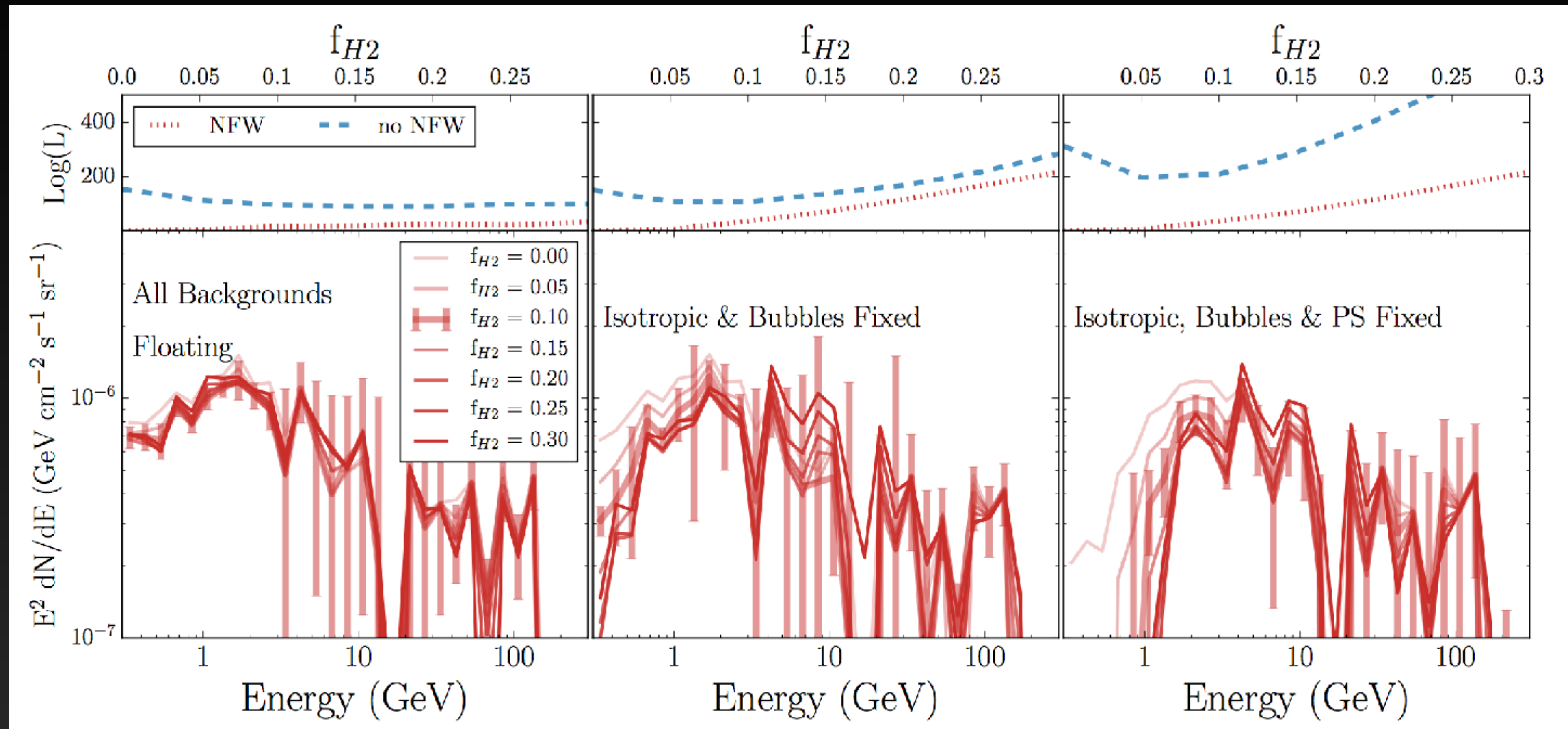


# Masking 1FIG Sources in the GC



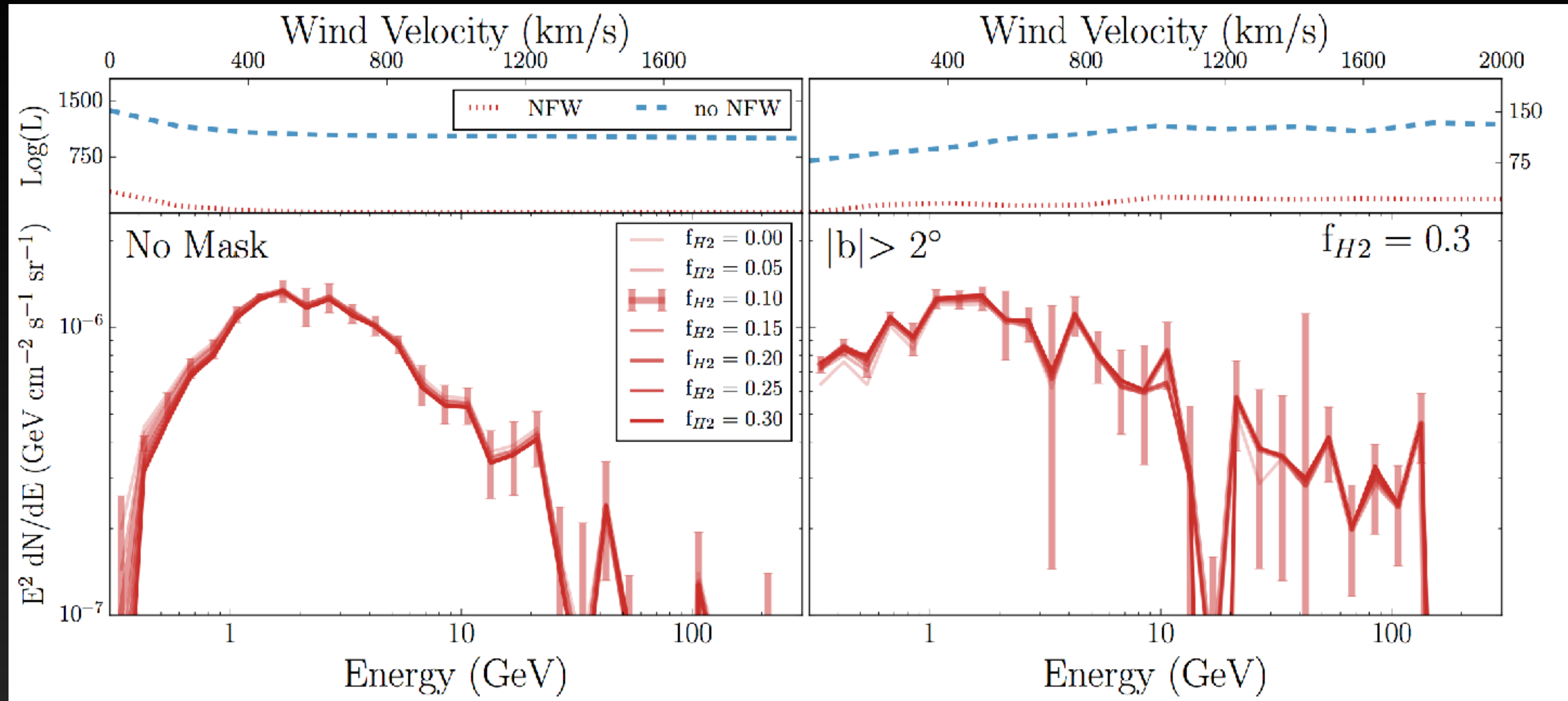
Changing the point source catalog from the 3FGL to the 1FIG has only a negligible effect on the gamma-ray excess.

# The Effect on the Galactic center Excess (masking $|b| < 2^\circ$ )



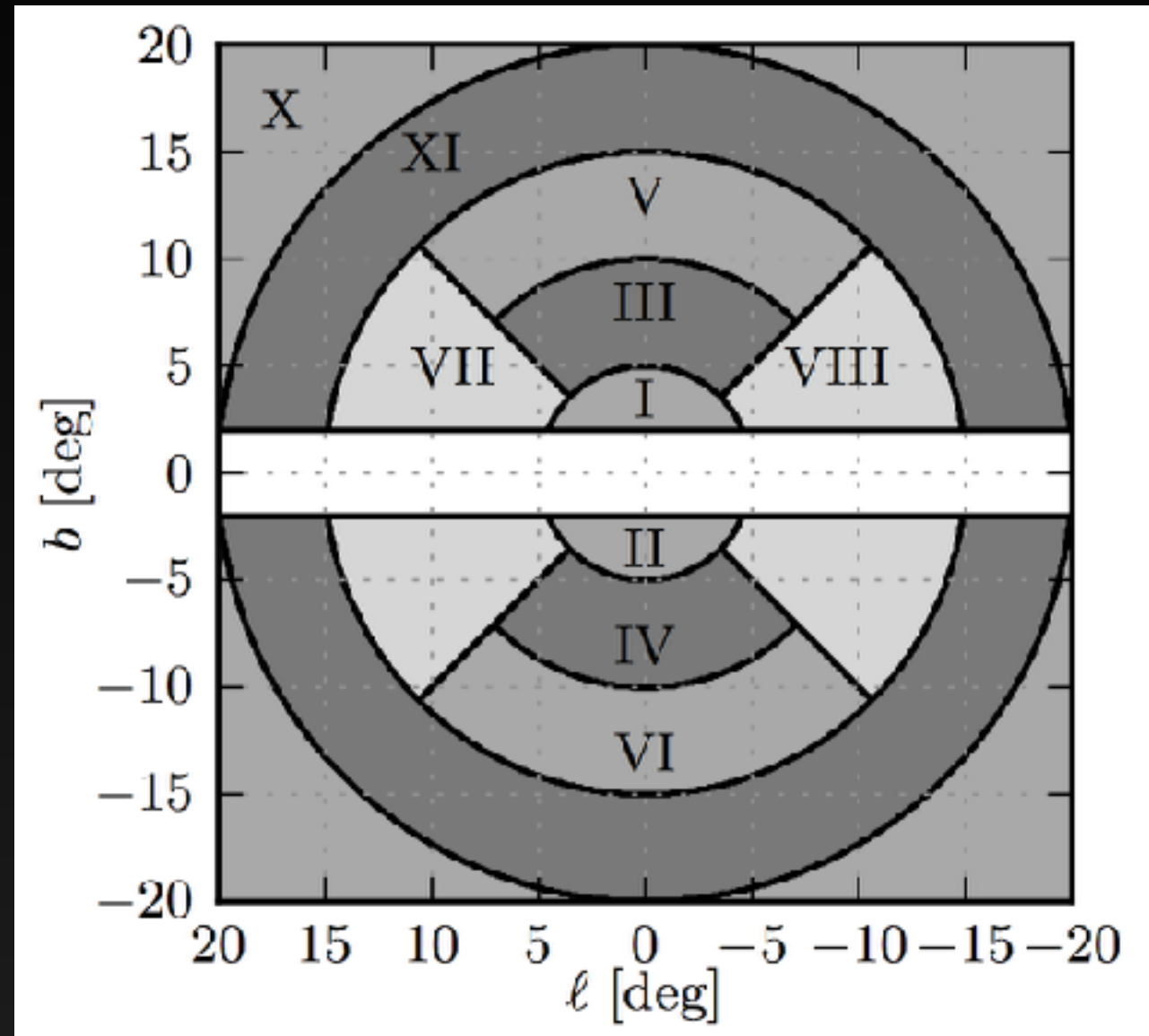
**Intriguingly, this persists even when the inner  $2^\circ$  are masked - implying that analyses of small ROIs favors the excess.**

# The Low Energy Spectrum



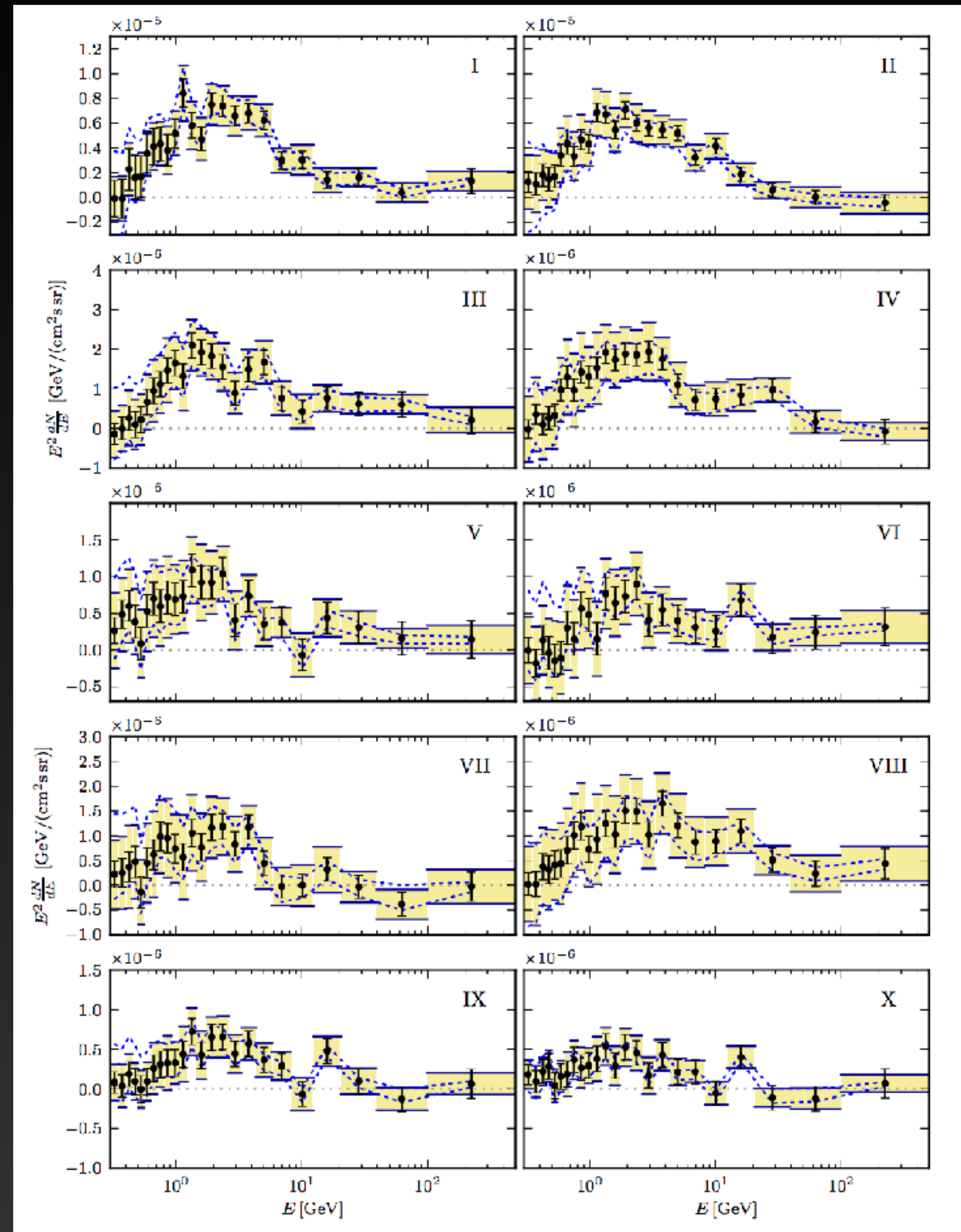
**The Galactic Center models contain only a small preference for the convective winds, and the spectrum and intensity of the Galactic center excess component remains resilient.**

# Analysis Far from the GC

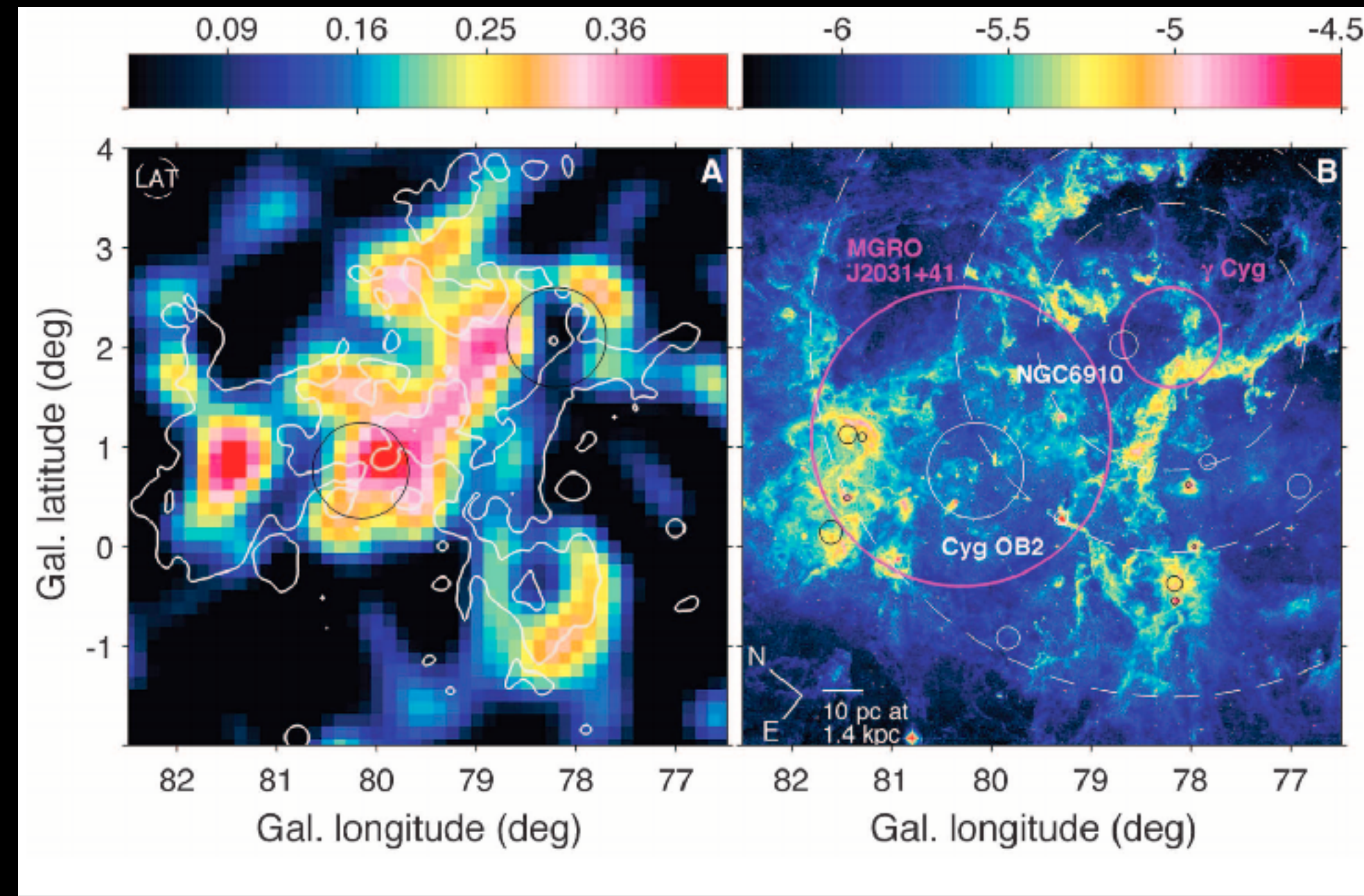


Analysis regions far from the GC also show an excess – not much star formation occurs a few degrees above the Galactic plane.

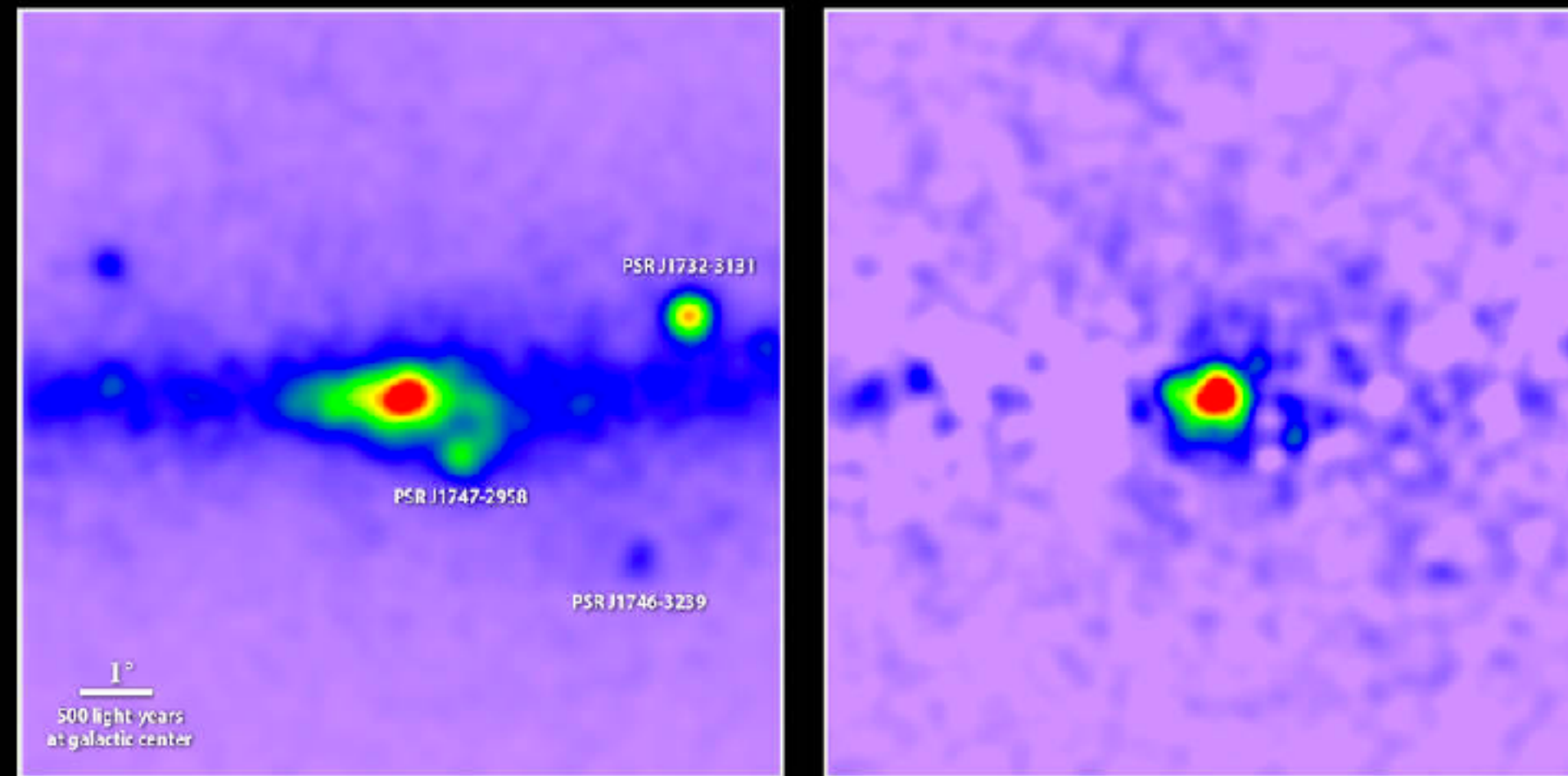
Calore et al. (2014, 1409.0042)



# Comparison to Cygnus-X



## Uncovering a gamma-ray excess at the galactic center



Unprocessed map of 1.0 to 3.16 GeV gamma rays

Known sources removed